Title
A Study of the Mechanism for Pollen Tube Growth

Author
Yan, An

Publication Date
2010

Peer reviewed|Thesis/dissertation

UNIVERSITY OF CALIFORNIA
RIVERSIDE

A Study of the Mechanism for Pollen Tube Growth

A Dissertation submitted in partial satisfaction
of the requirements for the degree of

Doctor of Philosophy

in

Plant Biology

by

An Yan

March 2011

Dissertation Committee:
Dr. Zhenbiao Yang, Chairperson
Dr. Guanshui Xu
Dr. Xuemei Chen

The Dissertation of An Yan is approved by:

_____

_____

_____
Committee Chairperson

University of California, Riverside

ACKNOWLEDGEMENTS

First, I would like to thank my two advisors Dr. Zhenbiao Yang and Dr. Guanshui Xu for their constant encouragement, devoted guidance during the past five years. I would like to thank Dr. Xuemei Chen for her kind help and guidance in my study.

I would also like to thank people in Yang Lab for their help, suggestions and encouragement. Especially, I would like to thank Dr. Gang Liu for fruitful collaboration in modeling of cell wall mechanical aspects in pollen tube growth. I would like to thank Dr. Yan Zhao for collaboration in study of endocytosis of pollen tubes. I would like to thank Dr. Yong-jik Lee, Dr. Jae-ung Hwang, Dr. Fan Yang, Dr. Ying Gu and Dr. Ying Fu for training me when I began my PhD study in Yang Lab.

I also got a lot of help from people outside Yang Lab. I would like to thank Dr. Jeffrey Harper for providing *aca9-2* seeds. I would like to thank Dr. Jean-Claude Mollet for providing JIM5 and JIM7 antibodies. I would like to thank Dr. Inhwan Hwang for providing anti-CHC antibody. I would like to thank Dr. David Carter for assistance in Microscopy. I would like to thank Dr. Masahiro Furutani and Dr. Tadaomi Takenawa for providing PIPs markers. I would like to thank Dr. Jose Feijo for sharing microarray data on PIPKs gene exprssion pattern.

Finally, I want to thank my wife and parents for their love and support all the years.

ABSTRACT OF THE DISSERTATION

A Study of the Mechanism for Pollen Tube Growth

by

An Yan

Doctor of Philosophy, Graduate Program in Plant Biology
University of California, Riverside, March 2011
Dr. Zhenbiao Yang, Chairperson

Through this PhD thesis work, the mechanism for pollen tube growth is studied using combined modeling and experimental approaches.

In chapter 1 of this thesis, we proposed mathematical models for ROP1 activity oscillation at apex of pollen tubes. Our combined theoretical and experimental studies suggested that ROP1 activity oscillation depends on downstream ROP1 signaling events, F-actin assembly and calcium accumulation, which positively and negatively feedback regulate ROP1 activity, respectively. Our findings suggested a key role for calcium in the negative feedback regulation of ROP1 activity.

In chapter 2 of this thesis, we proposed and experimentally validated a model coupling both active ROP1 polarity establishment and pollen tube morphogenesis. We revealed that exocytosis is the key process linking ROP1 GTPase polarity establishment, cell wall pectin distribution and polarized cell growth. Through exocytosis mediated positive feedback loop, RopGAP mediated global inhibition and lateral diffusion of ROP1

GTPase on plasma membrane, active ROP1 GTPases polarity can be established and maintained. Once maintained, active ROP1 controls cell wall mechanics via control of pectin exocytosis and thus determines the shape of pollen tubes. Experimentally, we also validated the model through both genetic (*ren1-1* mutant) and chemical (Latrunculin B treatment) perturbation of pollen tube morphogenesis process.

In Chapter 3 of this thesis, we studied the mechanism of endocytosis in pollen tubes. We revealed that two interconvertible phosphoinositides, PI(4,5)P2 and PI4P, function in different steps of clathrin-dependent endocytosis in pollen tubes. Whereas accumulation of PI(4,5)P2 is required for the initial steps of membrane invagination, PI4P is required for the later steps of closing and/or fission of invaginated membrane. Given previous findings that both the accumulation and the hydrolysis of PI(4,5)P_2 are required for clathrin-mediated endocytosis in yeast and animal cells, a balance between PI4P and PI(4,5)P_2 may provide a common mechanism underlying clathrin-dependent endocytosis in various eukaryotic systems.

Table of Contents

List of Tables

List of Figures

Introduction

Tip growth, a specialized cell growth where the expansion of cell surface only happens at a small region, is conserved throughout evolution. Many cell types in various biological systems including pollen tube, root hair (plant), neuron axon (animal) and fungal hyphae (fungi) demonstrate robust tip growth (Lee and Yang, 2008). During fertilization process of higher plant, pollen tube elongates rapidly within pistil to guarantee the successful delivery of sperm cells to ovules. Pollen tube is one of the most fast growing cells in plant and the speed of pollen tube elongation in tobacco can reach 1.5 mm/hour in vivo (Cheung and Wu, 2008). Many biological processes such as cell wall mechanics, vesicle trafficking, F-actin cytoskeleton dynamics, calcium dynamics and various signal transduction pathways are coupled together in a highly coordinated manner to ensure the sustained rapid tip growth of pollen tubes.

Cell wall mechanics is critical for pollen tube morphogenesis

From mechanical aspect, turgor pressure inside cell together with cell wall mechanical properties would determine the shape of plant cells. Several mathematical models have been built to successfully simulate pollen tube tip growth (Dumais et al., 2006; Lowery and Van Vactor, 2009; Fayant et al., 2010). The common assumption in these models for pollen tube growth is that anisotropic cell wall properties would lead to polarized pollen tube growth under the constant turgor pressure. Two lines of experimental evidence support this assumption. On one hand, direct experimental measurement using pressure

probe revealed that turgor pressure remains almost constant during pollen tube growth (Benkert et al., 1997). On the other hand, microindentation experiments also revealed that in growing pollen tubes, the cell wall softness display a steep gradient with highest value at apex (Parre and Geitmann, 2005; Zerzour et al., 2009).

The major component in pollen tube tip cell wall is pectin, thus pectin was assumed to be the key factor to determine cell wall mechanics. Consistently, removal of pectin by pectinase treatment caused depolarized growth in pollen tubes (Fayant et al., 2010). Furthermore, soft esterized pectin is highly enriched in cell wall at the apex of pollen tubes, while the hardened de-esterized pectin is enriched at distal cell wall of pollen tubes (Parre and Geitmann, 2005). The localization pattern of soft/hard pectin along cell wall is very similar to softness/extensibility profile of cell wall (Fayant et al., 2010). Newly synthesized soft pectin ester is exocytosed to pollen tube apex cell wall and gradually converted to hardened de-esterized pectin by pectin methyesterase (PME) (Bosch and Hepler, 2005; McKenna et al., 2009). Reduced PME activity would lead to burst of pollen tube and overexpression of PME would suppress pollen tube growth, supporting a critical role of pectin ester level on cell wall mechanical property regulation (Bosch and Hepler, 2005; Jiang et al., 2005).

Exocytosis in pollen tubes

During tip growth of pollen tubes, both cell wall material and plasma membrane (PM) are renewed via rapid exocytosis. The classical model about exocytosis assumed that

exocytosis happened at apex of pollen tube (Hepler et al., 2001). This model is supported by fluorescence recovery after photobleaching (FRAP) analysis using a plasma membrane localized RLK-GFP marker (Lee et al., 2008). After photobleach, the recovery of RLK-GFP signal is only observed at apex of pollen tube. Using the same method, Lee et al. also found that exocytosis of RLK-GFP is dependent on F-actin dynamics at apical region.

In yeast cells, exocyst complex tethers exocytic vesicles to PM (TerBush et al., 1996). The homologs of exocyst complex subunits genes have been characterized in plant cells and Arabidopsis exocyst subunits loss of function mutants show defective pollen germination and pollen tube growth (Hala et al., 2008). However, future study is needed to show a direct function of exocyst complex in exocytosis in pollen tubes. Rab GTPases controls various steps in vesicle trafficking including ER to Golgi, endosome recycling and secretion of pectin (Cheung et al., 2002; de Graaf et al., 2005; Szumlanski and Nielsen, 2009). However, details in the functional diversity of Rab GTPases in pollen tubes still need to be studied.

F-actin dynamics in pollen tube

During pollen tube growth, actin cytoskeleton dynamics is important for exocytosis and cell growth (Kost et al., 1998; Vidali et al., 2001). Actin dynamics of pollen tube has been studied using various GFP based markers, such as mTalin and ADF (Fu et al., 2001; Cheung and Wu, 2004). Actin forms stable thick cables in shank part of pollen tubes. In

apical and subapical region of pollen tube, actin exists as dynamical fine filaments called F-actin. Disruption of F-actin dynamics in pollen tube would inhibit exocytosis and pollen tube elongation, even when the thick actin cable is not severely affected, suggesting that these two actin populations had different functions (Vidali et al., 2001). One interesting feature of pollen tube is that during fast growth phase, the growth rate shows regular oscillation with period of 10-100 seconds. F-actin levels at apical and subapical region of pollen tubes oscillate ahead of growth oscillation, suggesting a causal relationship between F-actin polymerization and growth (Fu et al., 2001).

F-actin dynamics is regulated by many kinds of actin binding proteins (ABPs) in pollen tubes. For examples, formin proteins promote actin nucleation and polymerization (Cheung and Wu, 2004; Cheung et al., 2010), while profilin proteins bind with monomeric actin to inhibit actin polymerization (McKenna et al., 2004). There are also actin severing proteins such as ADFs (Allwood et al., 2002; Chen et al., 2002) and villins (Zhang et al., 2010), which can disrupt actin filaments into small fragments. These actin binding proteins balanced with each other to maintain the dynamics of F-actin in pollen tubes.

Calcium dynamics in pollen tube

Besides F-actin, calcium also shows fast dynamics during growth oscillation of pollen tubes. Cytosol calcium form steep gradient in the apical region of pollen tube (Pierson et al., 1994; Malho et al., 1995). In oscillating growing pollen tubes, cytosol calcium level

oscillates slightly behind growth oscillation and exocytosis oscillation, suggesting that calcium does not directly lead to growth (Pierson et al., 1994; Messerli et al., 2000; McKenna et al., 2009). Calcium enters pollen tube cells via calcium channels at apical PM (Malho et al., 1995). The molecular identity of selective calcium channels in pollen tube is still missing. The level of cytosol calcium is negatively regulated by PM localized calcium pumps (Schiott et al., 2004). Knock out mutant of *ACA9* gene, which encodes a PM localized calcium pump, shows inhibited pollen tube growth and reduced pollen fertility.

Calcium may control pollen tube growth through two different modes: 1). Calcium suppresses actin polymerization via binding with different ABPs (Kovar et al., 2000; Yokota et al., 2000; Wang et al., 2008); 2). Calcium may activate different calcium-dependent protein kinases to regulate downstream protein activity. Several CDPKs have been shown to perturb pollen tube polar growth (Yoon et al., 2006; Myers et al., 2009) and further research on calcium dependent signal transduction is needed to fully understand the role of calcium in regulating pollen tube growth.

ROP1 GTPase signaling pathway in pollen tube

ROP GTPases are versatile signal transduction switches regulating various pathways such as polar growth, hormonal response, disease defense and non-biotic stress response (Yang, 2008). In pollen tubes, ROP1 is the major ROP GTPase regulating polar growth. Like other small GTPase, ROP1 exists in two forms: GTP-bound active form and GDP-

bound inactive form. CA-ROP1 OX would lead to depolarized growth of pollen tubes while DN-ROP1 OX would suppress pollen tube growth (Kost et al., 1999; Li et al., 1999).

A group of ROP1 interacting proteins in pollen tube are RICs, which bind active ROP via CRIB motif (Wu et al., 2001). In pollen tubes, active ROP1 enhances F-actin polymerization and calcium accumulation through two distinct downstream factors RIC4 and RIC3, respectively. Moreover, RIC4-F-actin pathway and RIC3-calcium pathway can check and balance with each other to maintain fast exocytosis and pollen tube growth (Gu et al., 2005; Lee et al., 2008). In fast growing oscillating tobacco pollen tubes, ROP1 activity is also oscillating, slightly before growth rate oscillation, which is in phase with F-actin and exocytosis oscillation, while cytosol calcium oscillation is behind growth rate oscillation (Hwang et al., 2005; McKenna et al., 2009). The underlying mechanism for ROP1 activity and calcium oscillations is another open question. In Chapter 1 of this thesis, we built and validated models for addressing the molecular mechanism of coupled ROP1 activity and calcium oscillations.

In growing pollen tubes, the polarity of ROP1 is robustly maintained at the apical PM through balanced actions of upstream regulators of ROP1. RopGEFs are positive regulators of ROP1 activity, which can change GDP bound ROP1 to GTP bound ROP1 (Berken et al., 2005; Gu et al., 2006). In pollen tubes, overexpression of RopGEFs leads to depolarized pollen tube growth (Gu et al., 2006). The activity of pollen RopGEFs are

regulated by a pollen tube receptor like kinase PRK2. PRK2 phosphorylates the C-terminal of pollen RopGEFs to release the GEF activity (Zhang and McCormick, 2007). On the other hand, RopGAP and GDI are negative regulators of ROP1 activity. RopGAP down-regulates ROP1 activity by promotion of GTP to GDP conversion, and GDI suppresses ROP1 activity by sequestering free ROP1 in pollen tube cytosoplasm (Klahre et al., 2006; Klahre and Kost, 2006; Hwang et al., 2008; Hwang et al., 2010). Consistently, suppression of RopGAP and GDI leads to depolarized ROP1 activity and pollen tube growth and overexpression of RopGAP and GDI suppresses pollen tube growth. The mechanism for active ROP1 polarity establishment and pollen tube morphogenesis is one key open question in pollen tube biology. In Chapter 2 of this thesis, we used combined modeling and experimental approaches to address the mechanisms underlying ROP1 dependent pollen tube growth.

Endocytosis in pollen tubes

Opposite to exocytosis, endocytosis internalizes extracellular materials and retrieves excessive components from the plasma membrane. Using lipophilic FM dye staining, it has been revealed that endocytosis happened very rapidly in pollen tubes (within 10 minutes) (Parton et al., 2001). Endocytic pathways can be divided into clathrin dependent and independent endocytosis based on whether clathrin coat is required for initiation of the endocytic vesicles. Clathrin was reported to localize on subapcial PM of pollen tubes (Derksen, 1995; Blackbourn and Jackson, 1996), suggesting clathrin dependent endocytosis happens at subapical PM. Through tracking different nanogold particle

internalization routes into pollen tubes, it has been found that clathrin independent endocytosis happens at the apex of pollen tube (Moscatelli et al., 2007). Several different studies suggested that endocytosis is regulated by multiple signal transduction pathways such as calcium, ROP GTPase and phosphoinositides (Camacho and Malho, 2003; Monteiro et al., 2005; Sousa et al., 2008). However, molecular mechanisms for both clathrin dependent and independent endocytic pathways in pollen tubes still require future study. In Chapter 3 of this thesis, we studied the roles of phosphoinositides in regulation of clathrin depenedent endocytosis in pollen tubes.

References

Allwood, E.G., Anthony, R.G., Smertenko, A.P., Reichelt, S., Drobak, B.K., Doonan, J.H., Weeds, A.G., and Hussey, P.J. (2002). Regulation of the pollen-specific actin-depolymerizing factor LlADF1. Plant Cell **14,** 2915-2927.

Benkert, R., Obermeyer, G., and Bentrup, F.-W. (1997). The turgor pressure of growing lily pollen tubes. Protoplasma **198,** 1-8.

Berken, A., Thomas, C., and Wittinghofer, A. (2005). A new family of RhoGEFs activates the Rop molecular switch in plants. Nature **436,** 1176-1180.

Blackbourn, H.D., and Jackson, A.P. (1996). Plant clathrin heavy chain: sequence analysis and restricted localisation in growing pollen tubes. J Cell Sci **109,** 777-786.

Bosch, M., and Hepler, P.K. (2005). Pectin methylesterases and pectin dynamics in pollen tubes. Plant Cell **17,** 3219-3226.

Camacho, L., and Malho, R. (2003). Endo/exocytosis in the pollen tube apex is differentially regulated by Ca^{2+} and GTPases. J Exp Bot **54,** 83-92.

Chen, C.Y., Wong, E.I., Vidali, L., Estavillo, A., Hepler, P.K., Wu, H.M., and Cheung, A.Y. (2002). The regulation of actin organization by actin-depolymerizing factor in elongating pollen tubes. Plant Cell **14,** 2175-2190.

Cheung, A.Y., and Wu, H.M. (2004). Overexpression of an Arabidopsis formin stimulates supernumerary actin cable formation from pollen tube cell membrane. Plant Cell **16,** 257-269.

Cheung, A.Y., and Wu, H.M. (2008). Structural and signaling networks for the polar cell growth machinery in pollen tubes. Annu Rev Plant Biol **59,** 547-572.

Cheung, A.Y., Niroomand, S., Zou, Y., and Wu, H.M. (2010). A transmembrane formin nucleates subapical actin assembly and controls tip-focused growth in pollen tubes. Proc Natl Acad Sci U S A **107,** 16390-16395.

Cheung, A.Y., Chen, C.Y., Glaven, R.H., de Graaf, B.H., Vidali, L., Hepler, P.K., and Wu, H.M. (2002). Rab2 GTPase regulates vesicle trafficking between the endoplasmic reticulum and the Golgi bodies and is important to pollen tube growth. Plant Cell **14,** 945-962.

de Graaf, B.H., Cheung, A.Y., Andreyeva, T., Levasseur, K., Kieliszewski, M., and Wu, H.M. (2005). Rab11 GTPase-regulated membrane trafficking is crucial for tip-focused pollen tube growth in tobacco. Plant Cell **17,** 2564-2579.

Derksen, J. (1995). Quantitative analysis of the distribution of organelles in tobacco pollen tubes: implications for exocytosis and endocytosis. Protoplasma **188,** 267-276.

Dumais, J., Shaw, S.L., Steele, C.R., Long, S.R., and Ray, P.M. (2006). An anisotropic-viscoplastic model of plant cell morphogenesis by tip growth. Int J Dev Biol **50,** 209-222.

Fayant, P., Girlanda, O., Chebli, Y., Aubin, C.E., Villemure, I., and Geitmann, A. (2010). Finite Element Model of Polar Growth in Pollen Tubes. Plant Cell **22,** 2579-2593.

Fu, Y., Wu, G., and Yang, Z. (2001). Rop GTPase-dependent dynamics of tip-localized F-actin controls tip growth in pollen tubes. J Cell Biol **152,** 1019-1032.

Gu, Y., Li, S., Lord, E.M., and Yang, Z. (2006). Members of a novel class of Arabidopsis Rho guanine nucleotide exchange factors control Rho GTPase-dependent polar growth. Plant Cell **18,** 366-381.

Gu, Y., Fu, Y., Dowd, P., Li, S., Vernoud, V., Gilroy, S., and Yang, Z. (2005). A Rho family GTPase controls actin dynamics and tip growth via two counteracting downstream pathways in pollen tubes. J Cell Biol **169,** 127-138.

Hala, M., Cole, R., Synek, L., Drdova, E., Pecenkova, T., Nordheim, A., Lamkemeyer, T., Madlung, J., Hochholdinger, F., Fowler, J.E., and Zarsky, V. (2008). An exocyst complex functions in plant cell growth in Arabidopsis and tobacco. Plant Cell **20,** 1330-1345.

Hepler, P.K., Vidali, L., and Cheung, A.Y. (2001). Polarized cell growth in higher plants. Annu Rev Cell Dev Biol **17,** 159-187.

Hwang, J.U., Gu, Y., Lee, Y.J., and Yang, Z. (2005). Oscillatory ROP GTPase activation leads the oscillatory polarized growth of pollen tubes. Mol Biol Cell **16,** 5385-5399.

Hwang, J.U., Vernoud, V., Szumlanski, A., Nielsen, E., and Yang, Z. (2008). A Tip-Localized RhoGAP Controls Cell Polarity by Globally Inhibiting Rho GTPase at the Cell Apex. Curr Biol **18,** 1907-1916.

Hwang, J.U., Wu, G., Yan, A., Lee, Y.J., Grierson, C.S., and Yang, Z. (2010). Pollen-tube tip growth requires a balance of lateral propagation and global inhibition of Rho-family GTPase activity. J Cell Sci **123,** 340-350.

Jiang, L., Yang, S.L., Xie, L.F., Puah, C.S., Zhang, X.Q., Yang, W.C., Sundaresan, V., and Ye, D. (2005). VANGUARD1 encodes a pectin methylesterase that enhances pollen tube growth in the Arabidopsis style and transmitting tract. Plant Cell **17,** 584-596.

Klahre, U., and Kost, B. (2006). Tobacco RhoGTPase ACTIVATING PROTEIN1 spatially restricts signaling of RAC/Rop to the apex of pollen tubes. Plant Cell **18,** 3033-3046.

Klahre, U., Becker, C., Schmitt, A.C., and Kost, B. (2006). Nt-RhoGDI2 regulates Rac/Rop signaling and polar cell growth in tobacco pollen tubes. Plant J **46,** 1018-1031.

Kost, B., Spielhofer, P., and Chua, N.H. (1998). A GFP-mouse talin fusion protein labels plant actin filaments in vivo and visualizes the actin cytoskeleton in growing pollen tubes. Plant J **16,** 393-401.

Kost, B., Lemichez, E., Spielhofer, P., Hong, Y., Tolias, K., Carpenter, C., and Chua, N.H. (1999). Rac homologues and compartmentalized phosphatidylinositol 4, 5-bisphosphate act in a common pathway to regulate polar pollen tube growth. J Cell Biol **145,** 317-330.

Kovar, D.R., Drobak, B.K., and Staiger, C.J. (2000). Maize profilin isoforms are functionally distinct. Plant Cell **12,** 583-598.

Lee, Y.J., and Yang, Z. (2008). Tip growth: signaling in the apical dome. Curr Opin Plant Biol **11,** 662-671.

Lee, Y.J., Szumlanski, A., Nielsen, E., and Yang, Z. (2008). Rho-GTPase-dependent filamentous actin dynamics coordinate vesicle targeting and exocytosis during tip growth. J Cell Biol **181,** 1155-1168.

Li, H., Lin, Y., Heath, R.M., Zhu, M.X., and Yang, Z. (1999). Control of pollen tube tip growth by a Rop GTPase-dependent pathway that leads to tip-localized calcium influx. Plant Cell **11,** 1731-1742.

Lowery, L.A., and Van Vactor, D. (2009). The trip of the tip: understanding the growth cone machinery. Nat Rev Mol Cell Biol **10,** 332-343.

Malho, R., Read, N.D., Trewavas, A.J., and Pais, M.S. (1995). Calcium Channel Activity during Pollen Tube Growth and Reorientation. Plant Cell **7,** 1173-1184.

McKenna, S.T., Vidali, L., and Hepler, P.K. (2004). Profilin inhibits pollen tube growth through actin-binding, but not poly-L-proline-binding. Planta **218,** 906-915.

McKenna, S.T., Kunkel, J.G., Bosch, M., Rounds, C.M., Vidali, L., Winship, L.J., and Hepler, P.K. (2009). Exocytosis precedes and predicts the increase in growth in oscillating pollen tubes. Plant Cell **21,** 3026-3040.

Messerli, M.A., Creton, R., Jaffe, L.F., and Robinson, K.R. (2000). Periodic increases in elongation rate precede increases in cytosolic Ca2+ during pollen tube growth. Dev Biol **222,** 84-98.

Monteiro, D., Castanho Coelho, P., Rodrigues, C., Camacho, L., Quader, H., and Malho, R. (2005). Modulation of endocytosis in pollen tube growth by phosphoinositides and phospholipids. Protoplasma **226,** 31-38.

Moscatelli, A., Ciampolini, F., Rodighiero, S., Onelli, E., Cresti, M., Santo, N., and Idilli, A. (2007). Distinct endocytic pathways identified in tobacco pollen tubes using charged nanogold. J Cell Sci **120,** 3804-3819.

Myers, C., Romanowsky, S.M., Barron, Y.D., Garg, S., Azuse, C.L., Curran, A., Davis, R.M., Hatton, J., Harmon, A.C., and Harper, J.F. (2009). Calcium-dependent protein kinases regulate polarized tip growth in pollen tubes. Plant J **59,** 528-539.

Parre, E., and Geitmann, A. (2005). Pectin and the role of the physical properties of the cell wall in pollen tube growth of Solanum chacoense. Planta **220,** 582-592.

Parton, R.M., Fischer-Parton, S., Watahiki, M.K., and Trewavas, A.J. (2001). Dynamics of the apical vesicle accumulation and the rate of growth are related in individual pollen tubes. J Cell Sci **114,** 2685-2695.

Pierson, E.S., Miller, D.D., Callaham, D.A., Shipley, A.M., Rivers, B.A., Cresti, M., and Hepler, P.K. (1994). Pollen tube growth is coupled to the extracellular calcium ion flux and the intracellular calcium gradient: effect of BAPTA-type buffers and hypertonic media. Plant Cell **6,** 1815-1828.

Schiott, M., Romanowsky, S.M., Baekgaard, L., Jakobsen, M.K., Palmgren, M.G., and Harper, J.F. (2004). A plant plasma membrane Ca2+ pump is required for normal pollen tube growth and fertilization. Proc Natl Acad Sci U S A **101,** 9502-9507.

Sousa, E., Kost, B., and Malho, R. (2008). Arabidopsis phosphatidylinositol-4-monophosphate 5-kinase 4 regulates pollen tube growth and polarity by modulating membrane recycling. Plant Cell **20,** 3050-3064.

Szumlanski, A.L., and Nielsen, E. (2009). The Rab GTPase RabA4d regulates pollen tube tip growth in Arabidopsis thaliana. Plant Cell **21,** 526-544.

TerBush, D.R., Maurice, T., Roth, D., and Novick, P. (1996). The Exocyst is a multiprotein complex required for exocytosis in Saccharomyces cerevisiae. EMBO J **15,** 6483-6494.

Vidali, L., McKenna, S.T., and Hepler, P.K. (2001). Actin polymerization is essential for pollen tube growth. Mol Biol Cell **12,** 2534-2545.

Wang, H.J., Wan, A.R., and Jauh, G.Y. (2008). An actin-binding protein, LlLIM1, mediates calcium and hydrogen regulation of actin dynamics in pollen tubes. Plant Physiol **147,** 1619-1636.

Wu, G., Gu, Y., Li, S., and Yang, Z. (2001). A genome-wide analysis of Arabidopsis Rop-interactive CRIB motif-containing proteins that act as Rop GTPase targets. Plant Cell **13,** 2841-2856.

Yang, Z. (2008). Cell polarity signaling in Arabidopsis. Annu Rev Cell Dev Biol **24,** 551-575.

Yokota, E., Muto, S., and Shimmen, T. (2000). Calcium-calmodulin suppresses the filamentous actin-binding activity of a 135-kilodalton actin-bundling protein isolated from lily pollen tubes. Plant Physiol **123,** 645-654.

Yoon, G.M., Dowd, P.E., Gilroy, S., and McCubbin, A.G. (2006). Calcium-dependent protein kinase isoforms in Petunia have distinct functions in pollen tube growth, including regulating polarity. Plant Cell **18,** 867-878.

Zerzour, R., Kroeger, J., and Geitmann, A. (2009). Polar growth in pollen tubes is associated with spatially confined dynamic changes in cell mechanical properties. Dev Biol **334,** 437-446.

Zhang, H., Qu, X., Bao, C., Khurana, P., Wang, Q., Xie, Y., Zheng, Y., Chen, N., Blanchoin, L., Staiger, C.J., and Huang, S. (2010). Arabidopsis VILLIN5, an actin filament bundling and severing protein, is necessary for normal pollen tube growth. Plant Cell **22,** 2749-2767.

Zhang, Y., and McCormick, S. (2007). A distinct mechanism regulating a pollen-specific guanine nucleotide exchange factor for the small GTPase Rop in Arabidopsis thaliana. Proc Natl Acad Sci U S A **104,** 18830-18835.

Chapter 1

Calcium participates in the feedback regulation of the oscillating ROP1 Rho GTPase in pollen tubes

Abstract

Biological oscillation occurs at various levels from cellular signaling to organismal behaviors. Mathematical modeling has allowed quantitative understanding of slow oscillators requiring changes in gene expression (e.g., circadian rhythms), but few theoretical studies have focused on rapid oscillation of cellular signaling. The tobacco pollen tube, which exhibits growth bursts every 80 seconds or so, is an excellent system for investigating signaling oscillation. Pollen tube growth is controlled by a tip-localized ROP1 GTPase whose activity oscillates in a phase about 90 degrees ahead of growth. We constructed a mathematical model of ROP1 activity oscillation, which consists of interlinking positive and negative feedback loops involving F-actin and calcium, two ROP1 signaling targets that oscillate in a phase about 20 and 110 degrees behind ROP1 activity, respectively. The model simulates the observed changes in ROP1 activity caused by F-actin disruption and predicts a role for calcium in the negative feedback regulation of the ROP1 activity. Our experimental data strongly support this new role of calcium in tip growth. Therefore, our findings provide new insights into the mechanism of pollen tube growth and the oscillation of cellular signaling.

Introduction

Oscillation is a fundamental mechanism underlying homeostasis, efficiency, and robustness of many biological processes (Feijo et al., 2001; Forger and Peskin, 2003; Hwang et al., 2005; Heintzen and Liu, 2007). An interesting question is whether there exists a common design principle for highly diverse biological oscillation phenomena, ranging from circadian rhythms in various organisms to rapid cyclic changes in signaling events such as cellular calcium. It has been shown that oscillations with relatively long periods such as circadian clocks involve feedback-mediated oscillatory changes in the transcription of key transcription factors (Forger and Peskin, 2003; Geva-Zatorsky et al., 2006; Heintzen and Liu, 2007). However, some oscillatory changes are independent of gene expression, such as biochemical metabolism (Patnaik, 2003), cellular signaling (Maeda et al., 2004), calcium fluxes (Sneyd et al., 2004), and cytoskeletal dynamics-mediated cell movement (Giannone et al., 2004; Wolgemuth, 2005).

To deliver sperms to the ovule for fertilization in plants, pollen tubes rapidly elongate by tip growth in an oscillatory manner with a period ranging from 10 seconds to a few minutes (Feijo et al., 2001). Several ions like Ca^{2+}, H^{+} and K^{+} and signaling events in the apical region oscillate with the same period of growth oscillation in pollen tubes (Feijo et al., 2001). Cytosolic calcium forms a steep tip-focused gradient, and elimination of this gradient leads to growth arrest (Pierson et al., 1996; Holdaway-Clarke et al., 1997). The tip-localized calcium was proposed to regulate tip growth by regulating localized exocytosis (Roy et al., 1999; Lee et al., 2008). However, the peaks of the cytoplasmic

calcium level lag behind those of growth rates in oscillating pollen tubes (Messerli et al., 2000), suggesting that the apical calcium is not just to simply regulate exocytosis.

Another key oscillator in pollen tubes is the tip-localized ROP1 GTPase (Hwang et al., 2005), a central regulator of pollen tube growth (Lin et al., 1996; Kost et al., 1999; Li et al., 1999). Interestingly, the apical ROP1 activity oscillates in a phase approximately 90° ahead of growth and 120° ahead of the apical calcium (Hwang et al., 2005). ROP1 activates two downstream pathways that check and balance each other: RIC4-dependent assembly of tip-localized actin microfilaments (F-actin) and RIC3-mediated accumulation of the apical calcium (Gu et al., 2005).

In this study, we developed two mathematical models to simulate the interaction between the RIC4-F-actin and the RIC3-calcium pathways and experimentally tested the models. Our studies strongly support a role for the RIC4-actin pathway in the positive feedback regulation and suggest a new role for calcium in the negative feedback regulation of ROP1 signaling, and establish a molecular framework underpinning the oscillation of Rho GTPase signaling in the control of polarized cell growth.

Results

Model Structure

To model the oscillation of the apical ROP1 activity, we proposed the general structure of the ROP1 oscillation consisting of F-actin-mediated positive and calcium-mediated negative feedback loops (Figure 1).

Several previous observations support a role for the apical F-actin in the positive feedback loop. First, F-actin oscillates in a phase only slightly behind ROP1 activity (Hwang et al., 2005). Second, overexpression of the ROP1 effector RIC4, which promotes accumulation of the apical F-actin, induces a large increase in ROP1 activity (Gu et al., 2005; Hwang et al., 2005). Third, the RIC4-induced ROP1 activation was suppressed by Latrunculin B, an actin depolymerizing drug (Gu et al., 2005; Hwang et al., 2005). The apical F-actin promotes the apical targeting of exocytic vesicles (Vidali et al., 2001; Lee et al., 2008), which may carry positive regulators of ROP1 to the apical PM. We assumed that the positive feedback loop could reach saturation in part due to a limited amount ROP1 available for its activation. The cellular concentrations of Rho-family proteins (Rho, Rac, Cdc42) were estimated to range from 2.4 to 7.5 μM (Dawes and Edelstein-Keshet, 2007; Stites et al., 2007). Given the conserved functions of Rho proteins (including ROPs), we reasoned that the concentration of ROPs in pollen tubes would fall within this range. Accordingly the upper limit of ROP1 concentration in the PM was assumed to be 5 μM.

Another key assumption is an essential role for calcium in the negative feedback regulation of ROP1 activity. Rises in the apical calcium depend on the ROP1 activation of the RIC3 downstream pathway (Li et al., 1999; Gu et al., 2005), and lag behind those in the apical ROP1 by approximately 120° (Hwang et al., 2005). This suggests a time delay from ROP1 activation to the calcium increase. This delay can be explained by multiple biochemical and physical steps between ROP1 activation and calcium accumulation, because the ROP1 effector RIC3 is not a calcium channel but acts as an scaffolding protein (Wu et al., 2001; Gu et al., 2005). Once activated, RIC3 may signal to extracellular calcium influxes, which may subsequently activate calcium release from the internal calcium pool. We assumed that the rise in calcium levels leads to ROP1 inactivation, which is consistent with several observations. First, RIC3 overexpression suppresses the over-accumulation of the apical active ROP1 induced by RIC4 overexpression (Gu et al., 2005; Hwang et al., 2005). RIC3 suppression of the RIC4 overexpression phenotype is calcium-dependent and is not due to competition between these two ROP1 effectors (Gu et al., 2005; Hwang et al., 2005). Second, ROP1-dependent pollen tube elongation is suppressed when extracellular calcium is over a threshold level (Li et al., 1999; Gu et al., 2005). Third, loss-of-function mutant of *ACA9*, which encodes a PM-localized calcium pump, is impaired in pollen tube growth (Schiott et al., 2004) and has reduced localization of ROP1 to the apical PM (Figure 1.1).

We consider two possible modes of calcium action in the negative feedback loop (Figure 1.2). Calcium might promote the disassembly of the apical F-actin, leading to the down

regulation of the ROP1 activity by countering the F-actin mediated positive feedback (Figure 1.2A). Calcium is known to regulate several actin-binding proteins (Kovar et al., 2000; Yokota et al., 2000; Wang et al., 2008). Alternatively, calcium signaling might down regulate ROP1 activity by activating negative regulators of ROP1 (Figure 1.2B). In Arabidopsis pollen tubes, the apically localized REN1 RhoGAP participates in the negative feedback regulation of ROP1 and may be subject to regulation by calcium (Hwang et al., 2008).

Modeling ROP1 activity oscillation and its phase relationship with calcium oscillation

We formulated equations for the two different possible modes of calcium-dependent negative feedback. The biological contexts and values of parameters are listed in Table 1.1 and Table 1.2.

Equations for Model I (Calcium promotion of actin disassembly):

$$\frac{dx}{dt} = \beta_x f(x) g(x,y) - \alpha_x x \quad (1.1)$$

$$\frac{dy}{dt} = \beta_y [x(t-\tau) + b] - \alpha_y y \quad (1.2)$$

$$f(x) = \begin{cases} R_0 - x & x < R_0 \\ 0 & x \geq R_0 \end{cases} \quad (1.3)$$

$$g(x,y) = \begin{cases} \dfrac{kx(C_0 - y)}{R_0 C_0} & y < C_0 \\ 0 & y \geq C_0 \end{cases} \quad (1.4)$$

Equations for Model II (Calcium modulation of ROP regulators):

$$\frac{dx}{dt} = \beta_x f(x)g(x) - \alpha_x h(y)x \text{.....}(2.1)$$

$$\frac{dy}{dt} = \beta_y [x(t-\tau) + b] - \alpha_y y \text{.....}(2.2)$$

$$f(x) = \{ \begin{matrix} R_0 - x & x < R_0 \\ 0 & x \geq R_0 \end{matrix} \text{.....}(2.3)$$

$$g(x) = \frac{kx}{R_0} \text{.....}(2.4)$$

$$h(y) = \{ \begin{matrix} \frac{1}{M} & y < y_{\min} \\ \frac{1}{M}[1 + \frac{(M-1)(y - y_{\min})}{y_{\max} - y_{\min}}] & y_{\min} \leq y \leq y_{\max} \\ 1 & y > y_{\max} \end{matrix} \text{.....}(2.5)$$

We found that both models could reproduce observed oscillations of the ROP1 activity and the calcium concentrations (Figure 1.3A, B). Both ROP1 activity and calcium show sustained oscillation with periods around 80 seconds. The amplitudes for the ROP1 activity and the apical calcium level are 0-0.6 μM and 0.8-2.2 μM, respectively. Calcium oscillation is behind ROP1 activity oscillation by approximately 120°. Therefore, these models simulate typical ROP1 activity and calcium oscillations observed in tobacco pollen tubes (Messerli et al., 2000; Hwang et al., 2005). The interlinked positive and negative feedback loops of ROP1 activity do not automatically lead to the oscillations of ROP1 activity and calcium. An important factor that determines the oscillation patterns is the time delay τ between ROP1 activity and calcium increases. When τ is 8 seconds, our model reproduced the observed oscillation pattern for tobacco pollen tubes with an oscillation period of approximately 80 seconds. A short time delay (τ = 4 s or smaller) would destabilize the oscillation of ROP1 activity and calcium level (Figure 1.3C, D). If

the time delay is too large (τ = 12 s or larger), the period of oscillations would be significantly prolonged (Figure 1.3E, F).

As a negative regulator of ROPs, RhoGAP is critical for polarized pollen tube growth (Hwang et al., 2008). The simulation of our models predicted that ROP1 activity oscillation is highly sensitive to increasing amounts of RhoGAP (Figure 1.4). To experimentally test this prediction, we overexpressed different dosages of RopGAP1 and found that increasing amount of RopGAP1 would significantly suppress ROP1 activity oscillation, as predicted from our models (Figure 1.4).

Simulation and experimental validation of the effect of F-actin on ROP1 activity oscillation.

To test our models regarding the role of F-actin-mediated positive feedback, we simulated the effect of depleting and stabilizing the apical F-actin. The simulation predicted that severe depletion of the apical F-actin would lead to a dramatic reduction of ROP1 activity to a basal level (<0.1 μM) and the termination of its oscillation (Figure 1.5D-E), and that moderate depletion of the apical F-actin would dampen the ROP1 activity oscillation by reducing the oscillation amplitude (Figure 1.6C-D). We tested these predictions by experimentally manipulating the level of the apical F-actin. By sequestering G-actin (monomeric actin), Latrunculin B promotes F-actin depolymerization (Gibbon et al., 1999; Hwang et al., 2005). Treatment of tobacco pollen tubes with 5 nM Latrunculin B caused a significant decrease in the amount of the apical

F-actin and tip growth inhibition (Fu et al., 2001). None of the 30 observed pollen tubes treated with 5 nM Latrunculin B showed detectable active ROP1 cap and oscillation of the apical ROP1 activity (Figure 1.5F, J-K), whereas 6 of 10 control tubes exhibited normal oscillation (Figure 1.5C, J-K). Consistently, we previously showed that the oscillation amplitude of ROP1 activity is reduced by treatment with 0.5 nM Latrunculin B (Hwang et al., 2005).

We then investigated the effect of the F-actin stabilizing drug Jasplakinolide. Our models predicted that the stabilization of the apical F-actin would result in the accumulation of the non-oscillating ROP1 activity to a high level (Figure Figure1.5G-H). Indeed we found that tobacco pollen tubes treated with 100 nM Jasplakinolide exhibited sustained high levels of the apical ROP1 activity that did not oscillate (n=20) (Figure 1.5I, J-K). Taken together we conclude that the apical F-actin positively feedback regulates the apical ROP1 activity and thus is crucial for the oscillation of the ROP1 activity.

Simulation and experimental validation of the effect of calcium on the ROP1 activity

In our models, the apical cytosolic calcium is critical in the negative feedback loop of the ROP1 activity control. To validate this, we simulated and experimentally tested the effect of calcium on ROP1 activity using several means of perturbation of the apical calcium.

The simulation predicted that if the rate of calcium accumulation is greatly increased, the ROP1 activity would be persistently suppressed to a minimal level (about 0.05 μM) and

would rapidly lose its oscillation (Figure 1.7D-E). If the rate of calcium accumulation is increased moderately, the ROP1 activity would be moderately reduced and oscillate with smaller amplitudes (Figure 1.7H-I). To test these predictions, we first examined the effect of RIC3 overexpression on the ROP1 activity. RIC3 is a ROP1 effector responsible for the ROP1-dependent calcium accumulation, and overexpression of RIC3 increased calcium accumulation in pollen tube tips (Gu et al., 2005). Approximately 60% of control tubes exhibit typical oscillation pattern. When pollen was transformed with 0.1 μg RIC3 plasmid construct, the apical active ROP1 was depleted (n=30) and no ROP1 activity oscillation was seen in these pollen tubes (Figure 1.7F, L-M). When 0.02 μg RIC3 construct was used, 5 out of the 20 observed pollen tubes showed oscillation in the ROP1 activity with reduced amplitudes (Figure 1.7J, L-M), while remaining tubes did not oscillate.

We next manipulated an increase in cytosolic calcium by treating tobacco pollen tubes with A23187, a calcium ionophore that causes leakage of extracellular calcium into cells. We treated pollen tubes with different levels of A23187 to examine their effects on ROP1 activity in tobacco pollen tubes. At 1 μM A23187 treatment, the active ROP1 cap was depleted (n=20) and no ROP1 activity oscillation was seen in these pollen tubes (Figure 1.7G, L-M). When treated with 10 nM A23187, 3 out of 20 observed pollen tubes showed oscillation in the ROP1 activity with lower levels and reduced amplitudes (Figure 1.7K, L-M). Consistent with these results, we found that pollen tubes from the *aca9-2* knockout mutant exhibited greatly reduced amount of ROP protein in the apical PM

(Figure 1.1). The results further confirmed the model prediction that high calcium levels in pollen tubes would inhibit ROP1 activity and dampen its oscillation.

Finally, we predicted that a reduction in cytosolic calcium levels would significantly increase the apical ROP1 activity and eliminate its oscillation (Figure 1.8D-E). We tested this prediction by treating pollen tubes with $LaCl_3$, a calcium channel blocker, which has been shown to lower cytosolic calcium levels in pollen tubes (Malho et al., 1995). When treated with 10 μM $LaCl_3$, pollen tubes maintained a high level of the apical ROP1 activity (>1.6) and lost its oscillation (Figure 1.8F-H, n=20). Therefore all of our experimental data agree with our model predictions and support an important role for calcium in the negative feedback regulation of the apical ROP1 activity and its oscillation in pollen tubes.

Discussion

Our mathematical modeling has led to new insights into the mechanism underlying oscillatory pollen tube growth and Rho GTPase-dependent signaling circuitry. Our combined theoretical and experimental studies suggest that ROP1 activity oscillation depends on downstream ROP1 signaling events, F-actin assembly and calcium accumulation, which positively and negatively feedback regulate ROP1, respectively. These studies strongly support one of the first examples, if not the first, of oscillatory signaling circuitries that are dependent on the highly conserved Rho GTPase family. This may have implications in the understanding of Rho GTPase-mediated processes in other

systems. Rho-family GTPases control cellular processes involving cell polarization and/or oscillatory behaviors in various eukaryotic cells, e.g., oscillatory cell movement (Giannone et al., 2004; Wolgemuth, 2005). Similar oscillatory Rho GTPase signaling, as we show here for polarized pollen tube growth, might also regulate the oscillation of other Rho-dependent processes. Furthermore, the ROP1 signaling circuit provides a mechanism for calcium oscillation, which serves as an important temporal calcium signal. Given the conservation of both Rho GTPases and calcium oscillation, it is tempting to speculate that Rho GTPase-mediated calcium oscillation might also exist in other systems.

Our findings suggest a key role for calcium in the negative feedback regulation of ROP1 activity, which can explain the long-standing dilemma in the field of pollen tip growth, i.e., the oscillatory accumulation of calcium at the cell tip lags behind the increase in tip growth rate, albeit an essential role for calcium in tip growth. Our modeling predicts that either mode of calcium-dependent negative feedback is sufficient for the generation of oscillating ROP1 activity: calcium promotion of F-actin depolymerization to counter F-actin-mediated positive feedback and calcium activation of ROP1 inactivators, such as RopGAPs. Calcium sensors such as CDPKs are important for pollen tube growth (Yoon et al., 2006; Myers et al., 2009) and may act in the negative feedback regulation. Future studies of such calcium sensors should help to elucidate the mechanisms by which calcium feedback regulates ROP1 signaling in pollen tubes. Future research should also focus on modeling the linkage between the calcium- and F-actin-mediated feedback regulations and the polarization of the ROP1 activity.

Materials and Methods

Plant materials and growth conditions

Seeds of the *aca9-2* homozygote mutant were kindly provided by Dr. Jeffrey Harper (Schiott et al., 2004). Wild type Arabidopsis plants of WS ecotype were used as control plants. Arabidopsis plants were grown under 16 hours:8 hours (Light:Dark) period at 20°C and were used as the source for pollen for immuno-staining experiments. Wild type tobacco (*Nicotiana tabacum*) plants were grown under 12 hours:12 hours (Light:Dark) period at 25°C.

Detection of ROP1 localization using indirect immunofluorescence microscopy

Pollen grains of Arabidopsis flowers were germinated in solid germination medium for 4 hours at room temperature and then immuno-stained with Anti-Rop1Ps polyclonal antibody and FITC-conjugated goat anti-rabbit IgG antibody (Sigma) as described previously (Hwang et al., 2008). Mounted pollen tubes from WS wild type background and *aca9-2* mutant background were observed under a Leica SP2 Confocal Microscope. Median planes of pollen tubes were scanned to show the sub-cellular localization pattern of ROP1 protein.

Bollistics-mediated transient expression in tobacco pollen

Three DNA constructs as described previously (Gu et al., 2005; Hwang et al., 2005) were used for bollistics-mediated transient expression: pLAT52:RhoGAP1, pLAT52:RIC3 and

GFP-based ROP1 activity marker pLAT52:GFP-RIC4ΔC. DNA constructs were amplified in the E. coli strain DH5α and purified using Plasmid Mini Kit according to the manufacturer's instructions (Qiagen, Valencia, CA).

Particle bombardment-mediated transient expression in tobacco pollen was performed using method previously described (Hwang et al., 2005). 0.1 μg of LAT52:GFP-RIC4ΔC construct was transformed to show oscillation of ROP1 activity. To study the effect of RIC3 or RhoGAP1 overexpression on ROP1 activity, 0.1 μg or 0.02 μg pLAT52:RIC3 or pLAT52:RhoGAP1 were co-transformed with 0.1 μg GFP-RIC4ΔC. Pollen tubes were observed under a Leica SP2 Confocal Microscope 3-6 hours after germination.

Drug Treatments

To determine the role of F-actin, 3 hours after pollen germination, 5 μM Lat B and 100 μM Jasplakinolide stock solutions were added into pollen germination medium to a final concentration of 5 nM and 100 nM, respectively. For A23187 treatment, 1 mM A23187 stock solution was added into pollen germination medium to final concentrations of 1 μM (for high concentration treatment) and 10 nM (for low concentration treatment). For $LaCl_3$ treatment, 10 mM $LaCl_3$ stock solution was added into pollen germination medium to a final concentration of 10 μM.

Confocal Microscopy

For Confocal laser scanning microscopy, laser was focused on the median plane, where the apical PM localized GFP-RIC4ΔC was most clear. Imaging of GFP-RIC4ΔC was

performed using a Leica SP2 confocal microscope with 488 nm laser excitation and 500-570 nm emission for GFP. For time course analysis, images of pollen tube tips were collected using a 63× water immersion lens, zoomed with 4× with 512×512 frame and 400-Hz scanning speed at 10 seconds intervals.

Measurement of Relative ROP1 Activity

The relative ROP1 activity is defined as the ratio between the mean value of GFP-RIC4ΔC signal localized to the apical PM and that localized to the cytosol. The mean intensity of GFP-RIC4ΔC signals on the apical PM and in the cytosol was measured using MetaMorph 4.5 software (Universal Imaging, West Chester, PA) for each median scan of GFP-RIC4ΔC expressing pollen tubes. The mean intensity of cytosolic part was obtained from an area of 15 μm circumference in the middle of pollen tube, 2 μm away from the tip of pollen tubes.

Numerical Simulation of ODEs Model

The numerical simulation of the ODEs model was conducted using dde23 solver in Matlab 7.0 software.

References

Dawes, A.T., and Edelstein-Keshet, L. (2007). Phosphoinositides and Rho proteins spatially regulate actin polymerization to initiate and maintain directed movement in a one-dimensional model of a motile cell. Biophys J **92,** 744-768.

Feijo, J.A., Sainhas, J., Holdaway-Clarke, T., Cordeiro, M.S., Kunkel, J.G., and Hepler, P.K. (2001). Cellular oscillations and the regulation of growth: the pollen tube paradigm. Bioessays **23,** 86-94.

Forger, D.B., and Peskin, C.S. (2003). A detailed predictive model of the mammalian circadian clock. Proc Natl Acad Sci U S A **100,** 14806-14811.

Fu, Y., Wu, G., and Yang, Z. (2001). Rop GTPase-dependent dynamics of tip-localized F-actin controls tip growth in pollen tubes. J Cell Biol **152,** 1019-1032.

Geva-Zatorsky, N., Rosenfeld, N., Itzkovitz, S., Milo, R., Sigal, A., Dekel, E., Yarnitzky, T., Liron, Y., Polak, P., Lahav, G., and Alon, U. (2006). Oscillations and variability in the p53 system. Mol Syst Biol **2,** 2006 0033.

Giannone, G., Dubin-Thaler, B.J., Dobereiner, H.G., Kieffer, N., Bresnick, A.R., and Sheetz, M.P. (2004). Periodic lamellipodial contractions correlate with rearward actin waves. Cell **116,** 431-443.

Gibbon, B.C., Kovar, D.R., and Staiger, C.J. (1999). Latrunculin B has different effects on pollen germination and tube growth. Plant Cell **11,** 2349-2363.

Gu, Y., Fu, Y., Dowd, P., Li, S., Vernoud, V., Gilroy, S., and Yang, Z. (2005). A Rho family GTPase controls actin dynamics and tip growth via two counteracting downstream pathways in pollen tubes. J Cell Biol **169,** 127-138.

Heintzen, C., and Liu, Y. (2007). The Neurospora crassa circadian clock. Adv Genet **58,** 25-66.

Holdaway-Clarke, T.L., Feijo, J.A., Hackett, G.R., Kunkel, J.G., and Hepler, P.K. (1997). Pollen Tube Growth and the Intracellular Cytosolic Calcium Gradient Oscillate in Phase while Extracellular Calcium Influx Is Delayed. Plant Cell **9,** 1999-2010.

Hwang, J.U., Gu, Y., Lee, Y.J., and Yang, Z. (2005). Oscillatory ROP GTPase activation leads the oscillatory polarized growth of pollen tubes. Mol Biol Cell **16,** 5385-5399.

Hwang, J.U., Vernoud, V., Szumlanski, A., Nielsen, E., and Yang, Z. (2008). A Tip-Localized RhoGAP Controls Cell Polarity by Globally Inhibiting Rho GTPase at the Cell Apex. Curr Biol **18,** 1907-1916.

Kost, B., Lemichez, E., Spielhofer, P., Hong, Y., Tolias, K., Carpenter, C., and Chua, N.H. (1999). Rac homologues and compartmentalized phosphatidylinositol 4, 5-bisphosphate act in a common pathway to regulate polar pollen tube growth. J Cell Biol **145,** 317-330.

Kovar, D.R., Drobak, B.K., and Staiger, C.J. (2000). Maize profilin isoforms are functionally distinct. Plant Cell **12,** 583-598.

Lee, Y.J., Szumlanski, A., Nielsen, E., and Yang, Z. (2008). Rho-GTPase-dependent filamentous actin dynamics coordinate vesicle targeting and exocytosis during tip growth. J Cell Biol **181,** 1155-1168.

Li, H., Lin, Y., Heath, R.M., Zhu, M.X., and Yang, Z. (1999). Control of pollen tube tip growth by a Rop GTPase-dependent pathway that leads to tip-localized calcium influx. Plant Cell **11,** 1731-1742.

Lin, Y., Wang, Y., Zhu, J.K., and Yang, Z. (1996). Localization of a Rho GTPase Implies a Role in Tip Growth and Movement of the Generative Cell in Pollen Tubes. Plant Cell **8,** 293-303.

Maeda, M., Lu, S., Shaulsky, G., Miyazaki, Y., Kuwayama, H., Tanaka, Y., Kuspa, A., and Loomis, W.F. (2004). Periodic signaling controlled by an oscillatory circuit that includes protein kinases ERK2 and PKA. Science **304,** 875-878.

Malho, R., Read, N.D., Trewavas, A.J., and Pais, M.S. (1995). Calcium Channel Activity during Pollen Tube Growth and Reorientation. Plant Cell **7,** 1173-1184.

Messerli, M.A., Creton, R., Jaffe, L.F., and Robinson, K.R. (2000). Periodic increases in elongation rate precede increases in cytosolic Ca2+ during pollen tube growth. Dev Biol **222,** 84-98.

Myers, C., Romanowsky, S.M., Barron, Y.D., Garg, S., Azuse, C.L., Curran, A., Davis, R.M., Hatton, J., Harmon, A.C., and Harper, J.F. (2009). Calcium-dependent protein kinases regulate polarized tip growth in pollen tubes. Plant J. **59**, 528-539.

Patnaik, P.R. (2003). Oscillatory metabolism of Saccharomyces cerevisiae: an overview of mechanisms and models. Biotechnol Adv **21,** 183-192.

Pierson, E.S., Miller, D.D., Callaham, D.A., van Aken, J., Hackett, G., and Hepler, P.K. (1996). Tip-localized calcium entry fluctuates during pollen tube growth. Dev Biol **174,** 160-173.

Roy, S.J., Holdaway-Clarke, T.L., Hackett, G.R., Kunkel, J.G., Lord, E.M., and Hepler, P.K. (1999). Uncoupling secretion and tip growth in lily pollen tubes: evidence for the role of calcium in exocytosis. Plant J **19,** 379-386.

Schiott, M., Romanowsky, S.M., Baekgaard, L., Jakobsen, M.K., Palmgren, M.G., and Harper, J.F. (2004). A plant plasma membrane Ca^{2+} pump is required for normal pollen tube growth and fertilization. Proc Natl Acad Sci U S A **101,** 9502-9507.

Sneyd, J., Tsaneva-Atanasova, K., Yule, D.I., Thompson, J.L., and Shuttleworth, T.J. (2004). Control of calcium oscillations by membrane fluxes. Proc Natl Acad Sci U S A **101,** 1392-1396.

Stites, E.C., Trampont, P.C., Ma, Z., and Ravichandran, K.S. (2007). Network analysis of oncogenic Ras activation in cancer. Science **318,** 463-467.

Vidali, L., McKenna, S.T., and Hepler, P.K. (2001). Actin polymerization is essential for pollen tube growth. Mol Biol Cell **12,** 2534-2545.

Wang, H.J., Wan, A.R., and Jauh, G.Y. (2008). An actin-binding protein, LlLIM1, mediates calcium and hydrogen regulation of actin dynamics in pollen tubes. Plant Physiol **147,** 1619-1636.

Wolgemuth, C.W. (2005). Lamellipodial contractions during crawling and spreading. Biophys J **89,** 1643-1649.

Wu, G., Gu, Y., Li, S., and Yang, Z. (2001). A genome-wide analysis of Arabidopsis Rop-interactive CRIB motif-containing proteins that act as Rop GTPase targets. Plant Cell **13,** 2841-2856.

Yokota, E., Muto, S., and Shimmen, T. (2000). Calcium-calmodulin suppresses the filamentous actin-binding activity of a 135-kilodalton actin-bundling protein isolated from lily pollen tubes. Plant Physiol **123,** 645-654.

Yoon, G.M., Dowd, P.E., Gilroy, S., and McCubbin, A.G. (2006). Calcium-dependent protein kinase isoforms in Petunia have distinct functions in pollen tube growth, including regulating polarity. Plant Cell **18,** 867-878.

Parameter	Biological Meaning (Unit)	Value
β_x	Parameter for ROP1 activation rate (s^{-1})	0.1
β_y	Parameter for calcium accumulation rate (s^{-1})	0.25
α_x	ROP1 inactivation rate (s^{-1})	0.25
α_y	Calcium depletion rate (s^{-1})	0.05
x_0	Initial value for active ROP1 concentration (μM)	0.1
y_0	Initial value for calcium concentration (μM)	0.8
R_0	Parameter for saturated ROP1 concentration in cell (μM)	5
C_0	Parameter for high calcium threshold to decrease F-actin (μM)	3
τ	Time delay between ROP1 and calcium accumulation (s)	8
k	Parameter for ROP1 and calcium dependent F-actin level (1)	5
b	Parameter for calcium accumulation (μM)	0.05

Table 1.1. Parameter setting for standard oscillation of ROP activity in Model I

Parameter	Biological Meaning (Unit)	Value
β_x	Parameter for ROP1 activation rate (s^{-1})	0.1
β_y	Parameter for calcium accumulation rate (s^{-1})	0.25
α_x	ROP1 inactivation rate (s^{-1})	0.8
α_y	Calcium depletion rate (s^{-1})	0.05
x_0	Initial value for active ROP1 concentration (μM)	0.1
y_0	Initial value for calcium concentration (μM)	0.8
R_0	Parameter for saturated ROP1 concentration in cell (μM)	5
k	Parameter for ROP1 dependent F-actin level (1)	2.2
b	Parameter for basal calcium increase (μM)	0.05
τ	Time delay between ROP1 and calcium accumulation (s)	8
M	Parameter for piecewise activation of GAP by calcium (1)	10
y_{min}	Parameter for piecewise activation of GAP by calcium (μM)	0.5
y_{max}	Parameter for piecewise activation of GAP by calcium (μM)	5

Table 1.2. Parameter setting for standard oscillation of ROP activity in Model II

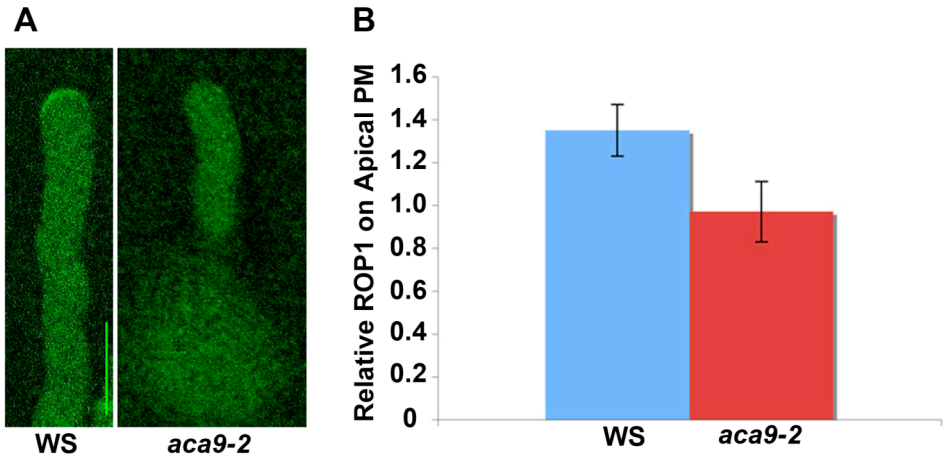

Figure 1.1. Localization of ROP1 protein in *aca9-2* mutant pollen tubes.
(A). Anti-Rop1 staining of a control WS wild type pollen tube and an *aca9-2* pollen tube. Bar=10 μm.
(B). Quantitative analysis of the plasma membrane-localized ROP protein in WS and *aca9-2* pollen tubes. Error bars indicate S. D., n=15, student's t-test $p<0.05$. The relative ROP1 amount on apical PM is defined as the ratio between the mean value of FITC signal localized to the apical PM and that localized to the cytosol. The mean intensity of FITC signals on the apical PM and in the cytosol was measured using MetaMorph 4.5 software (Universal Imaging, West Chester, PA) for each median scan of immunostained pollen tubes. The mean intensity of cytosolic part was obtained from an area of 15 μm circumference in the middle of pollen tube, 2 μm away from the tip of pollen tubes.

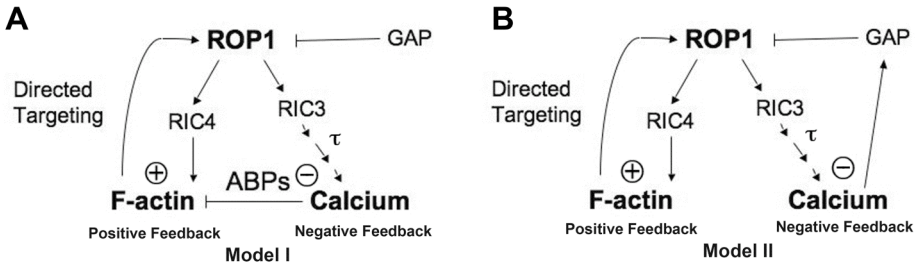

Figure 1.2. The structure of ROP1 oscillation models.
The oscillation models consist of two major feedback loops: (1) The F-actin mediated positive feedback loop (indicated with "+") and (2) the calcium-dependent negative feedback loop (indicated with "-"). Comparing to an increase in ROP1 activation rate, an increase in the rate of calcium accumulation in the tip is delayed, which is described as a time delay τ in oscillation models. Calcium is assumed to participate in the negative feedback regulation of ROP1 activity by either of the following mechanisms.
(A). Model I: Calcium signaling inhibits ROP1 activation by promoting F-actin depolymerization through the activation of actin binding proteins (ABPs).
(B). Model II: Calcium signaling promotes ROP1 deactivation by activating ROP1 negative regulators such as RhoGAP.

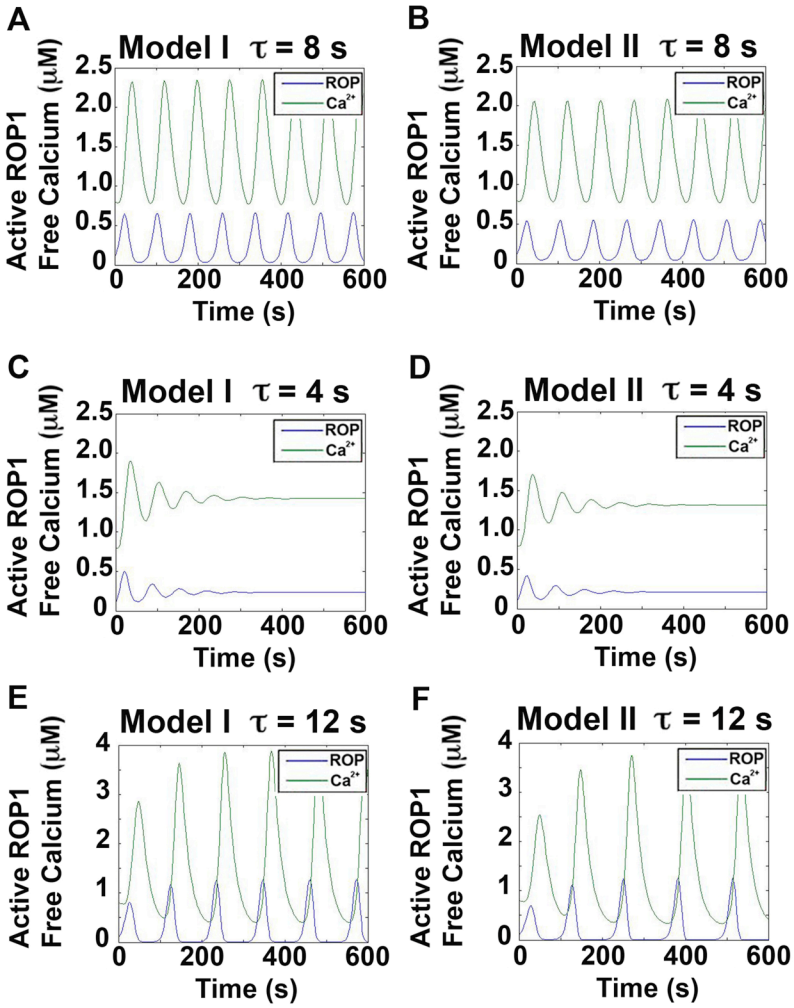

Figure 1.3. Simulating the effect of time delay on the oscillation of the apical ROP1 activity.
Simulation the effects of various time delays based on both Model I and II.
(A)-(B). Given a proper time delay (τ = 8 seconds), both Model I (A) and Model II (B) can reproduce the observed oscillation pattern for both active ROP1 and calcium. The simulation generates oscillation periods of approximately 80 seconds and amplitude of 0-0.6 μM and 0.8-2.2 μM for active ROP1 and calcium, respectively. Calcium oscillation is behind ROP1 activity oscillation by ≈120°. Parameter settings were shown in Table 1 and 2.
(C)-(D). Given short time delays (τ = 4 seconds), ROP1 activity and calcium oscillations are unstable. (C) Model I. (D) Model II.
(E)-(F). Given long time delays, the oscillation period would be greatly increased. The period is increased to ≈120 seconds when τ = 12 seconds. (E) Model I. (F) Model II.

Figure 1.4. Simulation and experimental validation of ROP1 activity oscillation in pollen tubes overexpressing RhoGAP.

(A)-(B). Simulation of ROP1 activity oscillation in control pollen tubes using Model I (A) and Model II (B).

(C). Experimental measurement of ROP1 activity oscillation in control pollen tubes. The relative ROP1 activity was measured as described in Figure 3. Shown is a typical oscillating pollen tube with an amplititude of 0.5 (from 0.8 to1.3) and a period of approximately 80 seconds. Six out of 10 pollen tubes showed similar oscillation pattern.

(D)-(E). Simulation from Model I (D) and Model II (E) predicted that the apical ROP1 activity would be reduced to a low level and be non-oscillating in pollen tubes overexpressing a high level of RhoGAP. For Model I, α_x=0.35 s^{-1}. For Model II, α_x=2 s^{-1}.

(F). Time-course analysis of ROP1 activity oscillation in a pollen tube with high level of RhoGAP overexpression. 0.1 μg RopGAP1 plasmid was used for transformaiton and the relative ROP1 activity was determined as described in Figure 3. Relative ROP1 activity was reduced to a basal level (<0.8) and did not oscillate. All 30 pollen tubes examined showed similar pattern.

(G)-(H). Simulation from Model I (G) predicted that a low level of RhoGAP overexpression would suppress the oscillation of the apical ROP1 activity and make it very unstable. Simulation from Model II predicted that ROP1 activity would still oscillate with much smaller amplititude when a very low level of RhoGAP is overproduced. For Model I, α_x=0.275 s^{-1}. For Model II, α_x=1.2 s^{-1}.

(I). Time-course analysis of ROP1 activity oscillation in a pollen tube with a low level of RopGAP1 overexpression. 0.02 μg RopGAP1 plasmid was used for transformaiton and the relative ROP1 activity was determined as described in Figure 3. Relative ROP1 activity was reduced to a low level and exibited fluctuations (1.1-1.2). Three out of 20 pollen tubes examined showed similar pattern. Due to the low level of ROP1 activity, it is difficult to determine whether the fluctuating ROP1 activity reflects unstable oscillation or measurement variation.

(J). Representative snapshot images of GFP-RIC4ΔC localization in control tubes and pollen tubes overexpressing low and high level of RopGAP1. Each figure is the representative from 20 pollen tubes. Bar=10 μm.

(K). Quantitative analysis of GFP-RIC4ΔC distribution to the apical PM. Shown is mean relative ROP1 activity in control tubes and tubes with low and high levels of RhoGAP overexpression in pollen tubes (Student's t-test $p<0.05$, n=20, Error bars indicate S. D.).

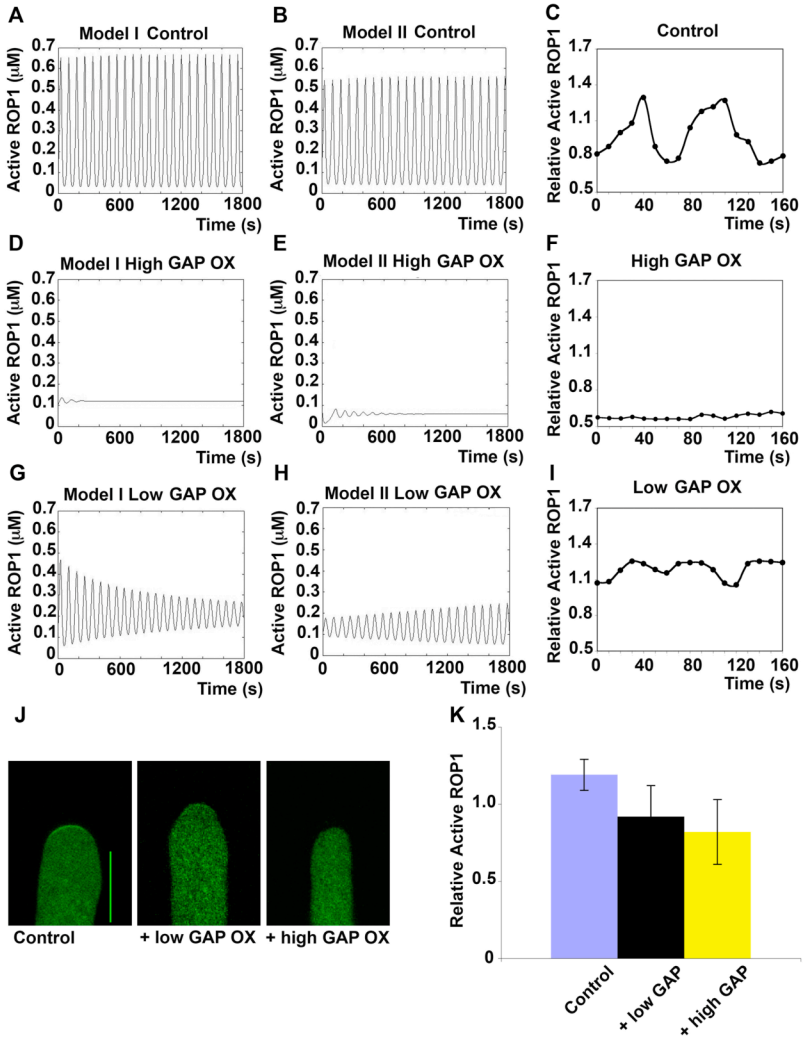
A
Model I Control
Active ROP1 (μM)
Time (s)
B
Model II Control
Active ROP1 (μM)
Time (s)
C
Control
Relative Active ROP1
Time (s)
D
Model I High GAP OX
Active ROP1 (μM)
Time (s)
E
Model II High GAP OX
Active ROP1 (μM)
Time (s)
F
High GAP OX
Relative Active ROP1
Time (s)
G
Model I Low GAP OX
Active ROP1 (μM)
Time (s)
H
Model II Low GAP OX
Active ROP1 (μM)
Time (s)
I
Low GAP OX
Relative Active ROP1
Time (s)
J
Control
+ low GAP OX
+ high GAP OX
K
Relative Active ROP1
Control
+ low GAP
+ high GAP

Figure 1.5. Simulation and experimental validation of F-actin's effect on ROP1 activity oscillation.
(A)-(B). Simulation of ROP1 activity oscillation in control pollen tubes using Model I (A) and Model II (B).
(C). Experimental measurement of ROP1 activity oscillation in control pollen tubes. The distribution of GFP-RIC4ΔC to the apical PM indicates the apical ROP1 activity (Hwang et al., 2005). The relative ROP1 activity was determined as the ratio between the mean PM GFP intensity and the mean cytosolic GFP intensity (Hwang et al., 2005). Shown is a typical oscillating pollen tube with an amplititude of 0.5 (from 0.9 to1.4) and a period of approximately 80 seconds. Six out of 10 pollen tubes exhibited this oscillation pattern.
(D)-(E). Simulations predicted that the apical ROP1 activity would be kept at very low level and would not oscillate in pollen tubes treated with 5 nM Latrunculin B (Lat B). For Model I, k=3. For Model II, k=1.3.
(F). Experimental validation of the predictions in D-E. In tubes treated with 5 nM Lat B, GFP-RIC4ΔC was depleted from the apical PM, and the relative ROP1 activity was consistently below 0.8. Shown is a representative of 30 tubes examined, which all showed low and non-oscillating ROP1 activity.
(G)-(H). Simulations predicted that the relative ROP1 activity would stay high and lose oscillation in pollen tubes treated with 100 nM Jasplakinolide (JAS). Under this condition, F-actin is always kept at high level. For Model I, g(x,y)=0.25. For Model II, g(x)=0.44.
(I). Experiemental validation of the predictions in G-H. The relative ROP1 activity stayed constantly above 1.3. Shown is a representative of 20 tubes examined, which all showed high and non-oscillating ROP1 activity.
(J). Representative snapshot images of GFP- RIC4ΔC localization in control, Lat B and JAS treated pollen tubes. Bar=10 μm.
(K). Quantitative analysis of the relative ROP1 activity in control, Lat B and JAS treated pollen tubes. Shown are mean relative ROP1 activity measured from snapshot images (Student's t test $p<0.05$, n=20, Error bars indicate S. D.).

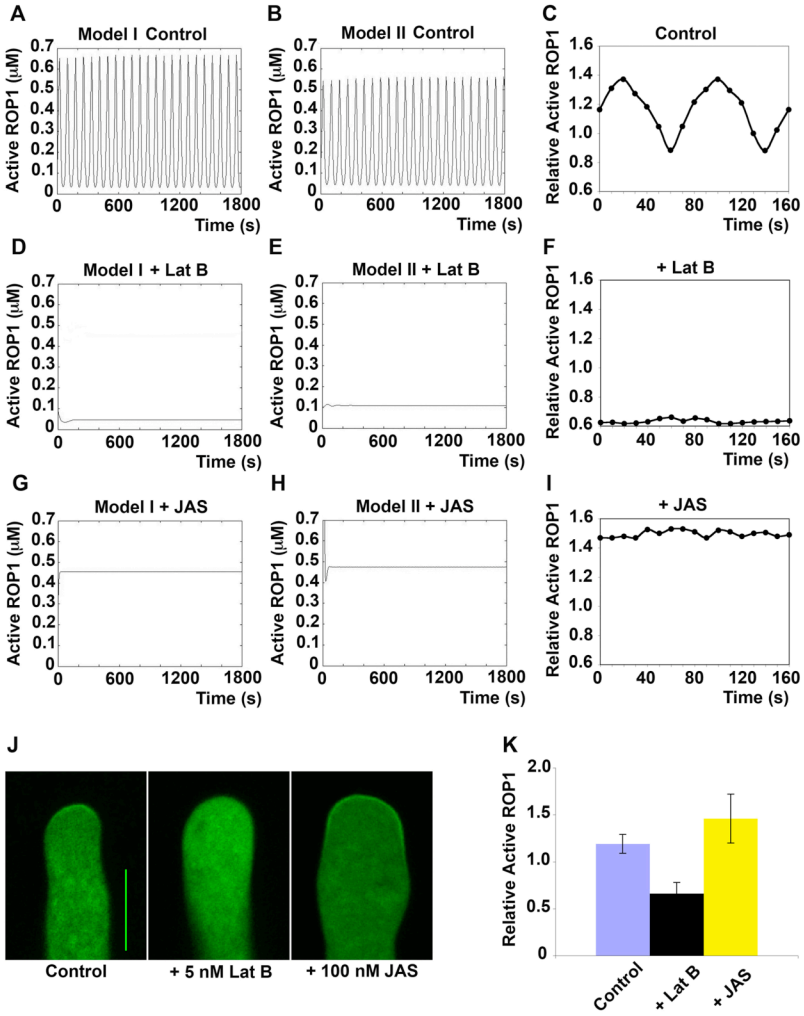
A
Model I Control
Active ROP1 (μM)
Time (s)
B
Model II Control
Active ROP1 (μM)
Time (s)
C
Control
Relative Active ROP1
Time (s)
D
Model I + Lat B
Active ROP1 (μM)
Time (s)
E
Model II + Lat B
Active ROP1 (μM)
Time (s)
F
+ Lat B
Relative Active ROP1
Time (s)
G
Model I + JAS
Active ROP1 (μM)
Time (s)
H
Model II + JAS
Active ROP1 (μM)
Time (s)
I
+ JAS
Relative Active ROP1
Time (s)
J
Control
+ 5 nM Lat B
+ 100 nM JAS
K
Relative Active ROP1
Control
+ Lat B
+ JAS

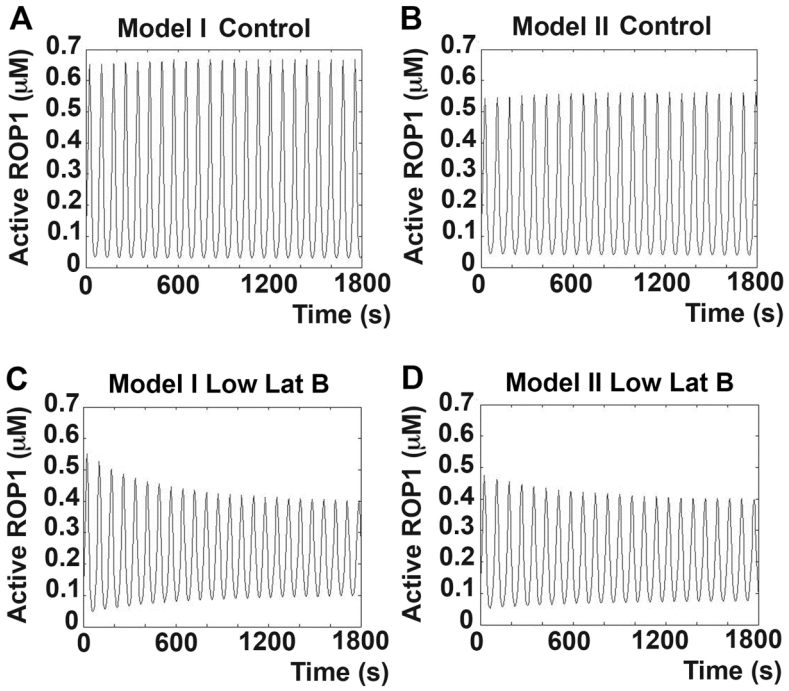

Figure 1.6. Model simulation of ROP1 activity oscillation in pollen tubes, in which F-actin level is reduced by Latruculin B treatment.

(A)-(B). Simulation of ROP1 activity oscillation in control pollen tubes using Model I (A) and Model II (B). (C)-(D). Simulations based on Model I (Figure C) and Model II (Figure D) predicted that the period of ROP1 activity oscillation would be unaffected but its amplitude would be reduced in pollen tube treated with low level of Lat B (0.5 nM). This prediction is consistent with the exprimental data that we reported previously (1). For Model I, k=4.8. For Model II, k=2.1.

Figure 1.7. Simulation and experimental validation of calcium's effect on ROP1 activity oscillation.
(A)-(B). Simulation of ROP1 activity oscillation in control pollen tubes using Model I (A) and Model II (B).
(C). Experimental measurement of ROP1 activity oscillation in control pollen tubes. The relative ROP1 activity was measured as described in Figure 3. Shown is a typical oscillating pollen tube with an amplititude of 0.5 (from 0.9 to1.4) and a period of approximately 80 seconds.
(D)-(E). Simulation from both Models I and II predicted that the apical ROP1 activity would stay low and lose oscillation in pollen tubes, in which the calcium accumulation rate is greatly increased. For both models, β_y=0.75 s^{-1}.
(F). Time-course analysis of the relative ROP1 activity in a pollen tube expressing a high level of RIC3 (i.e., 0.1 μg RIC3 plasmid DNA was used for transformation). Shown is a representative of 30 tubes examined, which all showed low and non-oscillating relative ROP1 activity (<0.8).
(G). Time-course analysis of the relative ROP1 activity in a pollen tube treated with 1 μM A23187 ionophore (high A23187). Shown is a representative of 20 tubes examined, which all showed low and non-oscillating relative ROP1 activity (<0.8).
(H)-(I). Simulation from both Models I and II predicted that the apical ROP1 activity could maintain oscillation but with much smaller amplitudes in pollen tubes with moderately increased calcium accumulation rate. For Model I, β_y=0.5 s^{-1}. For Model II, β_y=0.4 s^{-1}.
(J). Time-course analysis of the relative ROP1 activity in a pollen tube expressing a low level of RIC3 (i.e., 0.02 μg RIC3 was used for transformation). Relative ROP1 activity oscillates with similar periods but smaller amplitudes (0.3, from 0.8 to1.1) compared to control tubes. Shown is a representative of 5 tubes examined exhibiting a similar pattern.
(K). Time-course analysis of the relative ROP1 activity in a pollen tube treated with 10 nM A23187 ionophore (low A23187). Relative ROP1 activity oscillated with similar period but smaller amplitude (0.2, from 0.9 to 1.1). Shown is a representative of 3 tubes examined exhibiting a similar pattern.
(L). Representative snapshot images of GFP-RIC4ΔC localization in various treated tubes. Bar=10 μm.
(M). Quantitative analysis of the relative ROP1 activity in various treated pollen tubes. Shown are mean relative ROP1 activity measured from snapshot images (Student's t test $p<0.05$. n=20, Error bars indicate S. D.).

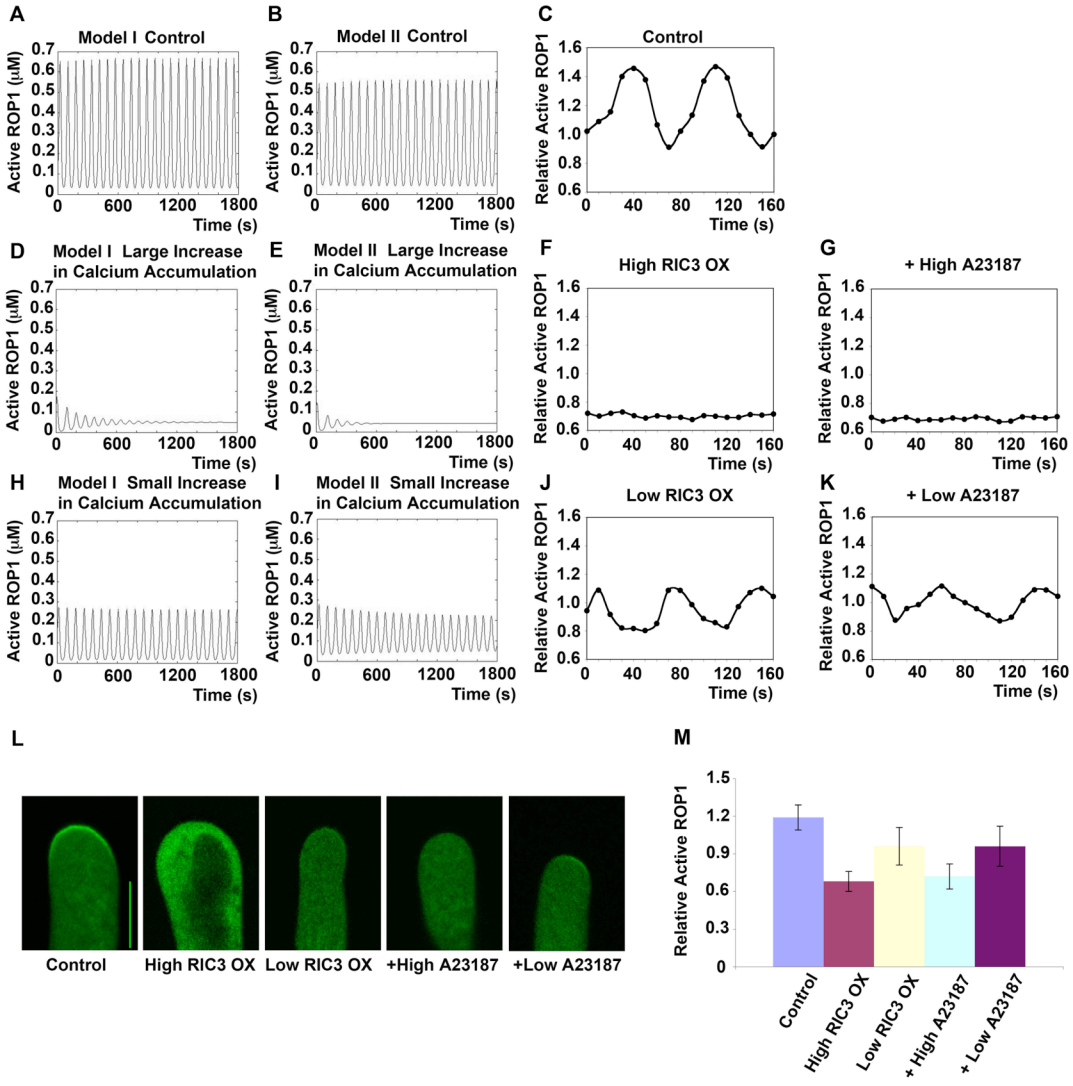
A
Model I Control
Active ROP1 (μM)
Time (s)
B
Model II Control
C
Control
Relative Active ROP1
D
Model I Large Increase in Calcium Accumulation
E
Model II Large Increase in Calcium Accumulation
F
High RIC3 OX
G
+ High A23187
H
Model I Small Increase in Calcium Accumulation
I
Model II Small Increase in Calcium Accumulation
J
Low RIC3 OX
K
+ Low A23187
L
Control
High RIC3 OX
Low RIC3 OX
+High A23187
+Low A23187
M
Relative Active ROP1
Control
High RIC3 OX
Low RIC3 OX
+ High A23187
+ Low A23187

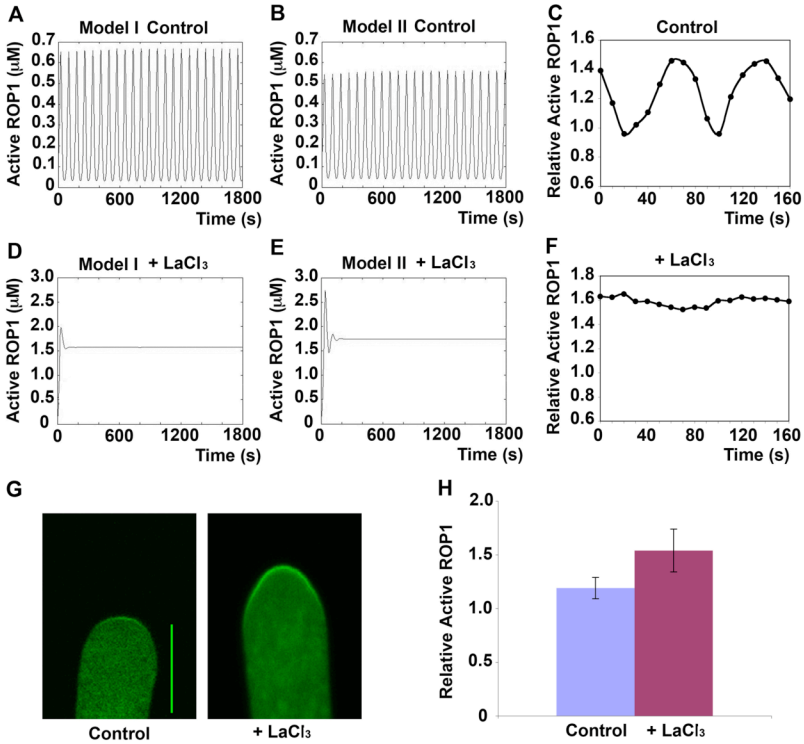

Figure 1.8. Model simulation and experimental validation of ROP1 activity oscillation in pollen tubes with reduction in calcium accumulation.

(A)-(B). Simulation of ROP1 activity oscillation in control pollen tubes using Model I (A) and Model II (B).

(C). Experimental measurement of ROP1 activity oscillation in control pollen tubes. The relative ROP1 activity was measured as described in Figure 3. Shown is a typical oscillating pollen tube with an amplititude of 0.5 (from 0.95 to1.45) and a period of approximately 80 seconds. Six out of 10 pollen tubes showed similar oscillation pattern.

(D)-(E). Simulation of ROP1 activity oscillation in pollen tubes defective in calcium accumulation. For Model I, β_y=0.025 s^{-1}. For Model II, β_y=0.025 s^{-1}.

(F). Time-course analysis of the relative ROP1 activity in a pollen tube treated with 10 μM $LaCl_3$. Relative ROP1 activity was constantly high (>1.5) and lacked oscillation. 20 pollen tubes checked showed similar pattern.

(G). GFP-RIC4ΔC localization in control and $LaCl_3$ treated pollen tubes. Bar=10 μm.

(H). Quantitative analysis of the relative ROP1 activity in control and $LaCl_3$ treated pollen tubes (Student's t-test $p<0.05$, n=20, Error bars indicate S. D.).

Chapter 2

A tip growth model of pollen tube

Abstract

Tip growth is a conserved theme throughout evolution of eukaryotes. We used combined modeling and experimental approaches to reveal the cell signaling and biomechanical principles driving pollen tube tip growth. We revealed that F-actin dependent exocytosis is the key process linking ROP1 GTPase polarity establishment, cell wall pectin distribution and polarized cell growth. Through exocytosis mediated positive feedback loop, RopGAP mediated global inhibition and lateral diffusion of ROP1 GTPase on plasma membrane, active ROP1 GTPases polarity can be established and maintained. Once maintained, active ROP1 controls cell wall mechanics via control of pectin exocytosis and thus determines the shape of pollen tubes. Our work revealed the interplay among ROP1 GTPase signaling, cell mechanics and cell morphogenesis via exocytosis. This mechanism might be applicable to other tip growth cell systems such as root hair and fungi hyphae.

Introduction

Tip growth, a highly polarized growth due to localized elongation of certain portion of cell surfaces, is highly conserved throughout evolution. Many cell types in various biological systems including pollen tube, root hair (plant) (Cheung and Wu, 2008; Lee and Yang, 2008), neuron axon (animal) (Lowery and Van Vactor, 2009) and fungal hyphae (fungi) (Fischer et al., 2008) demonstrate robust tip growth. Tip growth of pollen tubes, fundamental to the sexual production of higher plants, provides a good experimental system for study of the tip growth mechanism. Many previous modeling attempts had been made to simulate the tip growth of pollen tube (Dumais et al., 2006; Kroeger et al., 2008; Campas and Mahadevan, 2009; Fayant et al., 2010). Although several different simulation methods (including finite differences, finite element analysis) were used to describe the cell wall mechanics and shape formation of pollen tubes, previous models focused more on mechanical aspect, and did not reveal the underlying linkage between cell signaling and cell morphogenesis.

From axon initiation to hyphal extension, from root hair elongation to pollen tube growth, the polarized Rho-family GTPases signaling is the common theme for subsequent polarized growth (Fischer et al., 2008; Lee and Yang, 2008; Lowery and Van Vactor, 2009). Here, we have chosen the pollen tube cell as the model system to build a unifying theory for tip growth inter-connecting both cell signaling and biomechanics of the cell. Different from other biomechanical models for tip growth, our model focused on the underlying mechanism controlling tip growth, including two interlinked aspects: cellular

polarization of ROP1 GTPase activity and subsequent shape change controlled by active ROP1.

Results

Model for ROP1-driven tip growth

To build the model of ROP1 dependent growth, we separated the model to two sub-models: cell signaling model and biomechanics model (Figure 2.1). First, we established a cell-signaling model of ROP1 polarity formation and maintenance. We assumed that three processes together lead to ROP1 polarity formation: (1). A positive feedback loop mediated by exocytosis and ROP1 activators such as RopGEFs; (2). A global negative regulation mediated by cytosolic ROP1 inhibitors such as RopGAPs; (3). Slow lateral diffusion of ROP1 protein on apical plasma membrane. The rationale for these assumptions is as follow: (1). For exocytosis mediated positive feedback regulation, it has been shown that exocytosis in pollen tube tip region is essential for pollen tube growth and renewal of PM proteins (Lee et al., 2008; McKenna et al., 2009). Given that ROP1 and it activator RopGEFs are PM associated proteins (Kost et al., 1999; Li et al., 1999; Berken et al., 2005; Gu et al., 2005), we assumed that exocytosis is important for activation of ROP1 at apex of pollen tubes. Also, it has been shown recently that active ROP1 locally directed exocytosis at pollen tube tip region via control of F-actin dynamics (Gu et al., 2005; Lee et al., 2008), thus forming a positive feedback loop. (2). We included RopGAP mediated negative regulation of ROP1 activity because loss of function mutant of a cytosol RopGAP REN1 showed depolarized ROP1 distribution and

pollen tube growth (Hwang et al., 2008). (3). The diffusion of ROP1 GTPase on PM is assumed to be slow due to association with plasma membrane.

Next, we linked the local ROP1 activity with cell wall extensibility via exocytosis. Turgor pressure within the cell wall generated the tensile stress in the cell wall. In growing pollen tubes, turgor pressure is nearly constant (Benkert et al., 1997; Dumais et al., 2006; Winship et al., 2010). Previous modeling work revealed that under constant turgor pressure, the high extensibility at certain region of cell wall would lead to localized irreversible extension of cell wall under stress, giving rise to a cylinder like structure, such as pollen tube and root hair (Dumais et al., 2006). We assumed that exocytosis, which is guided by ROP1 activity, targets soft cell wall material pectin ester to apical region of pollen tube, thus allows localized extension of pollen tubes.

Estimation of Diffusion Constant of ROP1 on PM of pollen tubes

Before simulating active ROP1 distribution in pollen tubes, we first set out to measure diffusion constant of ROP1 on PM of pollen tubes. We used FRAP analysis on GFP-ROP1 OX pollen tubes of Arabidopsis to measure diffusion constant. First, we treated GFP-ROP1 OX pollen tubes with 20 nM Lat B for 10-15 minutes to suppress F-actin dependent exocytosis. Next, we photobleached GFP-ROP1 signal on a small region at apical PM to track the ROP1 protein movement along PM due to lateral diffusion. Finally, by fitting the distribution curves of GFP-ROP1 FRAP time course, we estimated the diffusion constant of GFP-ROP1 on apical PM of pollen tubes (Figure 2.2). From our

measurement, the diffusion constant of GFP-ROP1 on PM is 0.2±0.05 $\mu m^2/s$ (n=5, Ave±SD). The diffusion constant of GFP-ROP1 much larger than diffusion constant of PM proteins measured from yeast cells (Marco et al., 2007). One explanation is that pollen tube is fast growing cell compared to yeast cell, thus proteins on pollen tube PM may move at faster rate than proteins on yeast PM.

Simulation and experimental validation of ROP1 activity and pollen tube shape

We next simulated pollen tube growth in control pollen tubes using our mathematical model (parameters setting is listed in Table 2.1). Model simulation predicted that in WT pollen tubes, active ROP1 domain is confined to apical PM (within first 10 μm from apex) with the highest active ROP1 value at apex and the shape of pollen tube is a cylinder like structure with diameter of about 6 μm (Figure 2.3A, C). To visualize the active ROP1 in Arabidopsis pollen tubes, we generated a marker line expressing GFP-RIC1 under pollen specific Lat52 promoter. Our previous work has shown that RIC1 binds specifically with active form of ROP1 (Wu et al., 2001). In Arabidopsis pollen tubes, the GFP tagged RIC1 signal showed polarized active ROP1 localization at apical PM. Active ROP1 cap is within first 10 μm from the tip and the peak of intensity is at the apex of pollen tubes (Figure 2.3B, C). The experimentally measured GFP-RIC1 intensity distribution profile and pollen tube width can match surprisingly well with our model predictions (Figure 2.3A, C, I), suggesting our model indeed captured the most important features for pollen tube morphogenesis.

To further test our model for ROP1 dependent pollen tube growth, we simulated the pollen tube growth in a RopGAP null mutant *ren1-1*, which is defective in global inhibition of ROP1 activity (Hwang et al., 2008). We predicted that if global inhibition for ROP1 activity were defective, active ROP1 cap would be increased, thus leading to depolarized growth (Figure 2.3D, F). Active ROP1 cap is predicted to be within first 25 μm from the tip and the peak of intensity is at the apex of pollen tubes. The width of *ren1-1* pollen tube is predicted to be 13 μm, much larger than WT control. To validate these predictions from model, we generated *Lat52:GFP-RIC1 OX* line in *ren1-1* mutant background. In *ren1-1* mutant pollen tubes, the GFP-RIC1 showed depolarized localization and the pollen tube was much wider (Figure 2.3E). Both the active ROP1 distribution profile and pollen tube width exactly matched with our model predictions (Figure 2.3E, F, I).

Using our mathematical model, finally we attempted to validate the roles of F-actin dependent exocytosis in pollen tube morphogensis. In our model, exocytosis was assumed to be a versatile process with two different functions: (1). Positive feedback of ROP1 activity; (2). Targeting of new cell wall material to tip cell wall. From math model, we predicted when exocytosis activity was severely inhibited, the active ROP1 cap would disappear and pollen tube shape would not change. To further validate the model predictions, we experimentally tested this prediction by treating pollen tubes expressing GFP-RIC1 with F-actin polymerization inhibitor drug Latrunculin B. We found that 20 nM Lat B treatment abolished GFP-RIC1 signal at apical PM of Arabidopsis pollen tubes.

In Lat B treated pollen tubes, tube elongation was also stopped and the shape of pollen tubes remained unchanged as compared to WT pollen tubes. Again, these results fit well with model predictions for inhibition of exocytosis (Figure 2.3G, H, I).

ROP1 activity determines cell wall pectin distribution

One key assumption in our model is that active ROP1 locally controlled cell wall extensibility. We next examined the possible mechanism of how ROP1 activity determines cell wall extensibility. The apical region of pollen tube cell wall mainly consists of pectin, while the cellulose is the major component in distal cell wall of pollen tube (Parre and Geitmann, 2005). As a result, the extensibility of cell wall at growing domain is highly dependent on the property of pectin. A recent report has shown that removal of pectin by pectinase treatment will cause depolarized growth in pollen tubes (Fayant et al., 2010). Pectin was first synthesized at Golgi bodies as the less cross-linking (softer) methyl-esterized form (Bosch and Hepler, 2005; McKenna et al., 2009). Once pectin esters reached cell wall via exocytosis, they will be progressively de-esterified by PME and form highly cross-linked (harder) pectic acid wall structure with the action of calcium. Newly synthesized soft pectin esters were continuously secreted and inserted into existing apical wall structure via F-actin dependent exocytosis, reducing the strength of bonds between pectin molecules (Bosch and Hepler, 2005; McKenna et al., 2009). We hypothesized that active ROP1 control cell wall extensibility mainly through regulation of soft pectin exocytosis. To test this hypothesis, we observed pectin distributions in different pollen tubes. In WT control Arabidopsis pollen tubes, the JIM7 stained methyl-

esterified pectin is only concentrated at the apex cell wall, while the JIM5 stained de-esterified pectin accumulated from shoulder to distal cell wall (Figure 2.4A, D, G, H). In *ren1-1* mutant pollen tubes, we found that JIM7 stained soft pectin ester show much broader distribution and accordingly, JIM5 stained hardened pectin is depleted from a larger region of pollen tube apex (Figure 2.4B, E, G, H). On the other hand, in WT pollen tubes treated with Lat B, the JIM7 stained methyl-esterified pectin is decreased at the apex cell wall, while the JIM5 stained de-esterified pectin accumulated all along the pollen tube cell wall, from apex to distal region (Figure 2.4C, F, G, H). Taking the above data together, the distribution of pectin along pollen tubes cell wall is consistent with the assumption that ROP1 activity locally determines the soft pectin distribution via control of F-actin dependent exocytosis (Figure 2.4G, H).

Discussion

In summary, we successfully incorporated intracellular signaling event (ROP1 signaling in pollen tubes) with cell surface property (Cell wall pectins distribution) and cell growth (tip growth of pollen tubes) into one mathematical model. Through our combined modeling and experimental approaches, we not only simulated WT pollen tube ROP1 polarity establishment and pollen tube morphogenesis, but also simulated and experimentally validated the effect of genetic (*ren1-1*) and chemical (Lat B treatment) perturbations to ROP1 polarity control and cell morphogenesis. Although highly simplified, our model still captured the most important features for mechanism underlying tip growth of pollen tube: (1) F-actin dependent exocytosis mediates positive

feedback leading to ROP1 signaling polarity control and (2) Active ROP1 guided localized exocytosis of soft pectin molecules leads to cell wall extensibility polarity and morphogenesis of pollen tubes. Considering the conserved role of Rho GTPases signaling in control of tip growth phenotype, our model could shed light to future modeling work on other biological system such as root hair growth and hyphae extension.

Materials and methods

Mathematical model of pollen tube growth

We first described the active ROP1 polarity establishment process using a partial differential equation (1):

$$\frac{\partial R}{\partial t} = k_{pf}\left(R/R_0\right)^n\left(R_{\text{total}} - \int R\right)\left(\frac{R_{\max} - R}{R_{\max}}\right) - k_{gi}R + D\nabla^2 R \quad \ldots\ldots\ldots\ldots(1)$$

Next, we assumed the relation between ROP1 activity and cell wall extensibility follows equation (2):

$$\Phi = \Phi_0\left(\frac{R}{R_{tip}}\right)^m \ldots\ldots\ldots\ldots\ldots\ldots\ldots\ldots\ldots\ldots\ldots\ldots\ldots\ldots\ldots\ldots(2)$$

We then coupled equation (1) and (2) with a previous cell mechanical model to fully describe the pollen tube growth.

Equilibrium equations are listed as follows:

$$\sigma_s = \frac{P}{2\delta\kappa_\theta} \ldots\ldots\ldots\ldots\ldots\ldots\ldots\ldots\ldots\ldots\ldots(3)$$

$$\sigma_\theta = \frac{P}{2\delta\kappa_\theta}\left(2 - \frac{\kappa_s}{\kappa_\theta}\right) \ldots\ldots\ldots\ldots\ldots\ldots\ldots\ldots(4)$$

P is the turgor pressure. σ_s and σ_θ is the normal stress acting in the cell wall along meridional (s) and circumferential (θ) direction respectively. δ is the thickness of the cell wall. κ_s and κ_θ is the curvature of the cell wall along s and θ direction respectively.

Constitutive equations are listed as follows:

$$\dot{\varepsilon}_s = \Phi\left(\sigma_e - \sigma_y\right)\frac{\sigma_s - \nu\sigma_\theta}{K} \quad (5)$$

$$\dot{\varepsilon}_\theta = \Phi\left(\sigma_e - \sigma_y\right)\frac{\sigma_\theta - \nu\sigma_s}{K} \quad (6)$$

$\dot{\varepsilon}_s$ and $\dot{\varepsilon}_\theta$ are the strain rates. Φ is the extensibility of the cell wall and it is determined by ROP1 activity according to equation (2). σ_y is the yielding stress of the cell wall. ν is the flow coupling parameter to characterize the mechanical property affecting the distribution of strains between the principal directions. σ_e is the effective stress in the yielding criterion and can be expressed as:

$$\sigma_e = \sqrt{\sigma_s^2 + \sigma_\theta^2 - 2\nu\sigma_s\sigma_\theta} \quad (7)$$

$$K = \sqrt{\beta\sigma_s^2 + \beta\sigma_\theta^2 + \left(\beta - 6\nu\right)\sigma_s\sigma_\theta} \quad (8)$$

$$\beta = 2\nu^2 - 2\nu + 2 \quad (9)$$

Kinetic equations:

$$\dot{\varepsilon}_s = v_n\kappa_s + \frac{\partial v_s}{\partial s} \quad (10)$$

$$\dot{\varepsilon}_\theta = v_n\kappa_\theta + \frac{v_s\cos\phi}{r} \quad (11)$$

v_n and v_s is the local velocity of the cell wall along normal and s direction, the definition of s and ϕ. Numerical simulation of the model is carried out using Matlab professional software.

Plant growth conditions

Lat52:GFP-ROP1 line is described by Li et al., 1999. *ren1-1* line is described by Hwang et al., 2008. *Arabidopsis thaliana* plants were grown at 22°C in growth rooms under a light regime of 16 h of light and 8 h of dark. Pollen tubes were germinated on a solid medium (previously described by Hwang et al., 2008) for 3-4 hours before observation under microscope.

DNA manipulation and generation of *Lat52:GFP-RIC1 OX* lines in WT and *ren1-1* background

A GFP-RIC1 fragment was subcloned from pLGRIC1 construct (Described by Wu et al., 2001) into a binary vector pLat52:NOS (Described by Li et al., 1999) to generate the binary construct pLat52:GFP-RIC1 using *Xba* I and *Kpn* I sites. Lat52:GFP-RIC1 was introduced to wild type Col0 and ren1-1 background using Agrobacterium mediated flower dip method. Transgenic plants were selected on MS plates containing hygromycin.

Immunostaining of pectin in pollen tubes

Pollen tubes germinated in solid germination medium for 4 hours at room temperature were treated with fixative (4% paraformaldehyde, 3 mM $MgSO_4$, 2mM $CaCl_2$, 18%

Sucrose, 50 mM PIPES buffer, pH 6.9) for 1 hour. After washing gently with PBS buffer 3 times with 5 minutes each, pollen tubes were incubated with the purified JIM5 and JIM7 polyclonal antibodies (1:200 dilution with PBS buffer) at room temperature for 2 hours. After washing three times for 10 minutes each in PBS buffer, pollen tubes were incubated with secondary antibody, FITC-conjugated goat anti-rat IgG (1:300 dilution with PBS buffer) at room temperature for 2 hours. After three washes with PBS buffer, slides were mounted and observed under a confocal microscope (Leica SP2).

Confocal microscopy and image analysis

GFP-ROP1 or GFP-RIC1 expressing pollen tubes were observed under a Leica SP2 confocal microscope (488nm excitation, 500-540nm emission). For FRAP analysis of GFP-ROP1, 100% laser power (488 nm) was used to bleach the selected PM region, and time course images were take very 6 seconds. Matlab software was used to analyze GFP intensity profile on PM. FITC conjugated JIMs antibody images were taken under the same Leica SP2 confocal microscope (488nm excitation, 500-540nm emission). Image J software was used to analyze JIMs antibody localization profile along the PM.

References

Benkert, R., Obermeyer, G., and Bentrup, F.-W. (1997). The turgor pressure of growing lily pollen tubes. Protoplasma **198,** 1-8.

Berken, A., Thomas, C., and Wittinghofer, A. (2005). A new family of RhoGEFs activates the Rop molecular switch in plants. Nature **436,** 1176-1180.

Bosch, M., and Hepler, P.K. (2005). Pectin methylesterases and pectin dynamics in pollen tubes. Plant Cell **17,** 3219-3226.

Campas, O., and Mahadevan, L. (2009). Shape and dynamics of tip-growing cells. Curr Biol **19,** 2102-2107.

Cheung, A.Y., and Wu, H.M. (2008). Structural and signaling networks for the polar cell growth machinery in pollen tubes. Annu Rev Plant Biol **59,** 547-572.

Dumais, J., Shaw, S.L., Steele, C.R., Long, S.R., and Ray, P.M. (2006). An anisotropic-viscoplastic model of plant cell morphogenesis by tip growth. Int J Dev Biol **50,** 209-222.

Fayant, P., Girlanda, O., Chebli, Y., Aubin, C.E., Villemure, I., and Geitmann, A. (2010). Finite Element Model of Polar Growth in Pollen Tubes. Plant Cell.

Fischer, R., Zekert, N., and Takeshita, N. (2008). Polarized growth in fungi--interplay between the cytoskeleton, positional markers and membrane domains. Mol Microbiol **68,** 813-826.

Fu, Y., Wu, G., and Yang, Z. (2001). Rop GTPase-dependent dynamics of tip-localized F-actin controls tip growth in pollen tubes. J Cell Biol **152,** 1019-1032.

Gu, Y., Fu, Y., Dowd, P., Li, S., Vernoud, V., Gilroy, S., and Yang, Z. (2005). A Rho family GTPase controls actin dynamics and tip growth via two counteracting downstream pathways in pollen tubes. J Cell Biol **169,** 127-138.

Hwang, J.U., Vernoud, V., Szumlanski, A., Nielsen, E., and Yang, Z. (2008). A tip-localized RhoGAP controls cell polarity by globally inhibiting Rho GTPase at the cell apex. Curr Biol **18,** 1907-1916.

Kost, B., Lemichez, E., Spielhofer, P., Hong, Y., Tolias, K., Carpenter, C., and Chua, N.H. (1999). Rac homologues and compartmentalized phosphatidylinositol 4, 5-bisphosphate act in a common pathway to regulate polar pollen tube growth. J Cell Biol **145,** 317-330.

Kroeger, J.H., Geitmann, A., and Grant, M. (2008). Model for calcium dependent oscillatory growth in pollen tubes. J Theor Biol **253,** 363-374.

Lee, Y.J., and Yang, Z. (2008). Tip growth: signaling in the apical dome. Curr Opin Plant Biol **11,** 662-671.

Lee, Y.J., Szumlanski, A., Nielsen, E., and Yang, Z. (2008). Rho-GTPase-dependent filamentous actin dynamics coordinate vesicle targeting and exocytosis during tip growth. J Cell Biol **181,** 1155-1168.

Li, H., Lin, Y., Heath, R.M., Zhu, M.X., and Yang, Z. (1999). Control of pollen tube tip growth by a Rop GTPase-dependent pathway that leads to tip-localized calcium influx. Plant Cell **11,** 1731-1742.

Lowery, L.A., and Van Vactor, D. (2009). The trip of the tip: understanding the growth cone machinery. Nat Rev Mol Cell Biol **10,** 332-343.

Marco, E., Wedlich-Soldner, R., Li, R., Altschuler, S.J., and Wu, L.F. (2007). Endocytosis optimizes the dynamic localization of membrane proteins that regulate cortical polarity. Cell **129,** 411-422.

McKenna, S.T., Kunkel, J.G., Bosch, M., Rounds, C.M., Vidali, L., Winship, L.J., and Hepler, P.K. (2009). Exocytosis precedes and predicts the increase in growth in oscillating pollen tubes. Plant Cell **21,** 3026-3040.

Parre, E., and Geitmann, A. (2005). Pectin and the role of the physical properties of the cell wall in pollen tube growth of Solanum chacoense. Planta **220,** 582-592.

Winship, L.J., Obermeyer, G., Geitmann, A., and Hepler, P.K. (2010). Under pressure, cell walls set the pace. Trends Plant Sci **15,** 363-369.

Wu, G., Gu, Y., Li, S., and Yang, Z. (2001). A genome-wide analysis of Arabidopsis Rop-interactive CRIB motif-containing proteins that act as Rop GTPase targets. Plant Cell **13,** 2841-2856.

Table

Parameter	Biological meaning	Value	Unit
R_0	Reference ROP1 concentration	1	μM
k_{pf}	Parameter of positive feedback of ROP1 activity	1.5	/s
n	Power parameter of positive feedback for ROP1 activity	1.2	1
R_{total}	Total free ROP1	250	μM
R_{max}	Local saturation ROP1 concentration	10	μM
k_{gi}	Parameter of global inhibition for ROP1	0.5	/s
D	Diffusion parameter for ROP1	0.2	$\mu m^2/s$
Φ_{max}	Normalized maximum cell wall extensibility	1	1
P	Normalized tugur pressure	1	1
δ	Cell wall thickness	0.2	μm
ν	Flow coupling parameter	0.5	1

Table 2.1. Parameter setting for tip growth model.

Figures

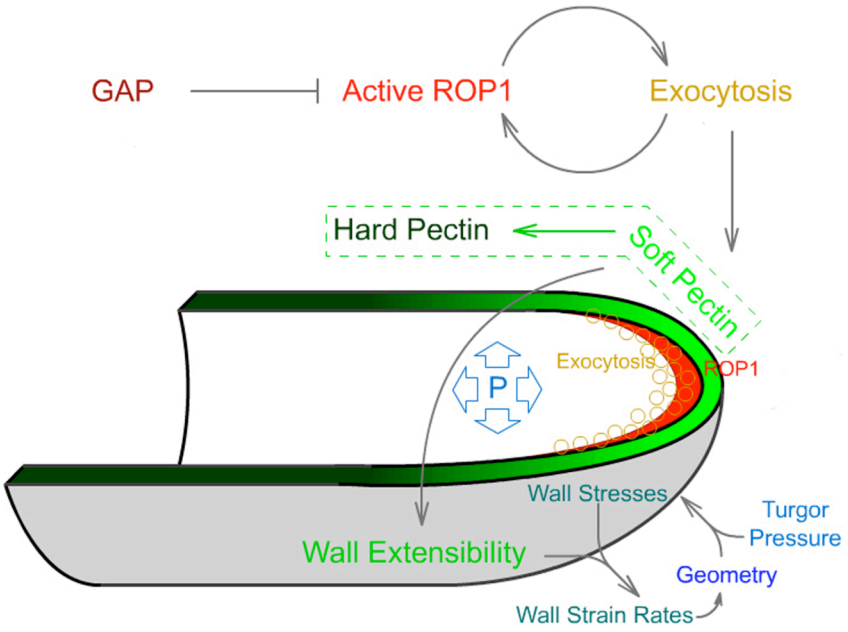

Figure 2.1. Conceptual model for ROP1 GTPase dependent pollen tube growth.
Upper part of this figure indicates a cell signaling model for ROP1 polarity establishment. Low part of this figure indicates a cell mechanical model for exocytosis dependent tip growth. Exocytosis is the key process linking the cell signaling model and the cell mechanical model.

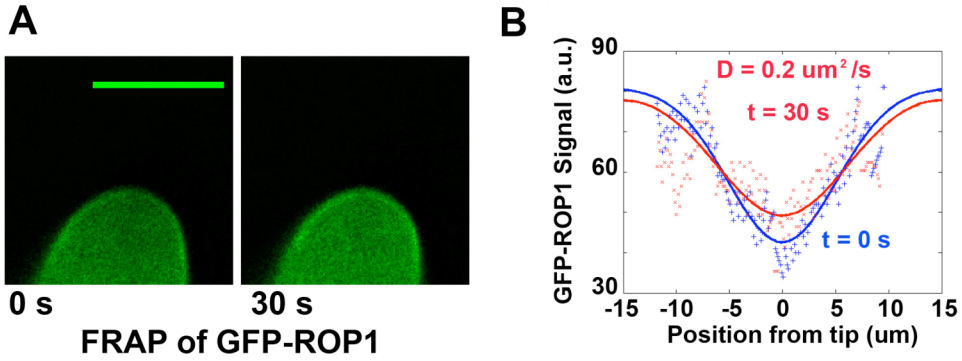

Figure 2.2. Estimation of GFP-ROP1 diffusion constant.
(A). FRAP analysis of GFP-ROP1 in pollen tubes treated with Lat B. Bar = 10 μm.
(B). Estimation of GFP-ROP1 diffusion constant on PM. Blue crosses indicate GFP-ROP1 intensity profile right after bleaching. Blue line is to fit the GFP-ROP1 intensity profile. Red crosses indicates GFP-ROP1 intensity profile at 30 seconds after bleaching. Red line is the model prediction for ROP1 localization (D = 0.2 $\mu m^2/s$), which matches GFP-ROP1 intensity profile.

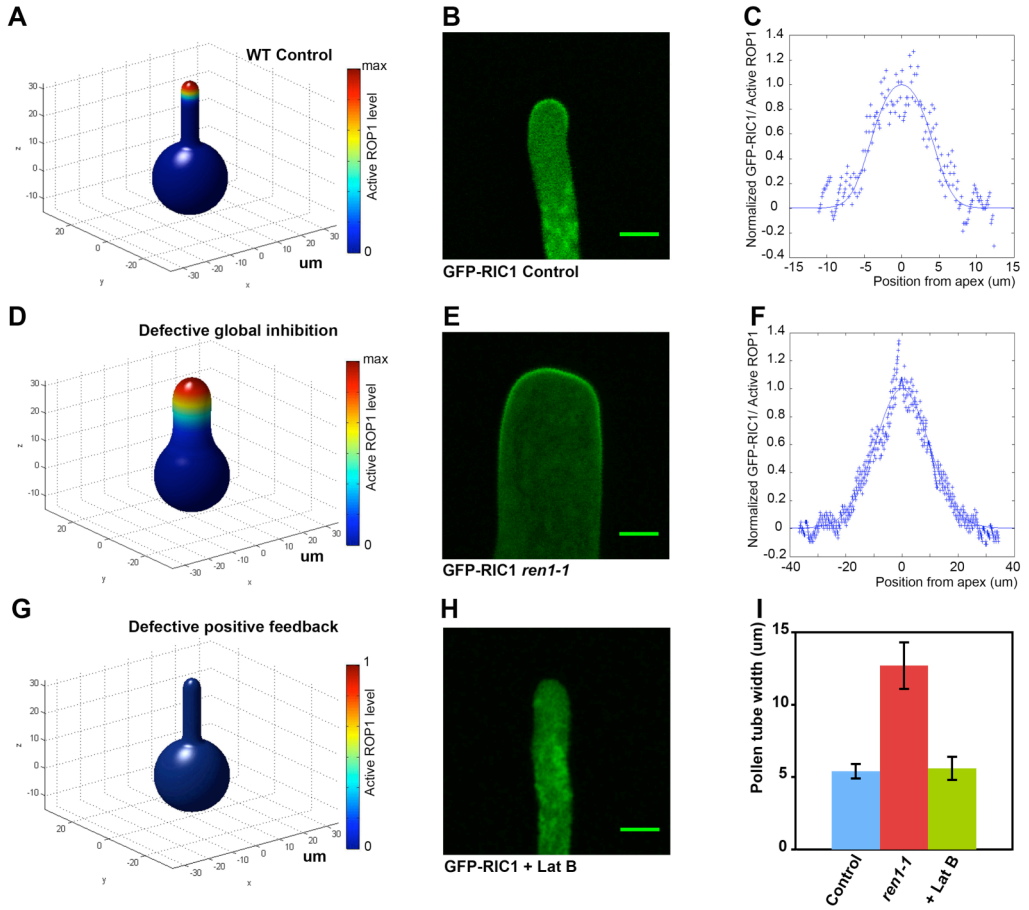

Figure 2.3. Simulation and experimental validation of ROP1 dependent pollen tube growth.
(A). Model prediction for pollen tube growth and active ROP1 localization in control pollen tubes.
(B). GFP-RIC1 localization in control pollen tubes. Bar = 5 μm.
(C). Validation of model prediction on active ROP1 localization in control pollen tubes. Blue crosses are GFP-RIC1 intensity profile in control pollen tube. Blue line is the model prediction for active ROP1 distribution in control pollen tube. Note that model prediction can match well with measured GFP-RIC1 intensity profile.
(D). Model prediction for pollen tube growth and active ROP1 localization in *ren1-1* pollen tubes.
(E). GFP-RIC1 localization in *ren1-1* pollen tube. Bar = 5 μm.
(F). Validation of model prediction on active ROP1 localization in *ren1-1* pollen tubes. Blue crosses are GFP-RIC1 intensity profile in *ren1-1* pollen tube. Blue line is the model prediction for active ROP1 distribution in *ren1-1* pollen tube. Note that model prediction can match well with measured GFP-RIC1 intensity profile.
(G). Model prediction for pollen tube growth and active ROP1 localization in pollen tubes with defective exocytosis.
(H). GFP-RIC1 localization in pollen tube with defective exocytosis. Bar = 5 μm.
(I). Width of pollen tubes with different ROP1 activity (n=30, error bar indicate SD.)

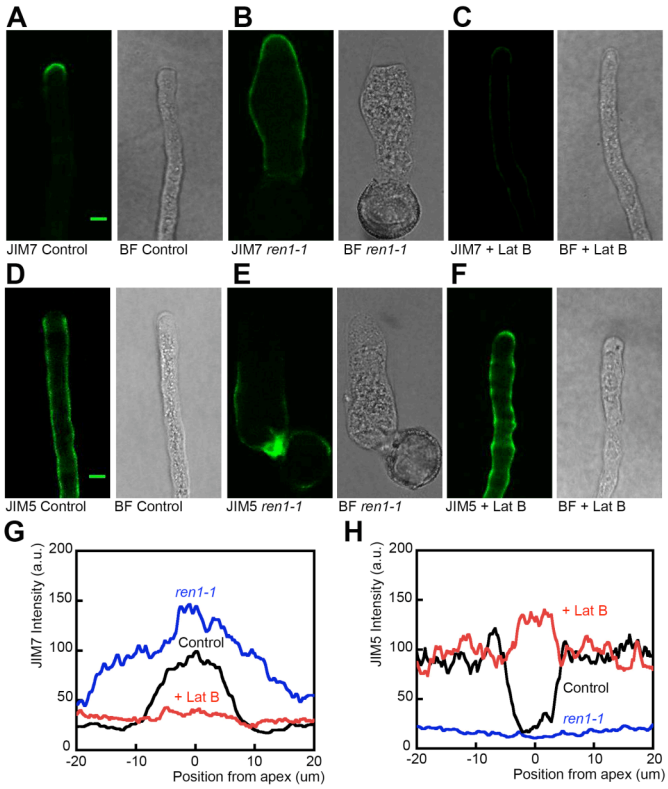

Figure 2.4. Active ROP1 controls cell wall pectin distribution via F-actin dependent exocytosis.
(A). JIM7 antibody staining in control Arabidopsis pollen tube. Left: FITC channel. Right: Bright Field channel. Bar = 5 μm.
(B). JIM7 antibody staining in *ren1-1* Arabidopsis pollen tube. Left: FITC channel. Right: Bright Field channel. Magnificantion is the same as in panel A.
(C). JIM7 antibody staining in Arabidopsis pollen tube treated with Lat B. Left: FITC channel. Right: Bright Field channel. Magnificantion is the same as in panel A.
(D). JIM5 antibody staining in control Arabidopsis pollen tube. Left: FITC channel. Right: Bright Field channel. Bar = 5 μm.
(E). JIM5 antibody staining in *ren1-1* Arabidopsis pollen tube. Left: FITC channel. Right: Bright Field channel. Magnificantion is the same as in panel D.
(F). JIM5 antibody staining in Arabidopsis pollen tube treated with Lat B. Left: FITC channel. Right: Bright Field channel. Magnificantion is the same as in panel D.
(G). JIM7 antibody averaged intensity profile in control, *ren1-1* and Lat B treated Arabidopsis pollen tubes (n=10).
(H). JIM5 antibody averaged intensity profile in control, *ren1-1* and Lat B treated Arabidopsis pollen tubes (n=10).

Chapter 3

Regulation of clathrin-dependent endocytosis by phosphoinositides at the tip of pollen tube

Abstract

Endocytosis modulates many key cellular processes such as cell polarity formation, polarized cell growth, and cytokinesis, but the molecular mechanisms underlying endocytosis are not well understood, especially in plant cells. We use the tip-growing pollen tube as a model to investigate these mechanisms. Here we show that phosphatidylinositol-4-phosphate 5-kinase 6 (PIP5K6)-mediated phosphoinositides are important regulators of clathrin-dependent endocytosis in pollen tubes. GFP-tagged PIP5K6 was preferentially localized to the shoulder of the apical plasma membrane (PM) in pollen tubes where it converts phosphatidylinositol 4-phosphate (PI4P) to phosphatidylinositol 4, 5-bisphosphate [PI(4,5)P_2]. RNAi-induced suppression of *PIP5K6* expression impaired tip growth and inhibited clathrin-dependent endocytosis in pollen tubes. In contrast, *PIP5K6* overexpression, which depleted PI4P and caused over-accumulation of PI(4,5)P_2 in the apical PM, induced massive aggregation of the PM in pollen tube tips. This PM abnormality was apparently due to excessive clathrin-dependent membrane invagination, because this defect was suppressed by the expression of a dominant negative mutant of clathrin heavy chain. These results support a role for PI(4,5)P_2 in promoting early stages of clathrin-dependent endocytosis, i.e., membrane invagination. Interestingly, the *PIP5K6* overexpression-induced PM abnormality was

partially suppressed not only by the overexpression of *PLC2*, which breaks down PI(4,5)P_2, but also by that of *PI4Kβ1*, which increases the pool of PI4P. Based on these observations, we propose that a proper balance between PI4P and PI(4,5)P_2 is required for clathrin-dependent endocytosis in the tip of pollen tubes. Given previous findings that both the accumulation and the hydrolysis of PI(4,5)P_2 are required for clathrin-mediated endocytosis in yeast and animal cells, a balance between PI4P and PI(4,5)P_2 may provide a common mechanism underlying clathrin-dependent endocytosis in various eukaryotic systems.

Introduction

Endocytosis internalizes extracellular materials and retrieves excessive components from the plasma membrane (PM), which can then be either degraded in lysosomes/vacuoles or recycled back to the PM. An increasing number of fundamental cellular processes such as cell polarity establishment, cytokinesis, polarized cell growth, and cellular signaling, have been shown to require endocytosis. In plant cells, endocytosis creates the polar localization of PINs (Dhonukshe et al., 2008; Kleine-Vehn and Friml, 2008; Yang, 2008), enhances brassinosteroid signaling (Geldner et al., 2007), and appears to regulate polarized cell growth (Helling et al., 2006; Moscatelli et al., 2007; Zonia and Munnik, 2008). Multiple pathways of endocytosis are known, but clathrin-dependent endocytosis is most extensively studied in yeast and in animal cells (Conner and Schmid, 2003; Mousavi et al., 2004). Clathrin-dependent endocytosis involves several stages, including assembly of clathrin and its adaptor proteins (such as AP-2 complex and AP-3) onto the

inner leaflet of the PM to form coated pits, invagination of coated pits, dynamin-mediated pinching of coated vesicles, and uncoating of clathrin from endocytic vesicles (Conner and Schmid, 2003; Mousavi et al., 2004). Evidence suggests that phosphatidylinositol 4, 5-bisphosphate [PI(4,5)P_2] localized in the inner leaflet of the PM promotes the formation and invagination of coated pits by binding to the AP-2 complex, AP-3, Dab2 and Epsin in yeast and animal cells (Mousavi et al., 2004; Di Paolo and De Camilli, 2006). Acute depletion of PI(4,5)P_2 caused loss of coated pits in mammalian COS-7 cells (Zoncu et al., 2007). PI(4,5)P_2 may also be important for membrane fission, as it also binds dynamin. Several recent studies show that PIP phosphatase-dependent metabolism of PI(4,5)P_2 is required for late stages of endocytosis in mammalian and yeast cells (Sun et al., 2005; Perera et al., 2006; Sun et al., 2007).

In contrast to yeast and mammalian cells, the molecular mechanism for clathrin-dependent endocytosis in plant cells remains poorly characterized, although clathrin-dependent endocytosis has been well-documented in plants and has been implicated in the polar localization of PIN proteins to the PM and polarized cell growth. As a single cell system, pollen tubes are particularly suited for the investigation of the mechanism for endocytosis and its role in polarized cell growth (Cheung and Wu, 2008; Lee and Yang, 2008; Yalovsky et al., 2008; Yang, 2008). Pollen tubes rapidly expand via tip growth that is dependent upon massive tip-targeted exocytosis. Thus it is conceivable that tip-localized endocytosis must be coordinated with exocytosis to control rapid tip growth. Indeed, both electron microscopy study and immunostaining of clathrin heavy chain

subunit suggest that clathrin is preferentially present at the shoulder of the apical PM of pollen tubes, and disruption of clathrin-dependent endocytosis in tobacco pollen tubes causes growth inhibition (Derksen et al., 1995; Blackbourn and Jackson, 1996; Moscatelli et al., 2007). Signaling mechanisms regulating polarized pollen tube growth, including tip-localized ROP GTPases (Lin et al., 1996; Kost et al., 1999; Li et al., 1999; Fu et al., 2001; Gu et al., 2005; Hwang et al., 2008; Lee et al., 2008), calcium gradients (Holdaway-Clarke et al., 1997), calcium-dependent protein kinases (Yoon et al., 2006; Myers et al., 2009), F-actin dynamics (Fu et al., 2001; Vidali et al., 2001), Rab GTPases (de Graaf et al., 2005) and PI(4,5)P_2 (Dowd et al., 2006; Helling et al., 2006), have been extensively studied. However, the mechanisms controlling clathrin-dependent endocytosis in pollen tubes are yet to be explored.

PI(4,5)P_2 has been reported to localize to the apical PM of pollen tubes and root hairs by using an in vivo PI(4,5)P_2 marker, a GFP-tagged pleckstrin-homology (PH) domain from phospholipase C (PLC), and has been implicated in the regulation of tip growth (Kost et al., 1999; Dowd et al., 2006; Helling et al., 2006). Recent studies suggest that the PM accumulation of PI(4,5)P_2 in pollen tubes may require one or more phosphatidylinositol-4-phosphate 5-kinases (PIP5Ks), which phosphorylate the D-5 position of the inositol ring of phosphatidylinositol-4-phosphate (PI4P). The Arabidopsis genome encodes 11 PIP5Ks divided into two groups: Type B (PIP5K1-9) containing Membrane Occupation and Recognition Nexus (MORN) repeats in the N-terminus and type A (PIP5K10 and 11) lacking MORN repeats (Mueller-Roeber and Pical, 2002; Im et al., 2007a). In

Arabidopsis root hairs, the production of PI(4,5)P_2 is through a Type B PIP5K, PIP5K3 (Kusano et al., 2008; Stenzel et al., 2008). Overexpression of *PIP5K3* causes abnormal root hair morphology and disruption of *PIP5K3* inhibits root hair growth. In pollen tubes, alteration of pollen-expressed PIP5K4 and PIP5K5 similarly affected pollen tube growth (Ischebeck et al., 2008; Sousa et al., 2008). It was proposed that these PIP5Ks affect either pectin exocytosis or recycling of endocytic vesicles (Ischebeck et al., 2008; Sousa et al., 2008). Although several studies have implicated phosphoinositides in the regulation of endocytosis in pollen tubes (Monteiro et al., 2005a; Monteiro et al., 2005b; Helling et al., 2006; Sousa et al., 2008), the role and the mode of action for phosphoinositides in endocytosis remain unclear.

In this report, we investigated the role of PI4P and PI(4,5)P_2 in the regulation of clathrin-mediated endocytosis in the tip of pollen tubes. We found that a pollen-enriched Arabidopsis PIP5K, PIP5K6, was preferentially localized to the shoulder of the apical PM in pollen tubes, as was clathrin. Importantly, down-regulation of PIP5K6 inhibited the assembly of clathrin onto the apical PM and endocytosis. In contrast, over-accumulation of PIP5K6 over-activated the early stage of clathrin-dependent endocytosis accompanied by a defect in the late stage of endocytosis, resulting in excessive aggregates of invaginated PM. The alteration of the apical PI(4,5)P_2 by inhibiting or overexpressing PLC did not cause this membrane deformation phenotype. Furthermore, PIP5K6-induced membrane deformation was suppressed by overexpression of either PLC2 or PI4Kβ1. Taken together, these findings support the hypothesis that PI(4,5)P_2

promotes the early stages of clathrin-dependent endocytosis (formation and invagination of clathrin-coated pits), whereas PI4P is required for the completion of clathrin-dependent endocytosis.

Results

PIP5K6 encodes a PI4P5K localized to the apical PM in pollen tubes

To investigate the role of the tip-localized PI(4,5)P_2 in the control of pollen tube tip growth, we sought to identify a PIP5K responsible for the synthesis of this PI(4,5)P_2 pool. Three Arabidopsis *PIP5K* genes *PIP5K4, 5* and *6* are specifically expressed in pollen (Zimmermann et al., 2004). Recent reports suggest that PIP5K4 and PIP5K5 are preferentially localized to the apical and sub-apical PM of pollen tubes (Ischebeck et al., 2008; Sousa et al., 2008). We found that PIP5K6-GFP was also localized to the apical and sub-apical PM with enrichment at the shoulder of the apex, while GFP alone was only found in the cytosol (Figure 3.1A, Figure 3.2A). In growing pollen tubes, PIP5K6-GFP was preferentially associated with sub-apical PM (Figure 3.1A). In contrast, in tubes that had ceased elongation, PIP5K6-GFP was preferentially localized to the tip of the apical PM (Figure 3.1B).

To test whether PIP5K6 is a functional PIP5K kinase *in vivo*, we visualized pollen PI(4,5)P_2 and PI4P using GFP-based markers, GFP-PLCδ1 PH and GFP-FAPP1 PH [GFP-tagged PH domains of the human PLCδ1 and phosphatidylinositol-4-phosphate adaptor protein-1 (FAPP1)], respectively (Furutani et al., 2006). PI(4,5)P2, marked by

GFP-PLCδ1 PH domain, accumulated at the apical PM of pollen tubes, consistent with previous reports in pollen tubes (Kost et al., 1999; Dowd et al., 2006). PI4P, marked by GFP-FAPP1 PH domain, accumulated at the apical PM and a vesicle-like structure (presumably TGN) in control pollen tubes, consistent with the PI4P localization pattern in root hair cells (Thole et al., 2008). Although considered as specific binding proteins for PI4P and PI(4,5)P2 in vitro, the phosphoinositides markers used in this study may compete with native proteins (including downstream effectors and native enzymes) for binding with PI4P and PI(4,5)P2. As a result, overexpression of these two markers might introduce some non-specific effects on pollen tube growth (Sousa et al., 2008). To minimize the unspecific effects caused by markers overexpression, we only used low-dosage DNA (0.1 μg per shot) for transient expression in tobacco pollen tubes. In addition we avoided pollen tubes expressing high levels of markers in our analyses. Using these two markers, we examined the effect of overexpressing (OX) active PIP5K6 on PI(4,5)P_2 and PI4P localization pattern in tobacco pollen tubes. Overexpression of the full-length *PIP5K6* significantly increased GFP-PLCδ1 PH distribution to the apical PM (Figure 3.2) and decreased GFP-FAPP1 PH distribution to the apical PM (Figure 3.3). Overexpression of a PIP5K-dead mutant PIP5K6 (K443S), in which the conserved K443 residue required for the catalytic activity of PIPK is mutated, seemed to have no significant effect on the distribution of PI(4,5)P2 and PI4P markers to the apical PM (Figure 3.2, 3.3). These observations indicate that PIP5K6 is an active enzyme locally keeping the balance between PI(4,5)P_2 and PI4P on the PM of pollen tubes.

***PIP5K6* overexpression causes PM deformation in pollen tube tips**

In the course of examining PIP5K6-GFP localization, we found that many *PIP5K6-GFP*-overexpressing tubes exhibited PIP5K6-GFP aggregates at the tip (Figure 3.4A). Similar phenotypes were observed in tobacco pollen tubes overexpressing PIP5K4-GFP and PIP5K5-GFP (Ischebeck et al., 2008; Sousa et al., 2008). To assess whether these aggregates were due to the PM deformation, multiple scanning at different focal planes were conducted in the tip of *PIP5K6-GFP* OX tubes. As shown in Figure 3.4A and B, in these abnormal tips PIP5K6-GFP appeared to be associated with the PM, which apparently retracted from the cell wall as a result of invagination, causing the overall deformation of the cytoplasm in the tip region. To confirm whether the aggregates were indeed due to invagination of the PM, we co-expressed untagged *PIP5K6* with the PM marker *RLK-GFP* (Lee et al., 2008), and found that the apical PM containing RLK-GFP displayed a similar invagination, as did PIP5K6-GFP (Figure 3.5).

PIP5K6-GFP OX pollen tubes exhibited different degrees of PM deformation. To better describe the severity of this phenotype, we arbitrarily categorized *PIP5K6-GFP* tubes into 3 groups: 1) those with the normal smooth PM; 2) those with moderate apical PM deformation; 3) those with severe apical PM deformation. At 4-5 hours after bombardment, the percentage of *PIP5K6-GFP* tubes falling into these three groups was 18%, 40% and 42%, respectively (n=100, Figure 3.4A). However, PM morphology was not altered by the overexpression of the GFP-tagged *PIP5K6 K443S* mutant (n=30,

shown in Figure 3.4A). Time-lapse imaging showed that the PM invagination started after PIP5K6-GFP localization invaded the extreme tip and became more severe over time (Figure 3.4C). These results suggest that excessive amount of PIP5K6 activity at the tip of pollen tubes caused the deformation of the PM.

The PM deformation occurred in *PIP5K6-GFP* OX tubes that had already stopped elongating (Figure 3.4C). At 4-5 hours after bombardment, *PIP5K6-GFP* OX tubes were shorter in length and wider in tips compared with control tubes expressing GFP alone (Figure 3.4D, E). The mean length decreased from 180 μm in control tubes to 113 μm in *PIP5K6-GFP* OX tubes (n=30, student's t-test value $p<0.05$). The mean width increased from 8.1 μm in control tubes to 12.4 μm in pollen tubes overexpressing *PIP5K6-GFP* (n=30, student's t-test value $p<0.05$). However, pollen tube growth arrest induced by other treatments such as overexpression of a dominant negative form of ROP1 did not cause PM deformation (data not shown), suggesting that the PM deformation is a specific effect of PIP5K6 overexpression, which is further supported by the suppression of the PM deformation by the inhibition of the early stage of clathrin-dependent endocytosis (see below).

Overexpression of *PIP5K6* causes over-initiated but aborted clathrin-dependent endocytosis

We hypothesized that one or both of the following membrane trafficking defects could contribute to the PM deformation induced by *PIP5K6* OX: 1) An increase in exocytosis that was not coupled with an increase in endocytosis or cell wall expansion, 2) a defect in a late stage of endocytosis, in which the apical PM was invaginated but not pinched off, as observed in the dysfunction of dynamin (Hill et al., 2001; Kang et al., 2003).

To investigate the effect of *PIP5K6* OX on exocytosis, we visualized exocytosis at the tip of tobacco pollen tubes by using the fluorescence recovery after photobleaching (FRAP) method (Lee et al., 2008). In pollen tubes expressing the *GFP-RLK* PM marker, we photobleached the apical PM region and tracked the recovery of the GFP signal. In control pollen tubes expressing *GFP-RLK* alone, the PM-associated GFP signal quickly recovered after photobleaching (n=10, average curve shown in Figure 3.6A, B). The PM signal recovered to about 70% of the original signal intensity within 3 min after photobleaching. In pollen tubes coexpressing *GFP-RLK* and *PIP5K6*, even at the early times when *PIP5K6* OX had not cause PM deformation, the recovery of the apical PM associated GFP signal was slower than control tubes (Figure 3.6A, C; student's t-test value $p<0.05$). At 3 min after photobleaching, the PM signal recovered to about 50% of the original signal intensity. This observation suggested that *PIP5K6* OX did not enhance but might suppress exocytosis in pollen tubes. In further support of this conclusion, we found that *PIP5K6* OX did not change the localization of a marker for exocytic vesicles YFP-RabA4d (Lee et al., 2008), as shown in Figure 3.7.

We then investigated whether *PIP5K6* OX altered endocytosis. FM 4-64 dye is commonly used as a marker for endocytosis, because it is incorporated in the PM and enters the cytoplasm only through endocytosis when applied to culture media. In normal elongating tobacco pollen tubes, FM4-64 dye labeled the PM, particular structures (likely endosomes), and the apical cytoplasm as an inverted cone pattern that is thought to contain both recycling and secretory vesicles (Figure 3.8A). Ten to fifteen minutes after 2.5 μM FM 4-64 was applied to *PIP5K6-GFP* tubes, FM 4-64 dye strongly stained the PM region and weakly stained the cytoplasm (Figure 3.8B-D). These observations are consistent with a previous report that *PIP5K4* OX inhibited FM dye uptake (Sousa et al., 2008) and support the hypothesis that *PIP5K6* OX over-activates the early stages (i.e., membrane invagination) but inhibits the later stage (i.e., fission of invaginated membrane) of endocytosis, resulting in excessive accumulation of deformed membranes at the tip of pollen tubes.

$PI(4,5)P_2$ is involved in recruiting clathrin and associated proteins required for the formation and invagination of coated pits in yeast and animal cells (Mousavi et al., 2004; Di Paolo and De Camilli, 2006). Thus a simple explanation for the PIP5K6-induced membrane deformation phenotype is that over-accumulation of $PI(4,5)P_2$ at the tip over-activated membrane invagination but not closure and pinching of endocytic vesicles during clathrin-dependent endocytosis. We tested this hypothesis using a dominant negative form of clathrin heavy chain (called "Clathrin Hub") (Liu et al., 1995; Dhonukshe et al., 2007), which contains the C-terminal part of the clathrin heavy chain

that can bind to and trap the clathrin light chain. Overexpression of *HUB* alone in tobacco pollen tubes slightly inhibited growth (Figure 3.9). When *PIP5K6-GFP* was co-overexpressed with *HUB*, the PM invagination phenotype was greatly suppressed (Figure 3.8E, F). Five to six hours after bombardment, the percentage of *PIP5K6-GFP*-overexpressing tobacco pollen tubes that displayed little, moderate, and severe PM invagination was 15%, 40% and 45%, respectively (Figure 3.8E, n=60). Under the same condition, 65% of pollen tubes overexpressing both *PIP5K6-GFP* and *HUB* showed normal smooth PM, while 35% exhibited moderate PM invagination and none had severe PM invagination (Figure 3.8F, n=60). To further test this hypothesis, we used a marker for early stage of clathrin dependent endocytosis, AP180 protein. AP180 is an adaptor protein responsible for clathrin cage assembly and thus participates in the initiation of clathrin-mediated endocytosis (Barth and Holstein, 2004). In control tobacco pollen tubes, GFP-AP180 was localized to the subapical PM, similar to clathrin localization pattern (Figure 3.10A-B). In pollen tubes co-overexpressing *GFP-AP180* and *PIP5K6*, the GFP-AP180 accumulated in both of the apex and the subapical PM, especially the invaginated sites of plasma membrane (Figure 3.10C-E). Taking together, these results strongly support the hypothesis that over-initiated but aborted clathrin-dependent endocytosis accounted for the PM deformation in *PIP5K6-GFP* OX pollen tubes.

PIP5K6 **RNAi inhibits endocytosis by blocking the PM recruitment of clathrin heavy chain**

If the PM-localized PI(4,5)P_2 indeed regulates the formation of coated pits by recruiting clathrin in pollen tubes as in yeast and animal cells, the suppression of PM-localized PIP5Ks is expected to inhibit clathrin-dependent endocytosis. We generated transgenic Arabidopsis plants expressing *PIP5K6* RNA interference (RNAi) construct under the control of *LAT52* promoter. *PIP5K6* RNAi lines exhibit reduced *PIP5K6* mRNA levels in pollen compared with wild type Arabidopsis plants (Figure 3.11A). Two representative lines examined showed similar phenotypes that are correlated with the reduction of mRNA levels in these lines. The *PIP5K6* RNAi pollen tubes were greatly shorter (around 60% reduction) than WT Col-0 pollen tubes (Figure 3.11B,C), similar to the previous findings with PIP5K4 mutants (Sousa et al., 2008). We also found that FM dye uptake was greatly inhibited in *PIP5K6* RNAi pollen tubes (Figure 3.11D, E).

We then analyzed the localization of clathrin heavy chain (CHC) in *PIP5K6* RNAi pollen tubes using an immunostaining method (Blackbourn and Jackson, 1996; Kim et al., 2001). In control pollen tubes, anti-CHC antibody staining was mainly localized to the subapical PM (Figure 3.11F). In *PIP5K6* RNAi pollen tubes, CHC antibody stained weakly at the PM (Figure 3.11F). In *pip5k4* KO pollen tubes (Sousa et al., 2008), CHC localization to the apical PM was also greatly reduced (Figure 3.11F). The relative PM associated CHC signal was significantly decreased in both *PIP5K6* RNAi and *pip5k4* mutant tubes (Figure 3.11G, n=20, error bar indicates SD, student's t-test value $p<0.05$.). Thus, deficiency in PIPK-dependent conversion of PI4P to PI(4,5)P_2 led to a defect in clathrin-dependent endocytosis. These results, together with *PIP5K6 OX* induced excessive

clathrin-dependent PM invagination, suggest that PI(4,5)P_2 production via type B PIP5Ks is important for the activation of the early stages (i.e., formation and invagination of coated pits) of clathrin-mediated endocytosis in the apical PM of pollen tubes.

Both over-accumulation of PI(4,5)P_2 and depletion of PI4P in the apical PM induced PM deformation in pollen tubes

Since *PIP5K6* OX not only caused over-accumulation of its product PI(4,5)P_2 but also depletion of its substrate PI4P in the apical PM (Figure 3.2, 3.3), either or both of PI4P depletion and PI(4,5)P2 over-accumulation could contribute to the observed PM invagination induced by PIP5K6 overexpression. To assess which of the *PIP5K6* OX effects was responsible for the *PIP5K6* OX phenotype, we first co-overexpressed *PIP5K6-GFP* with *Arabidopsis PLC2* in tobacco pollen tubes. Phospholipase C (PLC) hydrolyzes PI(4,5)P_2 into the second messengers IP3 and DAG. GFP-tagged Arabidopsis PLC2 was localized to both apical and sub-apical PM of tobacco pollen tubes (Figure 3.12). Overexpression of *PLC2* suppressed the over-accumulation of PI(4,5)P_2 caused by *PIP5K6* overexpression (Figure 3.13). When *PIP5K6-GFP* was co-expressed with *PLC2* in tobacco pollen tubes, the PM invagination phenotype was partially suppressed. At 4-5 hours after bombardment, 18%, 40% and 42% of tobacco pollen tubes overexpressing *PIP5K6-GFP*, displayed smooth normal PM, moderate PM invagination and severe PM invagination, respectively (Figure 3.14A, n=100). In contrast, 46%, 39%, and 15% of pollen tubes overexpressing both *PIP5K6-GFP* and *PLC2* exhibited smooth PM,

moderate PM invagination and severe PM invagination (Figure 3.14B, n=100, Fisher exact probability test value $p<0.05$), respectively. Thus, removal of PI(4,5)P_2 by PLC2 overexpression greatly but did not completely suppressed *PIP5K6* OX-induced PM invagination. This result supports the notion that over-accumulation of PI(4,5)P_2 contributed to, but was not solely responsible for the PM invagination phenotype. Consistent with this finding, we found that *PLC2* OX partially suppressed the growth phenotype of *PIP5K6* OX (Figure 3.14D-E, n=30, student's t-test value $p<0.05$).

Since suppression of PI(4,5)P_2 over-accumulation did not completely restore normal pollen tube tips, we hypothesized that *PIP5K6* OX-induced depletion of PI4P in the apical PM of pollen tubes also contributed to the *PIP5K6* OX phenotype. To test this hypothesis, we examined the effect of overexpressing *Arabidopsis PI4Kβ1*, which rescued the reduction of PI4P caused by *PIP5K6* overexpression (Figure 3.15). Co-overexpression of *PI4Kβ1* with *PIP5K6-GFP* not only partially suppressed PIP5K6 OX growth phenotype (Figure 3.14D-E, n=30, student's t-test value $p<0.05$), but also partially suppressed the PM invagination phenotype induced by *PIP5K6-GFP* overexpression (Figure 3.14C). At 4-5 hours after bombardment, the percentage of *PIP5K6-GFP* and *PI4Kβ1* co-overexpressing tobacco pollen tubes that displayed little, moderate and severe PM deformation was 30%, 45% and 25%, respectively (n=100, Fisher exact probability test value $p<0.05$). Furthermore, treatment of wild type pollen tubes with PLC inhibitor U73122, which increased PI(4,5)P_2 level without decreasing PI4P level on the PM (Figure 3.16) (Helling et al., 2006), did not cause PM invagination

(Figure 3.16, n=30). This results further support the notion that over-accumulation of PI(4,5)P_2 at the apical PM alone was insufficient to cause the PM invagination phenotype induced by *PIP5K6 OX*. Taken together our data suggest that the PM invagination phenotype in *PIP5K6 OX* pollen tubes was the result of simultaneous over-accumulation of PI(4,5)P_2 and reduction of its precursor PI4P.

Discussion

Several recent reports support a role for both PI4P and PI(4,5)P_2 in the regulation of tip growth in root hairs and pollen tubes (Monteiro et al., 2005a; Monteiro et al., 2005b; Dowd et al., 2006; Helling et al., 2006; Preuss et al., 2006; Ischebeck et al., 2008; Kusano et al., 2008; Sousa et al., 2008; Stenzel et al., 2008; Thole et al., 2008; Szumlanski and Nielsen, 2009), but the mechanism by which these membrane-localized signaling molecules affect polarized cell growth remained unclear. Our results provide evidence that both PI4P and PI(4,5)P_2 play a critical role in the regulation of clathrin-dependent endocytosis at the tip of pollen tubes and that a proper balance between PI4P and PI(4,5)P_2 accumulated in the apical PM is important for clathrin-dependent endocytosis. We propose that PI(4,5)P_2 promotes the formation and invagination of clathrin-coated pits as shown in yeast and animal cells, while PI4P participates in the final stage of clathrin-dependent endocytosis at the tip of pollen tubes.

PIPK-dependent conversion of PI4P to PI(4,5)P_2 promotes the early stages of clathrin-dependent endocytosis at the tip of pollen tubes

Our results strongly suggest that PIP5K-mediated conversion of PI4P to PI(4,5)P_2, which preferentially occurs at the shoulder of the apical PM of pollen tubes, promotes the early steps of clathrin-dependent endocytosis. This conclusion is based on two key findings: 1) RNAi-mediated suppression of PIP5K6 inhibits endocytosis and clathrin assembly onto the apical PM, and 2) PIP5K6 overexpression induces clathrin-dependent excessive PM invagination. Our results suggest that this excessive PM invagination was not caused by over-activation of exocytosis. On the contrary, we showed PIP5K6 overexpression appeared to inhibit exocytosis, a phenomenon consistent with a role for PI4P (PIP5K substrate) in the positive regulation of exocytosis (Preuss et al., 2006). It was recently proposed that PIP5K OX-induced PI(4,5)P_2 over-accumulation leads to over-activated exocytosis, causing the PM to fold backward from the cell wall (Ischebeck et al., 2008; Sousa et al., 2008). This proposition was based on the observation that pectin over-accumulated outside of the invaginated region of the PM in pollen tubes overexpressing PIP5K. An alternative explanation for this observation could be that the endocytosis of pectin components is abortive in these pollen tubes. Pectin is found to accumulate in BFA-induced compartments in plant cells, which are thought to be enlarged endocytic compartments (Baluska et al., 2002). Thus over-initiated abortive endocytosis could lead to pectin over-accumulation in the tip of PIP5K-overexpressing pollen tubes.

Is PIP5K-dependent endocytosis mediated by its immediate product PI(4,5)P_2 or secondary products?

PI(4,5)P_2 could be converted into PI(3,4,5)P3 by PI(4,5)P_2-3-kinase. Homologs of this enzyme are absent in plants and PI(3,4,5)P3 has not been detected in plants to date. Thus PI(3,4,5)P3 is unlikely to participate in clathrin-dependent endocytosis in plant cells. PI(4,5)P_2 could also be converted into IP3 and DAG by PLC. However, overexpression of PLC in tobacco pollen tubes did not induce excessive PM invagination seen in PIP5K overexpressing tubes (Helling et al., 2006), arguing against a role for PLC products in the promotion of early clathrin-dependent endocytosis. Importantly, we found that the clathrin-dependent PM invagination in PIP5K6-overexpressing tubes was partially suppressed when PI(4,5)P_2 level was reduced by overexpressing an apical PM-localized PLC2. PI(4,5)P_2 has been found in clathrin-enriched vesicles upon salt stress, supporting a link between calthrin-dependent endocytosis and PI(4,5)P_2 (Konig et al., 2008). Therefore, we propose that PI(4,5)P_2, not its products, promotes early steps of clathrin-dependent endocytosis.

A role for PI(4,5)P_2 in the regulation of clathrin-dependent endocytosis in pollen tubes is consistent with the findings in animal and yeast cells (Sun et al., 2005; Sun et al., 2007; Zoncu et al., 2007). Through the study of PI(4,5)P_2 dynamics and clathrin-dependent endocytic compartment, it was shown in yeast cells that PI(4,5)P_2-enriched region is

important for the initiation of clathrin-dependent endocytosis (Sun et al., 2005; Sun et al., 2007). The most convincing study that supports a direct involvement of PI(4,5)P_2 in clathrin-dependent endocytosis was the demonstration that acute depletion of PI(4,5)P_2 by inducible activation of PI(4,5)P_2 phosphatase causes loss of coated pits in mammalian COS-7 cells (Zoncu et al., 2007). Moreover, several PI(4,5)P_2-binding proteins, including AP2 and AP180, are involved in the assembly of clathrin coat and/or invagination of clathrin-coated pits. Importantly, homologs for AP180 are present in plants and are expressed in pollen (Holstein and Oliviusson, 2005). Therefore, PI(4,5)P_2 regulation of the early stage of clathrin-dependent endocytosis appears to be conserved in eukaryotic kingdoms.

PI(4,5)P2 also regulates the organization and dynamics of the actin cytoskeleton, which impacts clathrin-mediated endocytosis in yeast (Yin and Janmey, 2003; Kaksonen et al., 2006; Sun et al., 2007). Could PI(4,5)P2 regulation of actin be part of the mechanism by which PI(4,5)P2 promotes the early stages of clathrin-dependent endocytosis? When overexpressed, a dominant negative mutant of PLC was found to increase F-actin in pollen tubes, implicating the involvement of PI(4,5)P2 in the regulation of the actin cytoskeleton (Dowd et al., 2006). A previous report disrupted the idea that the membrane invagination induced by PIP5K4 and PIP5K5 overexpression could be contributed to changes in the actin cytoskeleton (Ischebeck et al., 2008). Nonetheless, actin as a potential bridge between PIP5Ks and endocytosis is worthy further investigation, given that PI(4,5)P2 regulation of endocytosis is conserved in different eukaryotic systems.

PI4P may participate in a late stage of clathrin-dependent endocytosis

Our results also support a requirement for the PI(4,5)P_2 precursor, PI4P, in the regulation of clathrin-dependent endocytosis. Using a PI4P marker, GFP-FAPP1 PH, we found that PI4P is enriched in the apical PM and is localized in putative Golgi-derived vesicles. Similar PI4P distribution was also found in root hairs (Vermeer et al., 2009). In plant cells, PI4P is the most abundant form of phosphoinositides, suggesting PI4P may have some significance in plant cell signal transduction (Im et al., 2007b). Genetic studies of enzymes involved in PI4P synthesis and degradation in root hairs have implicated PI4P in the regulation of polar exocytosis (Preuss et al., 2006; Thole et al., 2008). Because PI4P is the immediate precursor of PI(4,5)P_2, however, it has been difficult to determine whether PI4P merely provides a precursor for PI(4,5)P_2 or has a direct role in signaling.

The excessive PM invagination phenotype in PIP5K6-overexpressing pollen tubes provided us with a unique opportunity to investigate the role of PI4P. As discussed above, our findings suggest that over-accumulation of PI(4,5)P_2 contributes to this phenotype. However, this phenotype cannot be explained solely by overproduced PI(4,5)P_2, because inhibition of PLC, which also causes over-accumulation of PI(4,5)P_2, did not induce the PM invagination phenotype. Furthermore, co-overexpression with PLC2 was only able to partially suppress the PIP5K6 overexpression phenotype. Importantly, co-overexpression with PI4K, which synthesizes PI4P, also partially

suppressed the PIP5K6 overexpression phenotype. These observations suggest that PI4P not only provides a precursor for PI(4,5)P_2, but also plays a more direct role in the regulation of clathrin-dependent endocytosis.

In yeast, knockout mutants for *SJL* genes (which encode PI(4,5)P_2 5-phosphatases) show abnormal PM invagination (Sun et al., 2005; Sun et al., 2007), which highly resembles the PIP5K6 overexpression PM phenotype. Using markers for different stages of endocytosis, it was shown that the abnormal PM invagination in the *sjl* mutants was caused by a defect in the late stage of clathrin-dependent endocytosis. The PM invagination phenotype in *sjl* knock out yeast cells was due to over-accumulation of abortive endocytic compartment. Based on these observations, it was proposed that the process of hydrolyzing PI(4,5)P_2 into PI4P is required for the later steps of clathrin-dependent endocytosis. Our finding that increasing the pool of PI4P in PIP5K6-overexpressing tubes by overexpressing PI4K can rescue the PM invagination defect clearly supports a direct role for PI4P in the regulation of the late stage of endocytosis. Thus we propose that a PI4P-dependent process may provide a conserved mechanism underlying the completion of clathrin-dependent endocytosis, and that a right balance (or interconversion) between PI4P and PI(4,5)P_2 is critical for the initiation, progression, and maturation of clathrin-dependent endocytosis. Identification of PI4P-binding proteins involved in this process will be important for testing this hypothesis.

Materials and Methods

Plant Growth Conditions

Arabidopsis thaliana plants (Col-0) were grown at 22°C in growth rooms under a light regime of 16 h of light and 8 h of dark. *Nicotiana tabacum* plants were grown in growth chamber at 25°C under a light regime of 12 h of light and 12 h of dark.

Cloning of *PIP5K6*, *PLC2*, *PI4Kβ1*, *HUB and AP180* coding sequences

The *PIP5K6* coding cDNA without the stop codon was amplified from cDNA obtained from Col-0 flowers using forward (5'-GCTCTAGAATGTCGGTAGCACAC-GC-3') and reverse (5'-GCTCTAGAAGCGTCTTCAACGAAGAC-3') primers carrying XbaI site (underlined). The *PLC2* coding cDNA was amplified from cDNA obtained from Col-0 flowers using forward (5'- GCTCTAGAATGTCGAAGCAAAC-GTAC-3') and reverse (5'-CGGGATCCCCACAAACT-CCACCTTCACG-3') primers carrying XbaI and BamHI sites (underlined), respectively. The *PI4Kβ1* coding cDNA was amplified from cDNA obtained from Col-0 flowers using forward (5'-GCTCTAGAATGCCGATGGG ACGC-3') and reverse (5'-CGGGATCCCCAATATTCCA-TTTTAAGACCC-3') primers carrying XbaI and BamHI sites (underlined), respectively. *HUB* (1860 bp of C-terminal clathrin heavy chain At3g11130) coding cDNA was amplified from cDNA obtained from Col-0 flowers using forward (5'-CCATGGAGAAGAAGTTTAACTTA-AATGTTCAGGC-3') and reverse (5'-GGTACCTTAGTAGCCGCCCATCGGTGG-3') primers carrying NcoI and KpnI sites (underlined), respectively. Coding cDNAs for

PIP5K6, PLC2 and PI4Kβ1 were cloned into the vector pGEM-Teasy vector (Promega) and sequenced. Coding cDNA for *HUB* was cloned into vector pCR2.1 (Invitrogen) and sequenced. *AP180* coding cDNA was amplified from cDNA obtained from Col-0 flowers using forward (5'- GGGGACAAGTTTGTACAAAAAAGCAGGCTCCATGCCGA GCAAGCTTAAAAAAG-3') and reverse (5'-GGGGACCACTTTGTACAAGAAAGCT GGGTAACTCAAGTGCTTGGCTATGATC-3') primers, then cloned into GATEWAY DONR vector and sequenced.

Mutagenesis of the PIP5K6 coding sequence

To obtain the point mutated coding sequence of *PIP5K6 K443S*, two cDNA fragments were amplified from pGEM-T easy PIP5K6 using the primer combinations (5'-GCTCTAGAATG-TCGGTAGCACACGC-3'/ 5'-TTCTTCATAGTCGATATCATG-3') and (5'- CTACATGAT-ATCGACTATGAA-3'/5'-GCTCTAGAAGCGTCTTCAACG AAGAC-3'), then cloned into pGEM-Teasy, respectively. Sequencing confirmed the presence of the K443S mutation. These two fragments were then ligated using EcoRV site, generating the PIP5K6 K443S cDNA.

Constructs for transient expression in tobacco pollen tubes

To generate the pLAT52:PIP5K6-GFP construct, PIP5K6 coding cDNA was subcloned from pGEM-T easy-PIP5K6 into pUC pLAT52:GFP vector using Xba I site (in frame with 5' end of GFP sequence) (Fu et al., 2001). To generate the pLAT52:PIP5K6 K443S-GFP construct, PIP5K6 K443S coding cDNA was subcloned from pGEM-T easy-

PIP5K6 K443S into the pUC pLAT52:GFP vector using Xba I site (in frame with 5' end of GFP sequence). To generate the pLAT52:PIP5K6 construct, PIP5K6 coding cDNA was subcloned from pGEM-T easy-PIP5K6 into the pUC pLAT52:GFP vector using Xba I site. To generate the pLAT52:PIP5K6 K443S construct, PIP5K6 K443S coding cDNA was subcloned from pGEM-T easy-PIP5K6 into the pLAT52:GFP vector using Xba I site. The pLAT52:GFP-RLK PM marker construct has been described previously (Lee et al., 2008). Human PLCδ1 PH domain was cut using BglII and BamHI from YFP-PLCδ1 construct (from Dr. Furutani, (Furutani et al., 2006), then insert into the pUC pLAT52::GFP vector using BglII site (at downstream of 3' end of GFP) to obtain pLAT52:GFP-PLCδ1 PH. Human FAPP1 PH domain was cut using BglII and BamHI from pDriveFAPP1 construct ((Furutani et al., 2006), then inserted into pUC pLAT52:GFP using BglII site (at downstream of 3' end of GFP) to produce the pLAT52:GFP-FAPP1 construct. HUB coding cDNA was subcloned from pCR2.1-HUB construct into the pUC pLAT52 vector using NcoI and KpnI sites to produce the pUC pLAT52:HUB construct. PLC2 coding cDNA was subcloned from pGEM-T easy PLC2 construct into the pUC pLAT52 vector using XbaI and BamHI sites to generate the pUC pLAT52:PLC2 construct. PI4Kβ1 coding cDNA was subcloned from pGEM-T easy PI4Kβ1 construct into the pUC pLAT52 vector using XbaI and BamHI sites to obtain the pUC pLAT52:PI4Kβ1 construct. AP180 coding cDNA was subcloned from GATEWAY DONR vector to destination vector to obtain the pGWLAT52:GFP-AP180 construct.

PIP5K6 RNAi construct and transgenic lines

To generate the *PIP5K6* RNAi construct, a 340-bp antisense cDNA fragment of the specific sequence of the *PIP5K6* was amplified using primer combination (5'-AAATCGATTTA-CCCTTCGACTTCTTCC-3'/ 5'-AACCATGGCCTTTAGAG ATAGT-TTGTCCT-3'), cloned into the ClaI-SacI sites in the pGEM-7Zf vector, yielding the plasmid pGEM-7Z-PIP5K6A. The antisense fragment was cloned as an NcoI-SmaI fragment into pUC pLAT52:GFP vector; the LAT52:PIP5K6A fragment (HindIII/ SacI) was subcloned into the pBI121 vector by replacing the CaMV 35S promoter and GUS cassette, generating the plasmid pBI121 LAT52:PIP5K6A. The sense fragment of PIP5K6 amplified using the primer set (5'- AAGGATCCTTACCCTT-CGACTTCTTCC-3'/ 5'-AATCTAGACCTTTAGAGATAGTT-TGTCCT-3') was inserted into BamHI-XbaI sites in the vector pFGC5941 LAT52 to generate the sense construct pFGC594-LAT52-PIP5K6S (Gu et al., 2005). The intron-PIP5K6S fragment (ClaI/ XbaI) was inserted into the pGEM-3Zf vector, then the fragment of intron-PIP5K6S (KpnI/ XbaI) was ligated into the pBI121 LAT52:PIP5K6A, generating the plasmid pBI-LAT52-PIP5K6 RNAi construct.

PIP5K6 RNAi construct was introduced into *Agrobacterium tumefaciens* GV3101 and transformed into *Arabidopsis thaliana* (Col-0) using floral dipping method (Clough and Bent, 1998). Independent T3 homozygous plants were isolation using Kanamycin selection for further analysis. Pollen mRNA was extracted from WT and *PIP5K6* RNAi plants and then used for synthesis of cDNA using Qiagen RNAeasy Kit and Invitrogen

Superscript III Reverse Transcriptase Kit. RT-PCR experiments (30 cycles) with primer sets (PIP5K6-F: 5'- ATGTCGGTAG CACACGCAGA-3'/ PIP5K6-R: 5'-TAAGCATGAGTTCATAATTCTTATGACC-3'; UBQ10-F: 5'-GATCTTTGCCGGA AAACAATTGGAGGATGGT-3'/ UBQ10-R: 5'-CGACTTGTCATTAGAAAGAA AGAGATAACAGG-3') were carried out to determine mRNA level of *PIP5K6* in both WT Col0 and *PIP5K6* RNAi pollen.

Transient gene expression in tobacco pollen tubes

Mature pollen grains collected from tobacco flowers (*Nicotiana tabacum*) were used for transient expression using a particle bombardment procedure as described previously (Fu et al., 2001). For all plasmid constructs used in our experiments, 0.2-1 μg plasmid DNA was used for each bombardment. Bombarded pollen grains were germinated in liquid germination medium for various times before observation under a microscope (Fu et al., 2001).

Analysis of Arabidopsis pollen tube growth

Flowers from Arabidopsis thaliana plants two weeks after bolting were used as source of pollen. Pollen grains were germinated on a solid germination medium (Li et al., 1999). Unless indicated otherwise, approximately 3–5 hours after germination, image of pollen tubes were recorded through a cooled CCD camera (model C4742-95; Hamamatsu)

attached on an Eclipse inverted microscope (model TE300; Nikon). The images were analyzed using the MetaMorph v4.5 measurement function.

PLC inhibitor treatment

U-73122 (Sigma) PLC inhibitor (in 0.1% DMSO) was added into tobacco pollen to a final concentration of 10 μM right after bombardment with a particular construct. A mock treatment (0.1% DMSO) was used as control. Five hours after pollen germination, pollen tubes were examined under a confocal microscope (Leica, SP2).

FM 4-64 dye staining in pollen tubes

FM 4-64 dye staining was carried out at 4-5 hours after pollen germination. For tobacco pollen tubes, FM4-64 dye (Sigma) was added to a final concentration of 2.5 μM into liquid pollen germination medium. For Arabidopsis pollen tubes, a droplet (10 μL) of liquid Arabidopsis pollen germination medium containing 10 μM FM 4-64 dye was applied onto thin layers of solid Arabidopsis pollen germination medium. Pollen tubes were incubated with FM 4-64 dye for 10-15 minutes before examination under a confocal microscope (Leica, SP2 or Zeiss, LSM510).

Immunostaining of clathrin heavy chain in pollen tubes

Pollen grains of Arabidopsis flowers were germinated in solid germination medium for 4 hours at room temperature and stained as described previously (Hwang et al., 2008). Pollen tubes were treated with fixative (4% paraformaldehyde, 3 mM $MgSO_4$, 2mM

$CaCl_2$, 18% Sucrose, 50 mM PIPES buffer, pH 6.9) for 1 hour. After washing gently with PBST (0.05% Triton X-100) buffer 3 times with 5 minutes each, pollen tubes were treated with digestion buffer (2% cellulase R-10, 400 mM Mannitol, 5 mM $CaCl_2$, 15 mM MES buffer, pH 5.5) at room temperature for 3-5 min. Digested pollen tubes were washed gently with PBST buffer three times for 5 minutes each and then were blocked with 1% nonfat milk in PBS buffer at room temperature for 1 hr. Pollen tubes were incubated with the purified primary anti-CHC (anti-Clathrin Heavy Chain antibody) (Kim et al., 2001) polyclonal antibody (1:200 dilution with 1% nonfat milk in PBS buffer) at room temperature for 1 hour. After washing three times for 10 minutes each in PBST buffer, pollen tubes were incubated with secondary antibody, FITC-conjugated goat anti-rabbit IgG (1:300 dilution with 1% nonfat milk in PBS buffer) at room temperature for 2 hours. After three washes with PBST buffer, slides were mounted with mount solution (0.1% p-phenylenediamine, 50% glycerol, PBS buffer). Mounted pollen tubes were observed under a Confocal Microscope (Leica SP2).

Confocal microscopy and imaging analysis

GFP localization. Localization patterns for GFP-tagged proteins in pollen tubes were observed under a confocal microscope (Leica SP2 or Zeiss LSM510). The signal intensities of GFP on the PM and in the cytoplasm were measured using the MetaMorph v4.5 measurement function. The PM region for GFP intensity measurement was measured by defining the peripheral region of the pollen tube as the PM. Apical PM region for intensity measurement in Tobacco pollen tubes was defined as the first 6 μm

along PM from the apical point. A circular region (4 μm in diameter) 4 μm away from tip was chosen for the measurement of cytosolic GFP intensity. Relative localization of GFP-labeled protein on the PM was calculated as the ratio of PM intensity vs cytosolic intensity.

FM 4-64 dye localization.

FM 4-64 dye labeled pollen tubes were observed under Leica SP2 confocal microscope or Zeiss LSM510 confocal microscope. The signal intensities of FM dye on the PM and in the cytoplasm were measured using the MetaMorph v4.5 measurement function. Apical PM region for intensity measurement in tobacco and Arabidopsis pollen tubes were defined as the first 6 μm and 4 μm along PM from the tip point, respectively. A circlular region (4 μm in diameter) 4 μm away from tip was chosen for measurement of cytosol intensity. Relative localization of FM dye on the plasma membrane was calculated to show the degree of internalization of FM dye.

Clathrin heavy chain localization.

Arabidopsis pollen tubes stained with anti-CHC primary antibody and FITC conjugated secondary antibody were observed under a Leica SP2 Confocal microscope. Median planes of pollen tubes were scanned to show the sub-cellular localization pattern of clathrin heavy chain.

The signal intensities of FITC-antibody on the PM and in the cytoplasm were measured using the MetaMorph v4.5 measurement function. Apical PM region for intensity

measurement in Arabidopsis pollen tubes was defined as the first 4 μm along PM from the tip point. A circular region (4 μm in diameter) 4 μm away from tip was chosen for measurement of cytosol intensity. Relative localization of FITC-antibody on the PM was calculated as the ratio of PM intensity vs. cytosolic intensity.

FRAP analysis.

Tobacco pollen tubes expressing RLK-GFP PM marker alone and coexpressing RLK-GFP plama membrane marker and PIP5K6 were used for FRAP analysis (Lee et al., 2008). The apical region of pollen tubes was photobleached using a strong laser with wavelength of 488 nm, and the recovery of fluorescence in pollen tubes was tracked in the following 3 minutes using a confocal microscope (Leica SP2). Time interval between adjacent frames was 10 seconds. Relative intensity of membrane-localized RLK-GFP compared to fluorescence before photobleaching was used to quantify the speed of fluorescence recovery.

Accession Numbers

Sequence data from this article can be found in the Arabidopsis Genome Initiative database under following accession numbers: PIP5K6 (At3g07960), PLC2 (At3g08510), PI4Kβ1(At5g64070), RLK PM marker (At5g35390), CHC HUB (At3g11130) and AP180 (At1g05020).

References

Baluska, F., Hlavacka, A., Samaj, J., Palme, K., Robinson, D.G., Matoh, T., McCurdy, D.W., Menzel, D., and Volkmann, D. (2002). F-actin-dependent endocytosis of cell wall pectins in meristematic root cells. Insights from brefeldin A-induced compartments. Plant Physiol **130,** 422-431.

Barth, M., and Holstein, S.E. (2004). Identification and functional characterization of Arabidopsis AP180, a binding partner of plant alphaC-adaptin. J Cell Sci **117,** 2051-2062.

Blackbourn, H.D., and Jackson, A.P. (1996). Plant clathrin heavy chain: sequence analysis and restricted localisation in growing pollen tubes. J Cell Sci **109,** 777-786.

Cheung, A.Y., and Wu, H.M. (2008). Structural and signaling networks for the polar cell growth machinery in pollen tubes. Annu Rev Plant Biol **59,** 547-572.

Clough, S.J., and Bent, A.F. (1998). Floral dip: a simplified method for Agrobacterium-mediated transformation of Arabidopsis thaliana. Plant J **16,** 735-743.

Conner, S.D., and Schmid, S.L. (2003). Regulated portals of entry into the cell. Nature **422,** 37-44.

de Graaf, B.H., Cheung, A.Y., Andreyeva, T., Levasseur, K., Kieliszewski, M., and Wu, H.M. (2005). Rab11 GTPase-regulated membrane trafficking is crucial for tip-focused pollen tube growth in tobacco. Plant Cell **17,** 2564-2579.

Derksen, J., Rutten, T., Lichtscheidl, I.K., Win, A.H.N.d., Pierson, E.S., and Rongen, G. (1995). Quantitative analysis of the distribution of organelles in tobacco pollen tubes: implications for exocytosis and endocytosis. Protoplasma **188,** 267-276.

Dhonukshe, P., Aniento, F., Hwang, I., Robinson, D.G., Mravec, J., Stierhof, Y.D., and Friml, J. (2007). Clathrin-mediated constitutive endocytosis of PIN auxin efflux carriers in Arabidopsis. Curr Biol **17,** 520-527.

Dhonukshe, P., Tanaka, H., Goh, T., Ebine, K., Mahonen, A.P., Prasad, K., Blilou, I., Geldner, N., Xu, J., Uemura, T., Chory, J., Ueda, T., Nakano, A., Scheres, B., and Friml, J. (2008). Generation of cell polarity in plants links endocytosis, auxin distribution and cell fate decisions. Nature **456,** 962-966.

Di Paolo, G., and De Camilli, P. (2006). Phosphoinositides in cell regulation and membrane dynamics. Nature **443,** 651-657.

Dowd, P.E., Coursol, S., Skirpan, A.L., Kao, T.H., and Gilroy, S. (2006). Petunia phospholipase c1 is involved in pollen tube growth. Plant Cell **18,** 1438-1453.

Fu, Y., Wu, G., and Yang, Z. (2001). Rop GTPase-dependent dynamics of tip-localized F-actin controls tip growth in pollen tubes. J Cell Biol **152,** 1019-1032.

Furutani, M., Tsujita, K., Itoh, T., Ijuin, T., and Takenawa, T. (2006). Application of phosphoinositide-binding domains for the detection and quantification of specific phosphoinositides. Anal Biochem **355,** 8-18.

Geldner, N., Hyman, D.L., Wang, X., Schumacher, K., and Chory, J. (2007). Endosomal signaling of plant steroid receptor kinase BRI1. Genes Dev **21,** 1598-1602.

Gu, Y., Fu, Y., Dowd, P., Li, S., Vernoud, V., Gilroy, S., and Yang, Z. (2005). A Rho family GTPase controls actin dynamics and tip growth via two counteracting downstream pathways in pollen tubes. J Cell Biol **169,** 127-138.

Helling, D., Possart, A., Cottier, S., Klahre, U., and Kost, B. (2006). Pollen tube tip growth depends on plasma membrane polarization mediated by tobacco PLC3 activity and endocytic membrane recycling. Plant Cell **18,** 3519-3534.

Hill, E., van Der Kaay, J., Downes, C.P., and Smythe, E. (2001). The role of dynamin and its binding partners in coated pit invagination and scission. J Cell Biol **152,** 309-323.

Holdaway-Clarke, T.L., Feijo, J.A., Hackett, G.R., Kunkel, J.G., and Hepler, P.K. (1997). Pollen Tube Growth and the Intracellular Cytosolic Calcium Gradient Oscillate in Phase while Extracellular Calcium Influx Is Delayed. Plant Cell **9,** 1999-2010.

Holstein, S.E., and Oliviusson, P. (2005). Sequence analysis of Arabidopsis thaliana E/ANTH-domain-containing proteins: membrane tethers of the clathrin-dependent vesicle budding machinery. Protoplasma **226,** 13-21.

Hwang, J.U., Vernoud, V., Szumlanski, A., Nielsen, E., and Yang, Z. (2008). A tip-localized RhoGAP controls cell polarity by globally inhibiting Rho GTPase at the cell apex. Curr Biol **18,** 1907-1916.

Im, Y.J., Davis, A.J., Perera, I.Y., Johannes, E., Allen, N.S., and Boss, W.F. (2007a). The N-terminal membrane occupation and recognition nexus domain of Arabidopsis phosphatidylinositol phosphate kinase 1 regulates enzyme activity. J Biol Chem **282,** 5443-5452.

Im, Y.J., Perera, I.Y., Brglez, I., Davis, A.J., Stevenson-Paulik, J., Phillippy, B.Q., Johannes, E., Allen, N.S., and Boss, W.F. (2007b). Increasing plasma membrane phosphatidylinositol(4,5)bisphosphate biosynthesis increases phosphoinositide metabolism in Nicotiana tabacum. Plant Cell **19,** 1603-1616.

Ischebeck, T., Stenzel, I., and Heilmann, I. (2008). Type B phosphatidylinositol-4-phosphate 5-kinases mediate Arabidopsis and Nicotiana tabacum pollen tube growth by regulating apical pectin secretion. Plant Cell **20,** 3312-3330.

Kaksonen, M., Toret, C.P., and Drubin, D.G. (2006). Harnessing actin dynamics for clathrin-mediated endocytosis. Nat Rev Mol Cell Biol **7,** 404-414.

Kang, B.H., Busse, J.S., and Bednarek, S.Y. (2003). Members of the Arabidopsis dynamin-like gene family, ADL1, are essential for plant cytokinesis and polarized cell growth. Plant Cell **15,** 899-913.

Kim, Y.W., Park, D.S., Park, S.C., Kim, S.H., Cheong, G.W., and Hwang, I. (2001). Arabidopsis dynamin-like 2 that binds specifically to phosphatidylinositol 4-phosphate assembles into a high-molecular weight complex in vivo and in vitro. Plant Physiol **127,** 1243-1255.

Kleine-Vehn, J., and Friml, J. (2008). Polar targeting and endocytic recycling in auxin-dependent plant development. Annu Rev Cell Dev Biol **24,** 447-473.

Konig, S., Ischebeck, T., Lerche, J., Stenzel, I., and Heilmann, I. (2008). Salt-stress-induced association of phosphatidylinositol 4,5-bisphosphate with clathrin-coated vesicles in plants. Biochem J **415,** 387-399.

Kost, B., Lemichez, E., Spielhofer, P., Hong, Y., Tolias, K., Carpenter, C., and Chua, N.H. (1999). Rac homologues and compartmentalized phosphatidylinositol 4, 5-bisphosphate act in a common pathway to regulate polar pollen tube growth. J Cell Biol **145,** 317-330.

Kusano, H., Testerink, C., Vermeer, J.E., Tsuge, T., Shimada, H., Oka, A., Munnik, T., and Aoyama, T. (2008). The Arabidopsis Phosphatidylinositol Phosphate 5-Kinase PIP5K3 is a key regulator of root hair tip growth. Plant Cell **20,** 367-380.

Lee, Y.J., and Yang, Z. (2008). Tip growth: signaling in the apical dome. Curr Opin Plant Biol. **11,** 662-671.

Lee, Y.J., Szumlanski, A., Nielsen, E., and Yang, Z. (2008). Rho-GTPase-dependent filamentous actin dynamics coordinate vesicle targeting and exocytosis during tip growth. J Cell Biol **181,** 1155-1168.

Li, H., Lin, Y., Heath, R.M., Zhu, M.X., and Yang, Z. (1999). Control of pollen tube tip growth by a Rop GTPase-dependent pathway that leads to tip-localized calcium influx. Plant Cell **11,** 1731-1742.

Lin, Y., Wang, Y., Zhu, J.K., and Yang, Z. (1996). Localization of a Rho GTPase Implies a Role in Tip Growth and Movement of the Generative Cell in Pollen Tubes. Plant Cell **8,** 293-303.

Liu, S.H., Wong, M.L., Craik, C.S., and Brodsky, F.M. (1995). Regulation of clathrin assembly and trimerization defined using recombinant triskelion hubs. Cell **83,** 257-267.

Monteiro, D., Castanho Coelho, P., Rodrigues, C., Camacho, L., Quader, H., and Malho, R. (2005a). Modulation of endocytosis in pollen tube growth by phosphoinositides and phospholipids. Protoplasma **226,** 31-38.

Monteiro, D., Liu, Q., Lisboa, S., Scherer, G.E., Quader, H., and Malho, R. (2005b). Phosphoinositides and phosphatidic acid regulate pollen tube growth and reorientation through modulation of $[Ca^{2+}]c$ and membrane secretion. J Exp Bot **56,** 1665-1674.

Moscatelli, A., Ciampolini, F., Rodighiero, S., Onelli, E., Cresti, M., Santo, N., and Idilli, A. (2007). Distinct endocytic pathways identified in tobacco pollen tubes using charged nanogold. J Cell Sci **120,** 3804-3819.

Mousavi, S.A., Malerod, L., Berg, T., and Kjeken, R. (2004). Clathrin-dependent endocytosis. Biochem J **377,** 1-16.

Mueller-Roeber, B., and Pical, C. (2002). Inositol phospholipid metabolism in Arabidopsis. Characterized and putative isoforms of inositol phospholipid kinase and phosphoinositide-specific phospholipase C. Plant Physiol **130,** 22-46.

Myers, C., Romanowsky, S.M., Barron, Y.D., Garg, S., Azuse, C.L., Curran, A., Davis, R.M., Hatton, J., Harmon, A.C., and Harper, J.F. (2009). Calcium-dependent protein kinases regulate polarized tip growth in pollen tubes. Plant J **59,** 528-539.

Perera, R.M., Zoncu, R., Lucast, L., De Camilli, P., and Toomre, D. (2006). Two synaptojanin 1 isoforms are recruited to clathrin-coated pits at different stages. Proc Natl Acad Sci U S A **103,** 19332-19337.

Preuss, M.L., Schmitz, A.J., Thole, J.M., Bonner, H.K., Otegui, M.S., and Nielsen, E. (2006). A role for the RabA4b effector protein PI-4Kbeta1 in polarized expansion of root hair cells in Arabidopsis thaliana. J Cell Biol **172,** 991-998.

Sousa, E., Kost, B., and Malho, R. (2008). Arabidopsis phosphatidylinositol-4-monophosphate 5-kinase 4 regulates pollen tube growth and polarity by modulating membrane recycling. Plant Cell **20,** 3050-3064.

Stenzel, I., Ischebeck, T., Konig, S., Holubowska, A., Sporysz, M., Hause, B., and Heilmann, I. (2008). The type B phosphatidylinositol-4-phosphate 5-kinase 3 is essential for root hair formation in Arabidopsis thaliana. Plant Cell **20,** 124-141.

Sun, Y., Kaksonen, M., Madden, D.T., Schekman, R., and Drubin, D.G. (2005). Interaction of Sla2p's ANTH domain with PtdIns(4,5)P2 is important for actin-dependent endocytic internalization. Mol Biol Cell **16,** 717-730.

Sun, Y., Carroll, S., Kaksonen, M., Toshima, J.Y., and Drubin, D.G. (2007). PtdIns(4,5)P2 turnover is required for multiple stages during clathrin- and actin-dependent endocytic internalization. J Cell Biol **177,** 355-367.

Szumlanski, A.L., and Nielsen, E. (2009). The Rab GTPase RabA4d regulates pollen tube tip growth in Arabidopsis thaliana. Plant Cell **21,** 526-544.

Thole, J.M., Vermeer, J.E., Zhang, Y., Gadella, T.W., Jr., and Nielsen, E. (2008). Root hair defective4 encodes a phosphatidylinositol-4-phosphate phosphatase required for proper root hair development in Arabidopsis thaliana. Plant Cell **20,** 381-395.

Vermeer, J.E., Thole, J.M., Goedhart, J., Nielsen, E., Munnik, T., and Gadella, T.W., Jr. (2009). Imaging phosphatidylinositol 4-phosphate dynamics in living plant cells. Plant J **57,** 356-372.

Vidali, L., McKenna, S.T., and Hepler, P.K. (2001). Actin polymerization is essential for pollen tube growth. Mol Biol Cell **12,** 2534-2545.

Yalovsky, S., Bloch, D., Sorek, N., and Kost, B. (2008). Regulation of membrane trafficking, cytoskeleton dynamics, and cell polarity by ROP/RAC GTPases. Plant Physiol **147,** 1527-1543.

Yang, Z. (2008). Cell polarity signaling in Arabidopsis. Annu Rev Cell Dev Biol **24,** 551-575.

Yin, H.L., and Janmey, P.A. (2003). Phosphoinositide regulation of the actin cytoskeleton. Annu Rev Physiol **65,** 761-789.

Yoon, G.M., Dowd, P.E., Gilroy, S., and McCubbin, A.G. (2006). Calcium-dependent protein kinase isoforms in Petunia have distinct functions in pollen tube growth, including regulating polarity. Plant Cell **18,** 867-878.

Zimmermann, P., Hirsch-Hoffmann, M., Hennig, L., and Gruissem, W. (2004). GENEVESTIGATOR. Arabidopsis microarray database and analysis toolbox. Plant Physiol **136,** 2621-2632.

Zoncu, R., Perera, R.M., Sebastian, R., Nakatsu, F., Chen, H., Balla, T., Ayala, G., Toomre, D., and De Camilli, P.V. (2007). Loss of endocytic clathrin-coated pits upon acute depletion of phosphatidylinositol 4,5-bisphosphate. Proc Natl Acad Sci U S A **104,** 3793-3798.

Zonia, L., and Munnik, T. (2008). Vesicle trafficking dynamics and visualization of zones of exocytosis and endocytosis in tobacco pollen tubes. J Exp Bot **59,** 861-873.

Figures

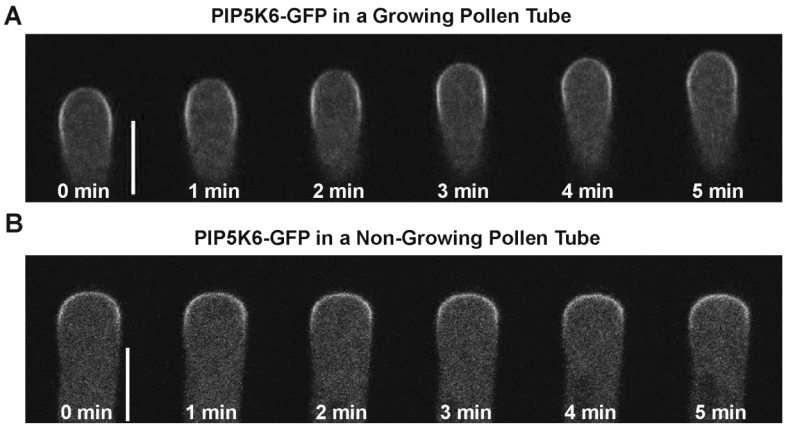

Figure 3.1. *PIP5K6*-GFP is localized to subapical PM in growing tobacco pollen tubes.
Localization of *PIP5K6*-GFP in tobacco pollen tubes were examined using bombardment mediated transient expression method. Median images were taken using Leica SP2 confocal microscope 4-5 hours after bombardment.
(A). Time course (5 minutes) of a growing tobacco pollen tube expressing PIP5K6-GFP. Bar = 10 μm. Note the strong PIP5K6-GFP signal at subapical PM.
(B). Time course (5 minutes) of a non-growing tobacco pollen tube expressing PIP5K6-GFP. Note the strong PIP5K6-GFP signal at apex of pollen tube.

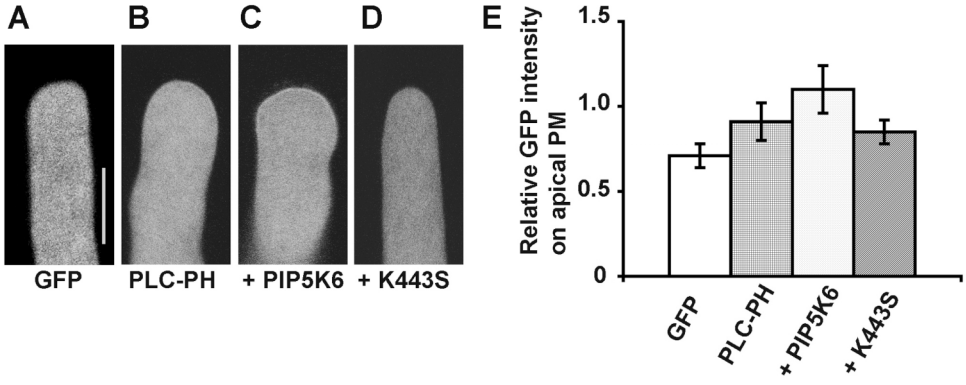

Figure 3.2. *PIP5K6* OX increases PI(4,5)P2 on apical PM of tobacco pollen tubes.
(A). A tobacco pollen tube transiently expressing GFP alone at 4 hours after bombardment. Note that GFP signal is not associated with PM. Bar = 10 μm.
(B). A tobacco pollen tube transiently expressing PI(4,5)P2 marker GFP-PLCδ1 PH at 4 hours after bombardment. This marker exhibited a weak signal in the apical PM.
(C). A tobacco pollen tube transiently expressing GFP-PLCδ1 PH marker and *PIP5K6* at 4 hours after bombardment. GFP-PLCδ1 PH Marker exhibited a stronger association with apical PM.
(D). A tobacco pollen tube transiently expressing GFP-PLCδ1 PH marker and *PIP5K6 K443S* at 4 hours after bombardment. GFP-PLCδ1 PH marker exhibited a weak association with apical PM.
(E). Relative GFP localization on the PM (PM GFP signal:cytosolic GFP signal) in GFP control, GFP-PLCδ1 PH marker alone, and GFP-PLCδ1 PH coexpressed with *PIP5K6* or *PIP5K6 K443S* co-expressed (Error bars indicate SD, n=15.). *PIP5K6* OX significantly increased PI(4,5)P2 level on the apical PM of pollen tubes (student's t-test value $p<0.05$), and *PIP5K6 K443S* OX did not significantly change PI(4,5)P2 level on the apical PM of pollen tubes (student's t-test value $p>0.05$).

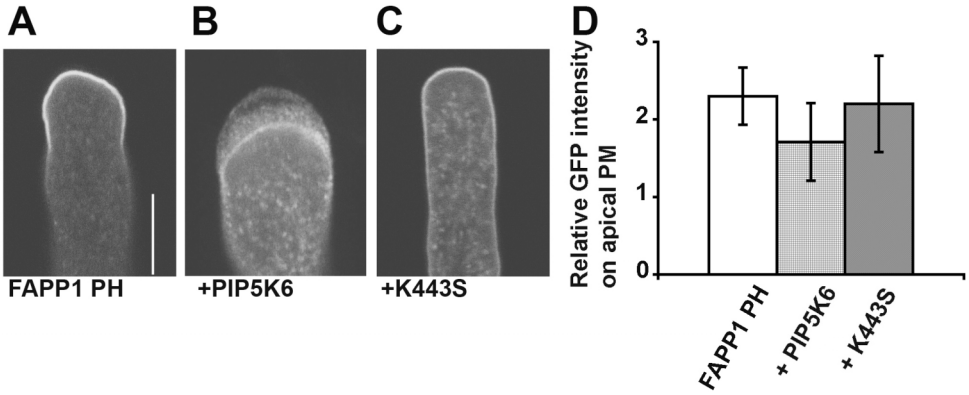

Figure 3.3. *PIP5K6* OX suppresses PI4P on apical PM of tobacco pollen tubes.
(A). A tobacco pollen tube transiently expressing PI4P marker GFP-FAPP1 PH at 4 hours after bombardment. Bar = 10 μm.
(B). A tobacco pollen tube transiently expressing GFP-FAPP1 PH marker and *PIP5K6* at 4 hours after bombardment. Note that increased localization of GFP-FAPP1 PH marker to vesicles in cell and decreased localization of GFP-FAPP1 PH marker to the PM.
(C). A tobacco pollen tube transiently expressing GFP-FAPP1 PH marker and *PIP5K6 K443S* at 4 hours after bombardment.
(D). Relative GFP-FAPP1 PH localization on the PM (PM GFP signal:cytosolic GFP signal) in control, *PIP5K6* and *PIP5K6 K443S* co-expressed pollen tubes (Error bars indicate SD, n=15.). *PIP5K6* OX significantly decreases PI4P level on the apical PM of pollen tubes (student's t-test value $p<0.05$), and *PIP5K6 K443S* OX does not significantly change the PI4P level on apical PM of pollen tubes (student's t-test value $p>0.05$).

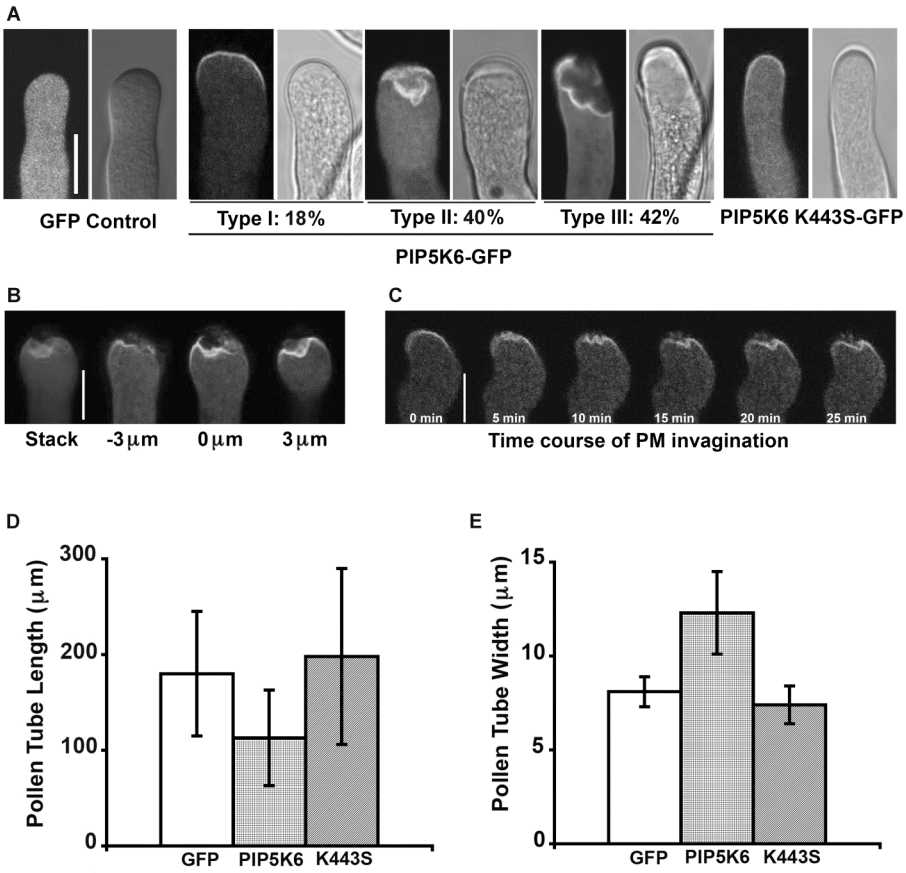

Figure 3.4. *PIP5K6* OX phenotype in tobacco pollen tubes.
Phenotype of tobacco pollen tubes transiently overexpressing *GFP, PIP5K6-GFP* and *PIP5K6 K443S-GFP*.
(A). Left two panels: GFP control is not PM associated and does not cause any defect of PM.
Middle 6 panels: Overexpression of *PIP5K6-GFP* causes PM deformation at the apical region of pollen tube. At 4-5 hours after bombardment, the percentage of *PIP5K6-GFP*-overexpressing tobacco pollen tubes that displayed little, moderate, and severe PM deformation was 18%, 40% and 42%, respectively (n=100). Bar = 10 μm. Right two panels: *PIP5K6 K443S-GFP*-overexpressing tobacco pollen tubes display no PM deformation. PIP5K6 K443S-GFP signal is strong at apical PM of pollen tube.
(B). Extensive PM deformation at different focal planes in a *PIP5K6-GFP*-overexpressing tobacco pollen tube. Stack image is shown on the left, and selected different images at different focal planes are shown on the right.
(C). Time course (25 minutes) of PM invagination event in a tobacco pollen tube expressing PIP5K6-GFP. Note that the pollen tube is not growing during PM invagination.
(D)-(E). Length and width of tobacco pollen tubes were measured 4-5 hours after bombardment. Overexpression of *PIP5K6-GFP* caused shorter and wider pollen tubes compared to *GFP* OX control (n=30, error bars indicate SD, student's t-test value $p<0.05$). *PIP5K6 K443S-GFP* OX does not have significant effect on pollen tube growth (n=30, error bars indicate SD, student's t-test value $p>0.05$).

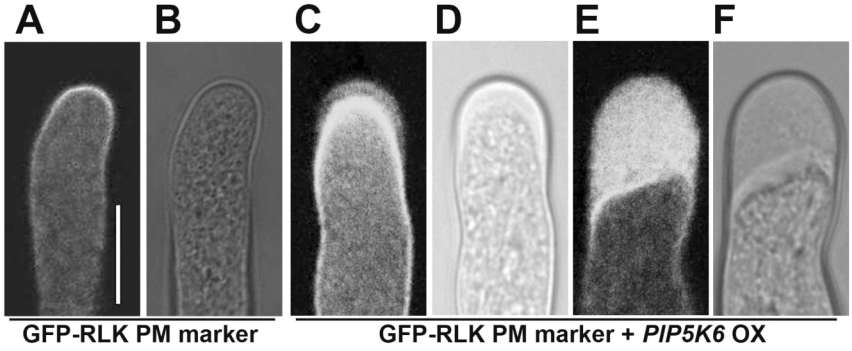

Figure 3.5. *PIP5K6* OX induces PM deformation in tobacco pollen tubes.
(A)-(B). A tobacco pollen tube transiently expressing *GFP-RLK* PM marker alone at 4 hours after bombardment. No PM deformation was observed. Bar = 10 μm. GFP channel: (A). Bright field channel: (B).
(C)-(F). Tobacco pollen tubes transiently co-expressing *GFP-RLK* PM marker and *PIP5K6*. Different degrees of PM deformation can be seen in these types of pollen tubes at 4 hours after bombardment. GFP channel: (C) and (E). Bright field channel: (D) and (F).

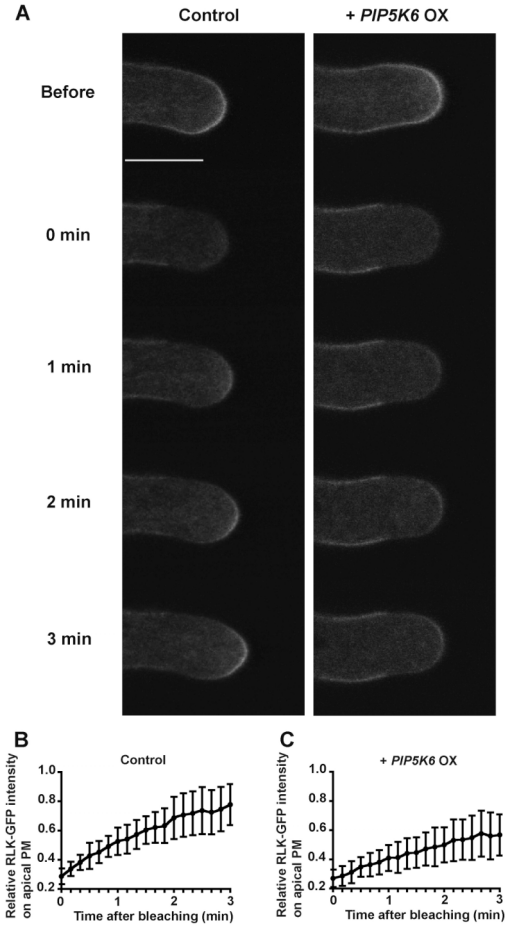

Figure 3.6. *PIP5K6* OX did not enhance exocytosis in tobacco pollen tubes.
To test whether PIP5K6 OX increased exocytosis in tobacco pollen tubes, fluorescence recovery after photobleaching (FRAP) method was used (Lee et al., 2008). The apical PM region of pollen tubes expressing GFP-RLK was photobleached using a strong laser with wavelength of 488 nm, and the recovery of fluorescence was tracked in the following 3 minutes using a confocal microscope (Leica SP2). The recovery of GFP-RLK signal indicates exocytosis.
(A). Left: A time course of FRAP in a tobacco pollen tube expressing GFP-RLK alone. Bar = 10 μm. Right: A time course of FRAP in a tobacco pollen tube co-expressing *GFP-RLK* and *PIP5K6*. Note that PIP5K6 OX pollen tubes analyzed were growing, but elongated at a slower rate than control tubes. The mean elongation rate for control pollen tubes and PIP5K6 OX tubes was 0.9 μm/min and 0.3 μm/min, respectively.
(B). Quantitative analysis of FRAP time courses of pollen tubes expressing *GFP-RLK* alone. Relative intensity of membrane-localized RLK-GFP compared to fluorescence before photobleaching was used to quantify the speed of fluorescence recovery. Mean values of FRAP signals are shown (n=10, error bars indicate SD).
(C). Quantitative analysis of FRAP time courses of pollen tubes expressing *GFP-RLK* and *PIP5K6*. Relative intensity of membrane-localized RLK-GFP compared to fluorescence before photobleaching was used to quantify the speed of fluorescence recovery. Mean values of FRAP signals are shown (n=10, error bars indicate SD). Recovery of GFP-RLK signal on the PM was significantly slower than that in control pollen tubes (student's t-test value $p<0.05$).

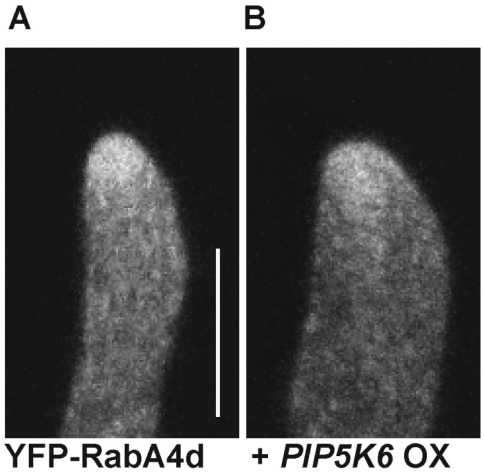

Figure 3.7. *PIP5K6* OX did not change RabA4d localization pattern in tobacco pollen tube tips.
Effect of *PIP5K6* OX on the distribution of exocytic vesicle marker RabA4d localization was analyzed by co-expressing *YFP-RabA4d* and *PIP5K6* using particle bombardment method.
(A). A tobacco pollen tube transiently expressing *YFP-RabA4d* at 4 hours after bombardment (n=20). YFP-RabA4d is an exocytic vesicle marker showing accumulation in the apical cytosol of tobacco pollen tubes. Bar = 10 μm.
(B). A tobacco pollen tube transiently expressing *YFP-RabA4d* and *PIP5K6* at 4 hours after bombardment (n=20). *PIP5K6* OX did not change accumulation of RabA4d in tobacco pollen tubes.

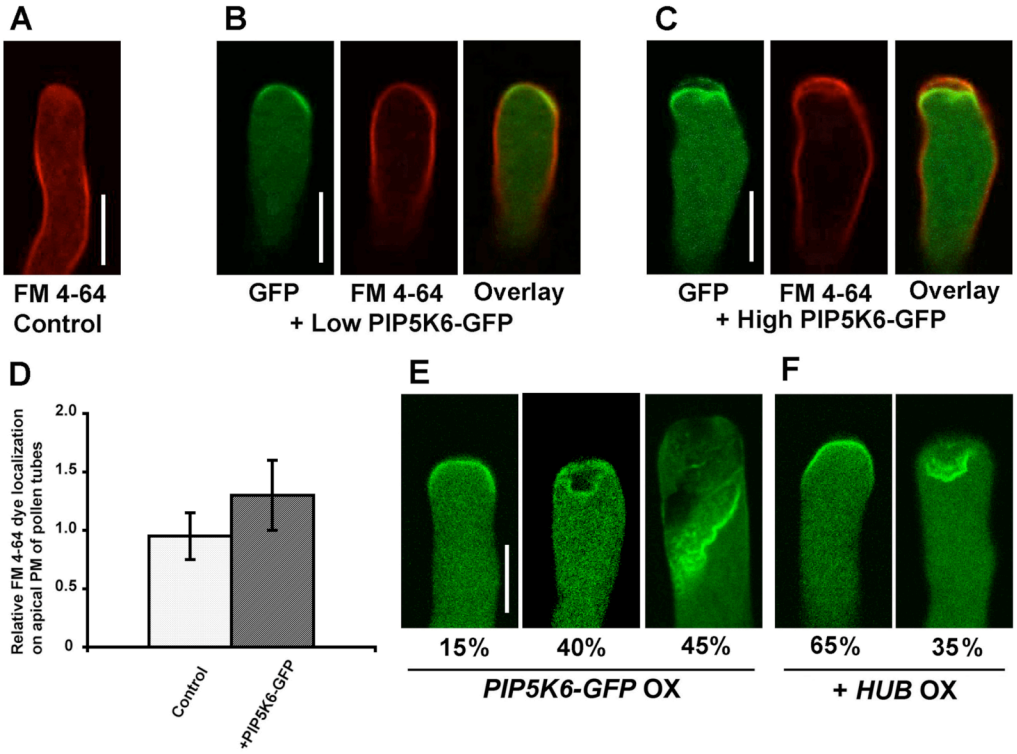

Figure 3.8. *PIP5K6* OX induces clathrin-dependent abortive endocytic compartments in pollen tubes.
(A). FM 4-64 dye uptake in a control tobacco pollen tube after 10-15 minutes of incubation.
Bar = 10 μm.
(B)-(C). FM 4-64 dye uptake in tobacco pollen tubes with different levels of *PIP5K6-GFP* overexpression.
(B): Low level of *PIP5K6-GFP* overexpression; (C): High level of *PIP5K6-GFP* overexpression.
(D). Analysis of relative FM 4-64 dye localization in control and *PIP5K6-GFP*-overexpressing tobacco pollen tubes. FM dye uptake is significantly suppressed by PIP5K6-GFP OX (n=20, student's t-test value $p<0.05$).
(E). 5-6 hours after bombardment, the percentage of *PIP5K6-GFP*-overexpressing tobacco pollen tubes that displayed little, moderate, and severe PM invagination was 15%, 40% and 45%, respectively (n=60).
(F). 5-6 hours after bombardment, 65% of pollen tubes overexpressing both *PIP5K6-GFP* and *HUB* showed normal smooth PM, while 35% exhibited moderate PM invagination, and none had severe PM invagination (n=60). *HUB* OX suppressed *PIP5K6-GFP* OX phenotype in tobacco pollen tubes (Fisher exact probability test value $p<0.05$).

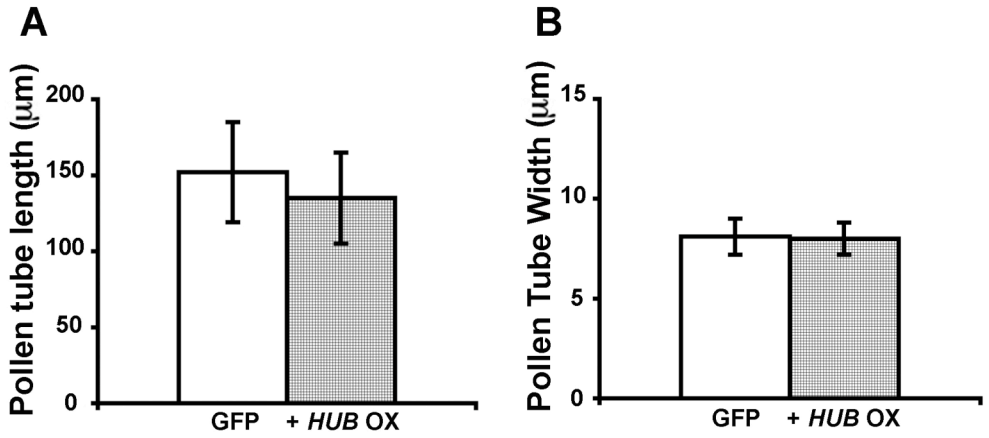

Figure 3.9. DN-CHC *HUB* OX slightly inhibits pollen tube growth.
The length (A) and width (B) of pollen tubes overexpressing GFP control and GFP with a dominant negative form of clathrin (*HUB*) in tobacco pollen tubes was determined at 4 hours after bombardment (Error bars indicate SD, n=30). Note that *HUB* OX only slightly inhibited pollen tube growth ($p<0.1$), and did not significantly change pollen tube width ($p>0.1$).

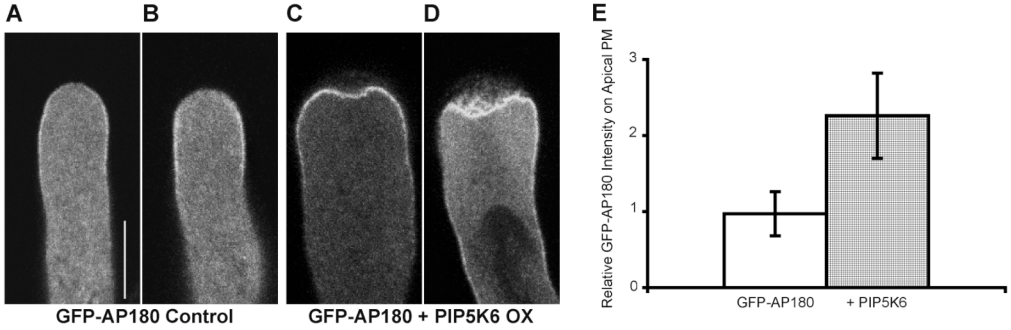

Figure 3.10. *PIP5K6* OX caused mislocalization of AP180.
Effect of *PIP5K6* OX on the localization of GFP-AP180 (a PIP2-binding proteins that reports the site of the initiation of clathrin-dependent endocytosis) was investigated by co-overexpressing *GFP-AP180* with *PIP5K6* using particle bombardment method.
(A)-(B). Tobacco pollen tubes transiently expressing *GFP-AP180* at 4 hours after bombardment. GFP-AP180 signal was preferentially localized to the subapical PM of pollen tubes. Bar = 10 μm.
(C)-(D). Tobacco pollen tubes transiently co-expressing *GFP-AP180* and *PIP5K6* at 4 hours after bombardment. Note that GFP-AP180 signal was preferentially localized to the apical PM and was associated with PM invagination sites, and the overall PM signal was greatly increased.
(E). Relative GFP-AP180 localization on apical PM (PM GFP signal:cytosolic GFP signal) in control and *PIP5K6* co-expressed pollen tubes (Error bars indicate SD, n=15.). *PIP5K6* OX significantly increases GFP-AP180 localization on the apical PM of pollen tubes (student's t-test value $p<0.05$).

Figure 3.11. *PIP5K6* RNAi inhibits clathrin-dependent endocytosis in Arabidopsis pollen tube.
(A). RT-PCR analysis of *PIP5K6* expression in *PIP5K6* RNAi pollen. Pollen RNA was extracted for RT-PCR analysis of *PIP5K6* mRNA expression.
(B). *PIP5K6* RNAi inhibits pollen tube growth by about 60%. Lengths of WT Col0 and *PIP5K6* RNAi pollen tubes are measured 4 hours after germination (n=100, error bars indicate SD, student's t-test value $p<0.05$.).
(C). WT Col0 and *PIP5K6* RNAi pollen tubes were cultured for 4 hours in solid germination medium. Bar = 100 μm.
(D). FM 4-64 dye staining in control and *PIP5K6* RNAi Arabidopsis pollen tubes. Bar = 10 μm. (E). The amount of the PM-localized FM 4-64 dye signal was quantified as FM 4-64 intensity at the apical PM divided by the cytosol FM 4-64 intensity. The mean value of this relative PM distribution of FM 4-64 dye at 15 minutes after incubation increased from 0.75 in control pollen tubes to 1.18 in *PIP5K6* RNAi pollen tubes (n=30, student's t-test value $p<0.05$).
(F). Immunostaining of clathrin heavy chain in WT Col0, *PIP5K6* RNAi and *pip5k4* pollen tubes. Bar = 10 μm. Median planes of pollen tubes were scanned to show the sub-cellular localization pattern of clathrin heavy chain. Arrow indicates PM localization of CHC antibody.
(G). Analysis of clathrin localization in WT Col0, *PIP5K6* RNAi and *pip5k4* pollen tubes. Both *PIP5K6* RNAi and *pip5k4* mutant pollen tubes show decreased clathrin association to PM. (n=20, error bars indicate SD, student's t-test value $p<0.05$).

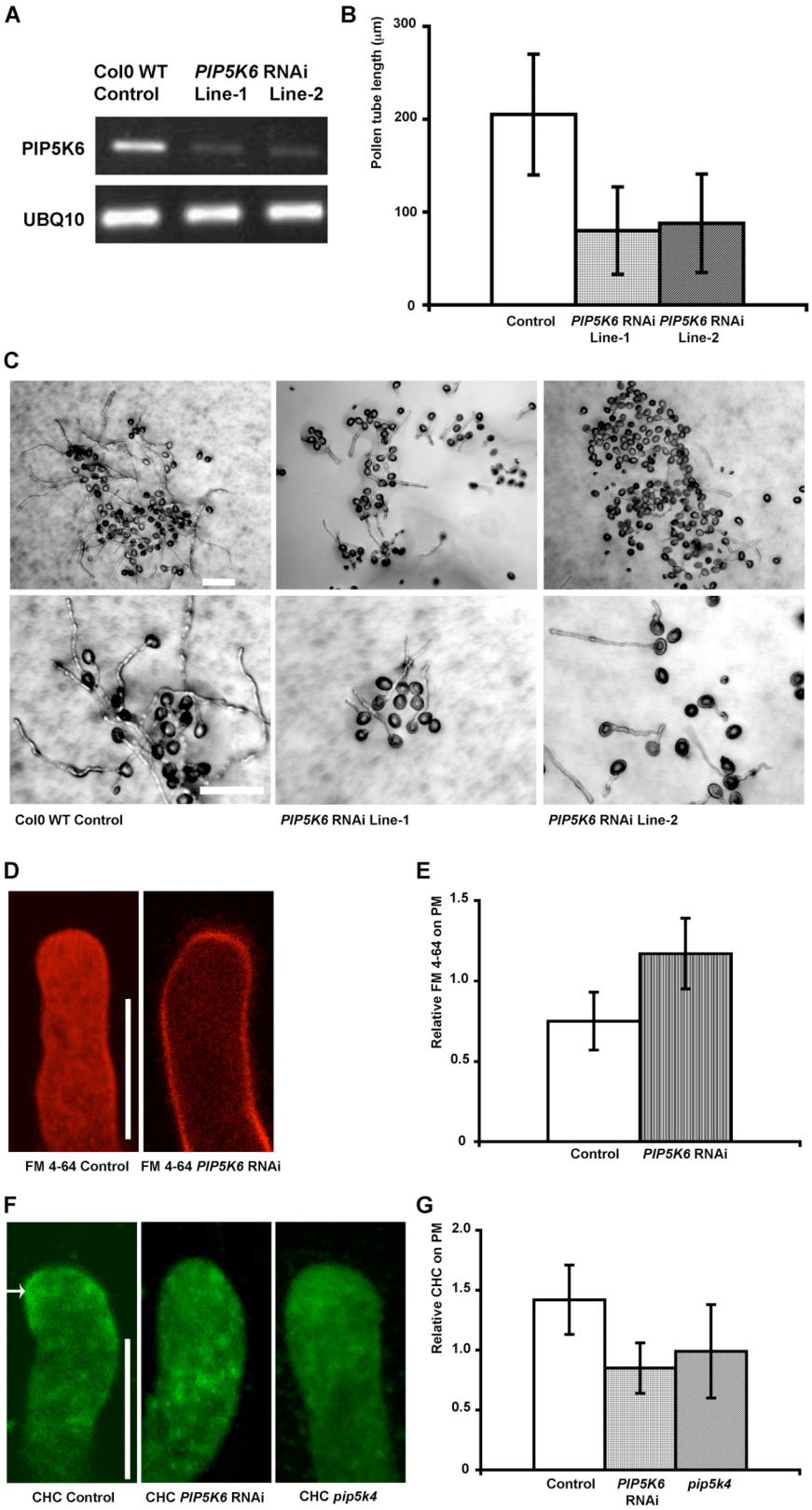
A
Col0 WT Control
PIP5K6 RNAi Line-1
PIP5K6 RNAi Line-2
PIP5K6
UBQ10
B
Pollen tube length (μm)
300
200
100
0
Control
PIP5K6 RNAi Line-1
PIP5K6 RNAi Line-2
C
Col0 WT Control
PIP5K6 RNAi Line-1
PIP5K6 RNAi Line-2
D
FM 4-64 Control
FM 4-64 PIP5K6 RNAi
E
Relative FM 4-64 on PM
1.5
1.0
0.5
0
Control
PIP5K6 RNAi
F
CHC Control
CHC PIP5K6 RNAi
CHC pip5k4
G
Relative CHC on PM
2.0
1.5
1.0
0.5
0
Control
PIP5K6 RNAi
pip5k4

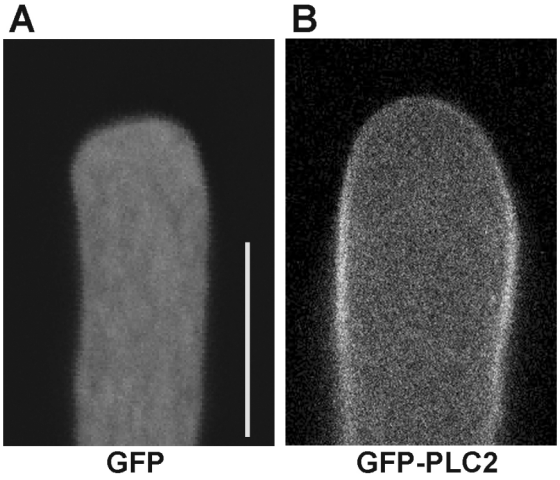

Figure 3.12. GFP-PLC2 was preferentially localized to the sub-apical PM of pollen tubes.
(A). A tobacco pollen tube transiently expressing *GFP* alone at 4 hours after bombardment. Note that GFP signal was not associated with the PM. Bar = 10 μm.
(B). A representative tobacco pollen tube transiently expressing *GFP-PLC2* at 4 hours after bombardment. Note that GFP-PLC2 was localized preferentially to the subapical PM, though weakly associated with the apical PM (n=15).

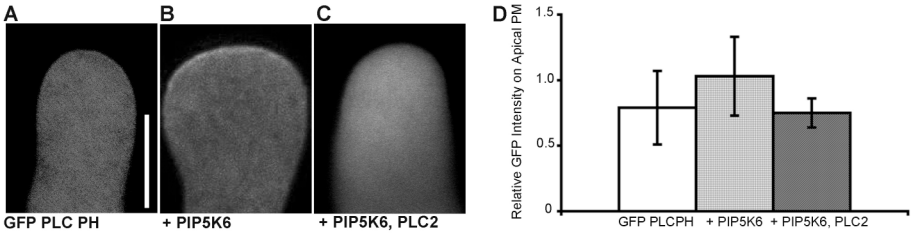

Figure 3.13. *PLC2* OX suppressed increase of PI(4,5)P2 induced by *PIP5K6* OX.
(A). A representative tobacco pollen tube transiently expressing PI(4,5)P2 marker *GFP-PLCδ1 PH* at 4 hours after bombardment. This marker exhibited a weak signal in the apical PM. Bar = 10 μm.
(B). A representative tobacco pollen tube transiently expressing *GFP-PLCδ1 PH* marker and *PIP5K6* at 4 hours after bombardment. GFP-PLCδ1 PH marker exhibited a stronger association with the apical PM when *PIP5K6* was overexpressed.
(C). To confirm that *PIP5K6* OX induced PI(4,5)P2 increase in the apical PM is suppressed by *PLC2* OX, PI(4,5)P2 marker *GFP-PLC δ1 PH* was used for co-bombardment with *PIP5K6* and *PLC2* into tobacco pollen tubes. Shown in (C) is a representative tobacco pollen tube at 4 hours after bombardment. Note that GFP-PLCδ1 PH marker is not associated with the apical PM.
(D). Relative GFP localization on the PM (PM GFP signal:cytosolic GFP signal) in GFP control, GFP-PLCδ1 PH marker alone, and GFP-PLCδ1 PH coexpressed with *PIP5K6* or *PIP5K6 plus PLC2* co-expressed (Error bars indicate SD, n>10.). *PIP5K6* OX significantly increased PI(4,5)P2 level on the apical PM of pollen tubes (student's t-test value $p<0.05$), and *PLC2* OX suppressed the increase in PI(4,5)P2 level on the apical PM of pollen tubes induced by *PIP5K6* OX (student's t-test value $p>0.05$).

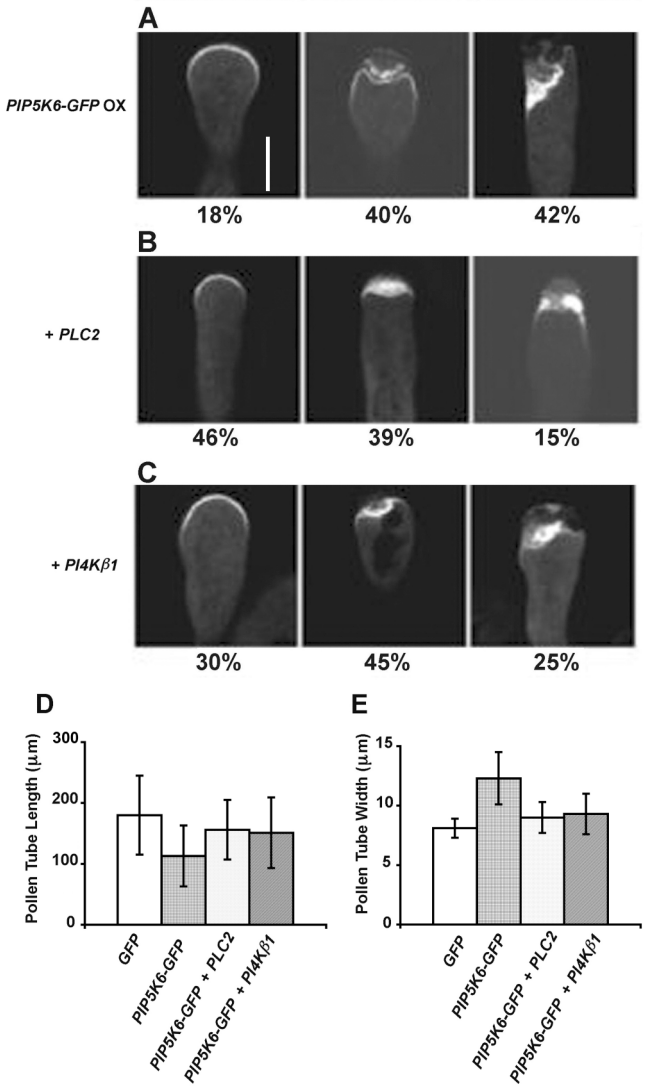

Figure 3.14. *PLC2* OX and *PI4Kβ1* OX suppress *PIP5K6* OX phenotype.
(A). *PIP5K6-GFP* OX phenotype in tobacco pollen tubes. At 4-5 hours after bombardment, the percentage of *PIP5K6-GFP* overexpressing tobacco pollen tubes that displayed little, moderate and severe PM deformation was 18%, 40% and 42%, respectively (n=100). Bar = 10 μm.
(B). At 4-5 hours after bombardment, the percentage of *PIP5K6-GFP* and *PLC2* co-overexpressing tobacco pollen tubes that displayed little, moderate and severe PM deformation was 46%, 39% and 15%, respectively (n=100). *PLC2* OX suppressed *PIP5K6-GFP* OX phenotype in tobacco pollen tubes (Fisher exact probability test value $p<0.05$).
(C). At 4-5 hours after bombardment, the percentage of *PIP5K6-GFP* and *PI4Kβ1* co-overexpressing tobacco pollen tubes that displayed little, moderate and severe PM deformation was 30%, 45% and 25%, respectively (n=100). *PI4Kβ1* OX suppressed *PIP5K6-GFP* OX phenotype in tobacco pollen tubes (Fisher exact probability test value $p<0.05$).
(D)-(E). Length and width of tobacco pollen tubes were measured 4-5 hours after bombardment. Overexpression of *PI4Kβ1* or *PLC2* both suppressed *PIP5K6* OX growth phenotype (n=30, error bars indicate SD, student's t-test value $p<0.05$).

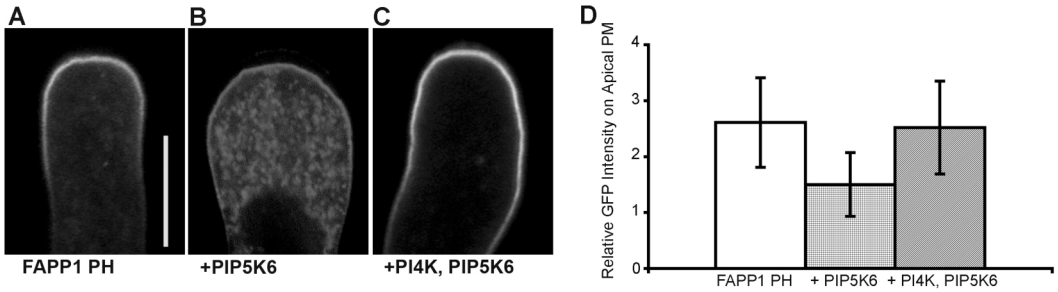

Figure 3.15. *PI4Kβ1* OX suppressed PI4P decrease induced by *PIP5K6* OX.
(A). A representative tobacco pollen tube transiently expressing PI4P marker *GFP-FAPP1 PH* at 4 hours after bombardment. Bar = 10 μm.
(B). A representative tobacco pollen tube transiently co-expressing *GFP-FAPP1 PH* marker and *PIP5K6* at 4 hours after bombardment. Note that increased localization of GFP-FAPP1 PH marker to vesicles in the cytosol and decreased localization of GFP-FAPP1 PH marker to PM.
(C). To confirm that *PIP5K6* OX induced PI4P reduction is rescued by *PI4Kβ1* OX, PI4P marker *GFP-FAPP1 PH* was used for co-bombardment with *PIP5K6* and *PI4Kβ1* into tobacco pollen tubes. Shown in (C) is a representative tobacco pollen tube at 4 hours after bombardment, no PI4P reduction is revealed by FAPP1 PH localization pattern.
(D). Relative GFP-FAPP1 PH localization on the PM (PM GFP signal:cytosolic GFP signal) in control, *PIP5K6* or *PIP5K6* and *PI4Kβ1* co-expressed pollen tubes (Error bars indicate SD, n=12.). *PIP5K6* OX significantly decreases PI4P level on the apical PM of pollen tubes (student's t-test value $p<0.05$), and *PIP5K6* plus *PI4Kβ1* OX does not significantly change the PI4P level on apical PM of pollen tubes (student's t-test value $p>0.05$).

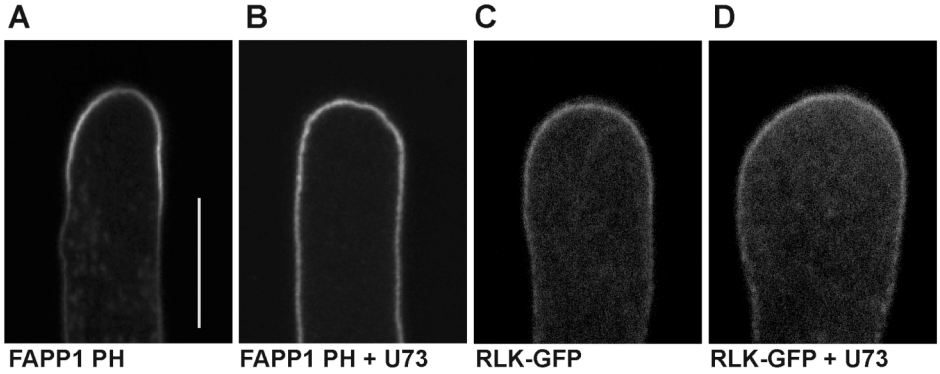

Figure 3.16. PLC inhibitor treatment increases PI4P localization and does not cause PM invagination in tobacco pollen tube.

(A)-(B) show the effect of PLC inhibitor U73122 treatment on PI4P distribution in tobacco pollen tubes. DMSO or U73122 were added into germination medium 3 hours after bombardment of *GFP-FAPP1 PH* construct into tobacco pollen. The inhibitor induced *GFP-FAPP1 PH* to distribute the whole PM.

(A). A representative tobacco pollen tube transiently expressing GFP-FAPP1 PH PI4P marker at 4 hours after bombardment and treated with 0.1% DMSO for 1 hour. Bar = 10 μm.

(B). A representative tobacco pollen tube transiently expressing GFP-FAPP1 PH PI4P marker at 4 hours after bombardment and treated with 10 μM U73122 for 1 hour. Note that GFP-FAPP1 PH marker localization is broader than control (n=30).

(C)-(D) show that treatment of U73122 alone cannot induce PM invagination phenotype in tobacco pollen tubes. DMSO or U73122 were added into germination medium 3 hours after bombardment of *RLK-GFP* construct into tobacco pollen.

(C). A tobacco pollen tube transiently expressing *RLK-GFP* PM marker at 4 hours after bombardment and treated with 0.1% DMSO for 1 hour.

(D). A tobacco pollen tube transiently expressing *RLK-GFP* PM marker at 4 hours after bombardment and treated with 10 μM U73122 for 1 hour. No PM invagination was observed (n=30).

Conclusion

Through this PhD thesis work, the mechanism for pollen tube growth is studied using combined modeling and experimental approaches. Overall, this research addressed three questions:

(1). What is the mechanism controlling ROP1 GTPase temporal dynamics at the apex of pollen tubes?

(2). What is the mechanism controlling ROP1 GTPase polarity establishment and pollen tube morphogenesis?

(3). What is the mechanism for clathrin mediated endocytosis in pollen tubes?

In chapter 1 of this thesis, we proposed mathematical models for ROP1 activity oscillation at apex of pollen tubes to answer the first question. Our combined theoretical and experimental studies suggest that ROP1 activity oscillation depends on downstream ROP1 signaling events, F-actin assembly and calcium accumulation, which positively and negatively feedback regulate ROP1 activity, respectively. Our findings suggest a key role for calcium in the negative feedback regulation of ROP1 activity, which can explain the long-standing dilemma in the field of pollen tip growth, i.e., the oscillatory accumulation of calcium at the cell tip lags behind the increase in tip growth rate, albeit an essential role for calcium in tip growth.

In chapter 2 of this thesis, we proposed and experimentally validated a model coupling both active ROP1 polarity establishment and pollen tube morphogenesis to answer the second question. We revealed that exocytosis is the key process linking ROP1 GTPase polarity establishment, cell wall pectin distribution and polarized cell growth. Through exocytosis mediated positive feedback loop, RopGAP mediated global inhibition and lateral diffusion of ROP1 GTPase on plasma membrane, active ROP1 GTPases polarity can be established and maintained. Once maintained, active ROP1 controls cell wall mechanics via control of pectin exocytosis and thus determines the shape of pollen tubes. Experimentally, we also validated the model through both genetic (*ren1-1* mutant) and chemical (Lat B treatment) perturbation of pollen tube morphogenesis process. The unique feature of our model is that we linked signal transduction pathway with cell wall mechanical pathway to fully describe the morphogenesis of tip-growing pollen tube cell. Since tip-growth is a universal theme throughout evolution, our modeling work done in pollen tube may provide useful clue for modeling tip growth in other cell system such as root hair and fungal hyphae.

In Chapter 3 of this thesis, we revealed that two interconvertible phosphoinositides, PI(4,5)P2 and PI4P, function in different steps of clathrin-dependent endocytosis in pollen tubes. Whereas accumulation of PI(4,5)P2 is required for the initial steps of membrane invagination, PI4P is required for the later steps of closing and/or fission of invaginated membrane. Given previous findings that both the accumulation and the hydrolysis of PI(4,5)P_2 are required for clathrin-mediated endocytosis in yeast and animal

cells, a balance between PI4P and PI(4,5)P_2 may provide a common mechanism underlying clathrin-dependent endocytosis in various eukaryotic systems.

Using combined modeling and experimental approaches, more mysteries hidden in pollen tube growth will surely be revealed. First, the pollen tube growth requires the balance between regulated exocytosis and endocytosis, but how exocytosis and endocytosis is coordinated is not well studied. To understand this mechanism, the relationship between ROP1 GTPase dependent exocytosis and phosphoinositides dependent clathrin mediated endocytosis need to be further studied. Secondly, we assumed that pollen tube growth direction is randomly chosen. In vitro, when guidance signal is missing, this assumption is acceptable. However, in vivo, the ability of pollen tube to turn toward the ovule is vital for the success of fertilization. Future studies will also focus on pollen tube growth direction change in presence of guidance signal to ensure the successful sexual plant reproduction.